

---ERRATA & ADDENDA---

- P8L11B FOR CONSTITUTIONAL READ CONSTITUTIONAL.  
P8L5B FOR ZEOLITE READ ZEOLITIC.  
P9L11B FOR ION-EXCHANGE READ ION-EXCHANGED.  
P10 SECTION HEADED EXAMPLES. THE SILICA GEL REFERRED TO CONTAINED CA 19WT% WATER. THE SODIUM ALUMINATE REFERRED TO CONTAINED 40WT% SODIUM OXIDE, 54.4WT% ALUMINIUM OXIDE. LOSS ON IGNITION 8.3WT%.
- P14L2B INSERT TRUNCATED BEFORE OCTAHEDRA.  
P16L1T INSERT TRUNCATED BEFORE OCTAHEDRAL.  
P26L7T FOR BEE READ BEEN.  
P28L15T MILLER SHOULD HAVE AN UPPER CASE M.  
P32L6T FOR SYMMETRY READ LATTICE.  
P34L10T LORENTZ SHOULD HAVE AN UPPER CASE L.  
P38L10T FOR 92 READ 98.  
P38L11T ANION SHOULD HAVE A LOWER CASE A.  
P39L6T FOURIER SHOULD HAVE AN UPPER CASE F. ALSO IN LATER TEXT.
- P50L13B FOR 11.2 READ 12.0.  
P58L3T FOR CAVITITES READ CAVITIES.  
P58L7B FOR AT HIGH TEMPERATURE READ AFTER HEAT TREATMENT.  
P67L7T FOR 800 READ 1380.  
P68 THE LAST FOUR SAMPLES IN TABLE 5.10 WERE NITRATE-RICH SODALITES NOT CANCRINITES AS ERRONEOUSLY STATED.
- P73L10T INSERT AND WATER MOLECULES AFTER IONS.  
P75L7B FOR THERWISE READ OTHERWISE.  
P79L14T FOR 48 READ 54.  
P79L4B IN BARLOCHER THE UMLAUT SHOULD BE ON THE A NOT THE O.  
P80L6T FOR CUBOCTAHEDRAL READ TRUNCATED OCTAHEDRAL.  
P80L17T FOR CUBOCTAHEDRAL READ TRUNCATED OCTAHEDRAL.  
P86L9B FOR OXIDITION READ OXIDATION.  
P88L6B INSERT AND BEFORE THE TUNGSTATE SYMBOL.  
P88L6B TUNGSTATE SYMBOL SHOULD HAVE CHARGE -2.  
P94L6B FOR TH READ THE.  
P94L5B FOR ARTIFICALLY READ ARTIFICIALLY.  
P95L12B FOR FOR READ FORM.  
P95L1B SYMBOL M SHOULD BE UPPER CASE.  
P96L8T INSERT BE AFTER NOT.  
P96L10T BRACES MISSING IN NUMERATOR OF EQN 8. INSERT LH BRACE AT FAR LHS & RH BRACE AFTER FIRST RH BRACKET.  
P96L17T NUMERATOR IN EQN 9. SUPERSCRIPIT ALPHA SHOULD BE BETA.  
P97L2T INSERT STOP BEFORE BARRER.  
P97L8T DELETE SUPERSCRIPIT ALPHA.  
P97L15T FOR CUBOCTAHEDRAL READ TRUNCATED OCTAHEDRAL.  
P97L11B FOR WHICH ARE READ WHICH IS.  
P100L5T LHS OF THE LAST IDENTITY. SUBSCRIPT FOR N SHOULD BE 100 NOT 110.  
P103L17T DENOMINATOR OF EQN 27. SUBSCRIPT FOR R IN SQUARE BRACKETS SHOULD BE 1 NOT 2.
- P104L4T INSERT EXTERNAL AFTER THE.  
P108L17T FOR AGREE READ AGREED.  
P112L15B FOR DESCRUBE READ DESCRIBE.  
P115L14T INSERT REF. (69) AFTER MEASURE.  
P115L16T INSERT REF. (94) AFTER FOLLOWS.  
P121L3B FOR 1968 READ 1969.  
P122L11B AFTER 162 INSERT 346, (1932).  
P122L9B FOR 1968 READ 1969.  
P123L11T FOR STUDIEREN READ STUDIEN.

Anion Entrainment During Hydrothermal Crystallization

by

John Francis Cole, M.Sc.

A Thesis submitted to The University of London

for the Degree of Doctor of Philosophy.

Physical Chemistry Laboratories,  
Imperial College of Science and  
Technology,  
South Kensington, London.

January, 1969.

## Abstract.

A study has been made of the low temperature hydrothermal reactions of raw kaolinite with sodium hydroxide solutions which contain additional alkali-stable salts. These systems produced predominantly a variety of sodalite and cancrinite salt inclusion aluminosilicates whose physical and chemical properties have been investigated in moderate detail. Some of these compounds were shown to have potential usefulness as ion-exchangers, storage media for chemically compounded gases and, after suitable pretreatment, as catalysts.

The several effects upon crystal properties of anion entrainment have been discussed and possible extensions to molecular sieve synthesis noted.

Salt inclusion isotherms on sodalite were obtained for a number of salts, and these were found to follow a Langmuir type law. A phenomenological theory of salt trapping from solution during the sodalite crystallization, coupled with a Donnan-type phase equilibrium was found to qualitatively account for the observations.

Acknowledgements.

I wish to record my indebtedness to Professor R.M. Barrer, F.R.S., who, during my three year stay in his laboratory, was a constant and enthusiastic source of advice, example and encouragement.

I am also indebted to my colleague Hans Villiger, who has contributed much to my practical understanding of X-ray Crystallography and digital computing.

I was supported by The Agricultural Research Council of Great Britain and by W.R. Grace and Co., of Baltimore, Maryland, U.S.A., and acknowledge with gratitude my indebtedness to these bodies.

The manuscript was typed by Mrs. M. Michael, whose work speaks for itself.

London, December 1968.

## Contents.

| Section No.* |  | Page No. |
|--------------|--|----------|
| 1            | Introduction concerning Definitions, and<br>Statement of Objectives .                  | 1        |
| 2            | Experimental Methods in Zeolite Chemistry.   | 6        |
| 3            | Properties and Structure of Sodalite and<br>Cancrinite.                                | 14       |
| 4            | X-ray Powder Diffraction Methods in Zeolite<br>Chemistry.                              | 28       |
| 5            | Preparation and Properties of Salt-rich Sodalites<br>and Cancrinites, with Discussion. | 42       |
| 6            | Theories of Hydrothermal Crystallization.  | 87       |
| 7            | Theory of Anion Entrainment During Hydrothermal<br>Crystallization.                    | 93       |
| 8            | Conclusions.   | 110      |
| Appendix 1.  | Mathematical and computational methods.  | 111      |
| References.  |  | 119      |

\* Tables, figures and mathematical equations are numbered consecutively in each section. Tables and figures have their numbers prefixed by the number of the section.

## SECTION 1.

### Introduction Concerning Definitions.

#### Hydrothermal Crystallization. <sup>(1,2)</sup>

The word "hydrothermal", used in the earth sciences, implies the solvent action of hot water in dissolving, transporting, redepositing or otherwise changing minerals of the earth's crust. In the laboratory the word "minerals" can be replaced by the phrase "mixtures of compounds which are themselves components of naturally occurring minerals". The scope of this definition is very wide, and recent work has shown that even synthetic organic molecules of some complexity can take part in hydrothermal reactions, producing entirely new mineral-type compounds.<sup>(3)</sup> Early work in hydrothermal chemistry was undertaken at considerably elevated temperatures and pressures, and required expensive and troublesome apparatus.<sup>(2,4)</sup> However, the chemical interest in the last twenty years has shifted to low temperature reactions, and as new methods have been developed, work at 100°C has become commonplace. This area will be discussed in most detail in the present work, and for this reason the specialized high temperature and pressure technology more appropriate to mineralogical and geological studies, will not be discussed.

#### Mineral Chemistry.

This subject was much investigated by the great European School of Mineral Chemists during the last century. Unfortunately, we have not seen their like since, and for nearly fifty years the chemistry of silicon and aluminium, two of the most important and abundant elements, has been relatively neglected. Few academic chemists are today engaged in research on silicon and aluminium and most modern texts on inorganic chemistry devote only minimal coverage to these areas, while expounding coordination chemistry in detail. Despite this, materials scientists and industrial chemists are continually finding new uses for mineral type compounds, and there is a growing demand for methods of producing "laboratory pure" minerals. The small amount of basic chemistry done here in the last twenty-five years has yielded impressive rewards. Perhaps the most handsome results of chemical

and physico-chemical endeavour with silicon and aluminium and hydro-thermal methods are found in the science and technology of molecular sieves. <sup>(5)</sup> From early beginnings in Barrer's laboratory, followed by commercialization at the hands of Union Carbide Corporation, this field is increasingly contributing to the petroleum and other industries. <sup>(6)</sup> The molecular sieves found in solvent bottles and drying tubes in the laboratory today are the cracking and isomerization catalysts used to process a major part of the world's crude oil. They are also used to dry and sweeten enormous quantities of natural gas, and to separate and dry mixtures of gases and liquids in numerous processes in chemical technology. Molecular sieves are found in submarines, space capsules and household refrigerators, and replace older adsorbents in many dehydration and purification processes.

The saving, increased production, and purity achieved by the use of sieves amounts yearly, in fiscal terms, to many hundreds of millions of dollars, <sup>(7,8)</sup> and the importance of these discoveries is becoming comparable with such things as the discovery of polyethylene.

#### Framework alkali aluminosilicates.

Early work on the structures of minerals revealed some very interesting geometrical features of Si and Al. In many such compounds atoms of these elements were surrounded by oxygen atoms in fourfold coordination, and the oxygens surrounding each Al or Si were at the corners of a regular, or nearly regular tetrahedron. These tetrahedra were able to share corners through oxygen bridges, and the reason for the variety of the mineral species was at once seen to be very similar to that responsible for the variety of organic compounds. Pauling <sup>(9)</sup> showed that the sharing of faces and edges of these tetrahedra would tend to decrease stability, so that sharing of corners should be most common, and so far most, if not all structures were found to substantiate this rule. Another important finding was that in these tetrahedra the Si-O bond length ( $\sim 1.63 \overset{0}{\text{Å}}$ ) and the Al-O bond length ( $\sim 1.73 \overset{0}{\text{Å}}$ ) were nearly the same and were almost constant.

Here then was the possibility of building an infinite variety of open, rigid three dimensional frameworks. If the Al-O<sub>4</sub> and Si-O<sub>4</sub> tetrahedra alternated or were mixed in some way in these structures, a negatively

charged framework would result, and the charges on the  $Al$  atoms would need to be compensated by cations. When these conditions obtain and the cations are members of group Ia of the periodic table, we speak of framework alkali aluminosilicates.<sup>(10)</sup> The zeolites, natural and synthetic, are examples of such compounds. These are built in such a way that unusually spacious internal channels and cavities result, which are normally filled with water. When this water is removed by heat or evacuation the zeolites are "activated" and behave as extremely efficient adsorbents for water and other molecules. By choice of zeolite and molecules we can selectively adsorb components from a mixture of different sized molecules, or "sieve" molecules. Since the cations in framework alkali aluminosilicates are only electrostatically bound, these compounds undergo the phenomenon of ion exchange and exhibit ion-sieve characteristics. These sorptive<sup>(11)</sup> and ion-exchange<sup>(12)</sup> properties of zeolites are used extensively in laboratory and industry. One of the most startling discoveries about zeolites was made as late as 1960, but was embryonic years before. Thirty years ago Pauling<sup>(9)</sup> compared an  $Al$  atom forming an oxygen tetrahedron whose corners were shared with silicon tetrahedra, with a perchlorate ion, and stated that "the acid obtained by replacing the potassium ion of mica by hydrogen ion should be very strong". When, ten years later, Barrer<sup>(13)</sup> heated  $NH_4^+$  forms of zeolites to form the  $H^+$  variety, no-one realized that a decade later hydrogen zeolites would prove to be the most powerful cracking catalysts ever found. Latest work shows that zeolites are excellent catalysts for many other kinds of reactions,<sup>(14)</sup> and we confidently await a whole range of new reactions at low temperatures, catalysed by these remarkable solids.

#### Salt Inclusion Alkali aluminosilicates.

Certain of these frameworks are more condensed than others, and during their formation in nature or in the laboratory, salt molecules are trapped in their cavities and channels. Just as the polarizable water molecules take up residence in open molecular sieves during synthesis, under certain circumstances, anions do the same thing in condensed zeolites.<sup>(15,16)</sup> If a zeolite happens to have two or more different sized framework cavities, synthesis in



a suitable salt solution can fill one of these with anions and the larger with water. The zeolite known in this laboratory as  $K-F^{(17,18)}$  is an example. It can trap  $KCl$  or  $KBr$ , but at the same time a substantial proportion of intracrystalline space is still available for water. Such compounds are entirely interesting and have very unusual ion-exchange characteristics.

The case when only one kind of cavity is present is found in nature in the mineral sodalite, and much of the present work will deal with its unusual chemistry. The mineral cancrinite, also the subject of this work, is another example in which two kinds of framework cavities exist. In these salt inclusion aluminosilicates, the anion takes up crystallographic positions in the framework and is associated with cations. Normally, due to its larger size relative to the openings controlling ingress and egress, these anions cannot be removed by dialysis or exchange, but are encapsulated in the structure.

Experiments with these compounds have thrown light on mechanisms of formation of zeolites in the laboratory, and some of the individual species are of potential usefulness. For example, various hydrothermally prepared sodalites are being investigated as possible photochromic detectors for solid state information storage,<sup>(19)</sup> and as storage media for chemically compounded gases, and alkali metals.<sup>(20)</sup>

#### Statement of Objectives.

The formal subject of this work is "Anion Entrainment During Hydrothermal Crystallization". One object of the work was to study salt uptake by porous crystals during their formation. This necessitated a general qualitative study of various synthetic systems to develop general experimental methods, and to enable the choice of systems suitable for quantitative studies. A second objective was the investigation of physical and chemical properties of salt-rich porous crystals. Having found that the sodalite system was suitable for quantitative work, it was hoped to determine salt inclusion isotherms, to attempt their theoretical explanation, and to try to correlate the results with the field of molecular sieve synthesis. An overall aim was to develop new methods for the experimental and theoretical treatment of the

subject, and to develop possibilities of future work in this relatively unstudied area.

The arrangement of the work is as follows. An account is first given of the reaction compositions and methods used in alkali aluminosilicate syntheses, and the routine experimental methods used to evaluate crystalline products. This account has been illustrated by practical details of a number of important examples. Next, the crystal structures and some other properties of sodalite and cancrinite have been given, since the bulk of what follows concerns these compounds. Some experimental details of x-ray powder photography, as applied to silicate chemistry, are then discussed, since this was one of the most important techniques used. Experimental materials and reaction compositions are then recorded, followed by a summary account of crystalline salt inclusion compounds produced, and their physical and chemical properties. After an intermediate discussion, the theoretical treatment of salt entrainment has been described and discussed at some length in relation to the experimental salt inclusion isotherms. An appendix contains a description of mathematical and computational methods employed in connection with the theory.

## SECTION 2.

### Reaction Compositions for Zeolite Synthesis.

The aluminium and silicon required for zeolite synthesis can be initially in a variety of forms. Aluminium hydroxide gel, sodium and potassium aluminate, aluminium phosphates and other salts are typical sources of Al, while sodium and potassium silicate, silica gel, precipitated silica, silica glasses, and commercially available aqueous silica sols are normally used as sources of silica. Waste material, for example from alkali bauxite-leaching plant, after suitable enrichment, can be used to advantage. Alkali is normally added directly in the form of hydroxides, or hydrolysable compounds such as carbonates and phosphates are mixed with the charges. A variety of additives such as certain salts, organic compounds and surfactants, are used to produce specific effects. These processes are to a large extent kept secret by the companies using them.

Increasing use has been made of cheap and plentiful natural sources of reactants. Kaolinite, halloysite, pyrophyllite, allophane and certain allied minerals have recently been used as raw materials for zeolite synthesis, and transformation of common natural and synthetic zeolites to other more desirable materials is becoming steadily more important.<sup>(21,22,23,24)</sup> Several representative examples of zeolite syntheses are given later in this section.

### Exact descriptions of reaction mixtures.

A precise description of the way in which reactants are prepared for zeolite syntheses is often important for success. An example will illustrate this. Kerr<sup>(25)</sup> has shown that either zeolite X or zeolite B (Barrer P) may be prepared by refluxing a mixture of 83.8g of sodium metasilicate nonahydrate and 18.3g of sodium aluminate with 400 mls of water. If the silicate in 250 mls of boiling water is added rapidly (5 sec) with vigorous stirring to the aluminate in 150 mls of boiling water and afterwards stirring is discontinued, in 3-4 hours, pure, well crystallized zeolite X is formed. If the silicate in 100 mls of boiling water is added slowly (25-35 sec) with stirring

to the aluminate in 300 mls. of boiling water, and stirring is continued until the end of the reaction (4-5 hours), pure, well crystallized zeolite B is formed. Thus, a description of this method, without details of order of addition, times and rates of stirring of reactants and so on, is of limited use, since the nature of the product depends on these variables. Many such details were found at great pains and expense, and for these reasons are not generally available. Their importance is, however, underlined.

#### Methods of Zeolite Synthesis.

The reactive mixtures, having been compounded from materials already described, are filled into suitable vessels of metal, plastic or glass and maintained at the desired temperature and pressure for predetermined periods. Times of from one hour to several weeks are common. During this period the vessels are often stirred, shaken, rolled or rocked. The type and rate of mechanical action may have profound effects on the products finally obtained. In addition, components may be added to, or removed from the reaction vessel during the experiments. At the end of the predetermined period, the solids are removed from the mother liquor by filtration, centrifugation, flotation or other means, and in industrial practice the latter is analysed, reconstituted and recycled. The solids are washed free of soluble reactants with water, or dilute ammonia solution, and stored for further use. The procedure described can be used on a laboratory scale to produce 0.5-20g lots of zeolites for research purposes, and is used industrially. For example, the Baltimore plant of W.R. Grace and Co. produces about 20 tons of zeolite Y a day, by the same general methods.

#### Methods of Zeolite Characterization.

Observation of the filtration behaviour, thixotropic character of zeolitic pastes and many other properties such as the feel and consistency of powdered products can immediately inform the experienced investigator whether he has a well-crystallized sample or a mixture of gel and other amorphous material. This information is usually supplemented by a rapid optical examination under a microscope. After this preliminary

evaluation, the procedure is now standardised as follows:

- (1) An x-ray powder diffraction photograph is made after suitable sample preparation. For this purpose a Guinier camera is much more useful than a Debye-Scherrer camera. The major phase or phases can normally be identified on sight. Measurement of a few lines of the Guinier photograph with a mm. rule ( $4\theta$  values) followed by a quick scan of computer-produced catalogues<sup>(29)</sup> of all known zeolites normally suffices to establish what is present, and the approximate proportions thereof. Unrecognizable patterns are treated as in section 4. In addition the powder photograph provides much extra information about the types of atoms in the crystals, the particle size, the degree of crystallinity and the arrangement of atoms in the crystal unit-cell. Some of these aspects will be further discussed in section 4.
- (2) If the product is essentially a single phase as evidenced by a unique x-ray powder photograph and is for some reason worthy of further interest, the thermal dehydration is next investigated. The sample is equilibrated in an atmosphere of water vapour under known conditions, and then heated in a controlled atmosphere at a prescribed rate. Various commercial instruments are available for this purpose. The weight of the sample is monitored continuously and also its temperature relative to that of a stable inert reference material being heated under the same conditions. If the sample is pure and highly crystalline, these thermogravimetric and differential-thermal data relate the amount of water held by the porous crystals, and the temperature range over which it is lost, the temperature at which constitutional water is lost, and the amount thereof, and the temperature at which the crystal is destroyed, by recrystallization to another phase, or by sintering to a glass. Further useful information is sometimes obtained by subjecting the ignition product to x-ray powder photography.
- (3) When it has been established that the sample holds an appreciable amount of zeolite water which can be reversibly removed without consequent destruction of the crystal lattice, the next step is usually an attempt to replace this water by other molecules. The crystals are outgassed in vacuum and their weight is continuously monitored while other gases and vapours are allowed to come into contact with them. Automatic apparatus with chart and/or digital

output is now available for this purpose. By judicious choice of sorbates of known molecular dimensions the effective pore size of the crystals can be determined,<sup>(30)</sup> and the sorption capacity, or internal volume available to guest molecules may be estimated.

(4) If the procedures already followed have all given interesting results, further synthesis experiments are made in order to optimize the quality of the product. At this point the experienced investigator will attempt to grow a large batch of the pure material, sufficient for all further researches. This may involve a great deal of further work on kinetics of formation, method of charge composition, and so on. The product will then be accurately analysed several times by wet chemical methods, and instruments such as the electron microprobe and electron microscope employed to obtain further details of constitution and morphology.

(5) If the material appears to be novel and the problems of producing it economically in a pure well-characterized state have been overcome, a search for potential uses of the new material may be commenced. This means, usually, investigating its catalytic properties. In the oil industry, a successful new or improved molecular sieve catalyst generally means, in fiscal terms, a return of many millions of dollars. This investigation therefore proceeds without delay, in the utmost secrecy.

Attempts are first made to make and characterize ion-exchange forms of the material, in particular the hydrogen form and the ammonium form. The latter can sometimes be transformed to the  $H^+$  form by calcination<sup>(13)</sup>. Since in a great many cases the whole investigation has been directed towards producing new catalysts, desirable features such as large pore-size, high thermal and steam stability, high Si/Al ratio must be established as properties of the new material. Deficiencies in any of these qualities need not however render the product useless, since new catalytic uses are constantly being found in areas where, for instance, high steam stability need not be important, and in any case other uses for zeolites are always being found.<sup>(14,31)</sup>

The potential catalyst is placed in a reactor, pretreated, and held at the

required conditions while feed mixtures of gases, oils or vapours are passed through or over it. The products are analysed by chromatographic techniques and the composition, cation content and other crucial variables are adjusted so as to maximise the yield of desirable products and to minimize such things as the temperature, poisoning, coking and decomposition of the catalyst. Other types of catalytic behaviour may be investigated by activating the catalyst and introducing interesting molecules at low temperatures, for example at 20 °C. The catalytic action of some zeolitic materials is so great that certain exothermic reactions take place even under these mild conditions. <sup>(32,33)</sup>

(6) The importance of preparing a pure, well crystallized specimen before making detailed measurements of the kind described cannot be overemphasised. Since amorphous material often has surprising sorptive properties <sup>(34)</sup> and shows curious thermal effects, mixtures of such impurities with crystalline material may lead to novel but worthless results. Also, amorphous material found alongside the zeolites often has the same chemical composition as the crystalline phase <sup>(18,35)</sup> so that chemical analysis is not always a good guide. The most powerful methods in this area employ the optical and electron microscopes, and electron diffraction techniques.

#### Examples of Zeolite Syntheses.

The best way of illustrating the methods of zeolite synthesis is to offer several widely differing examples with practical details. The following are mainly new examples from the literature and modifications used in this laboratory. Where the latter is the case, reference is given to original preparations.

Example 1. Synthesis of the elementary zeolite sodalite. <sup>(54)</sup> When pure kaolinite is heated with agitation in a sealed polypropylene bottle with excess 4M aqueous sodium hydroxide solution, at 80 °C for 24 hours, pure "basic" or "hydroxyl" sodalite is formed. The excess of imbibed NaOH may be extracted under nitrogen in a soxhlet apparatus. <sup>(55)</sup>

Example 2. Synthesis of the elementary zeolite cancrinite<sup>(18)</sup> with imbibed sodium nitrate. If the reaction mixture in example 1 contains, in addition, 0.1 moles  $\text{NaNO}_3$ , the product will be cancrinite, with imbibed  $\text{NaNO}_3$ , which may not be washed out.

Example 3. Synthesis of zeolite A (Union Carbide Zeolite type A, Linde Sieve A)<sup>(36)</sup>. A solution of commercial sodium aluminate (Hopkin and Williams) is prepared by dissolving 82g. in 1 litre of water and filtering. 120g. of sodium hydroxide (reagent grade) is added to 500 ml. of water and 60g. of precipitated silica gel (BDH) is dissolved therein by heating. The resulting solution is filtered through a sintered glass disc. This solution is then diluted by addition of a further 500 ml. water. When gels formed by mixing 5 parts by volume of aluminate solution with 3 parts by volume of silicate solution are heated at  $100^\circ$  without agitation for 24 hours, zeolite A is formed.

Example 4. Synthesis of zeolite X (Union Carbide Corporation Zeolite type X, Linde Sieve X)<sup>(37)</sup>. The method of example 3 is followed, except that the gels are made from 1 part of aluminate and 2 parts of silicate.

Example 5. Synthesis of zeolite P (R.M. Barrer Zeolite Na-P, cubic variety)<sup>(17)</sup>. The method of example 3 is followed, except that gels are made from one part of aluminate and 4 parts of silicate. By varying the method of gel preparation using the same solutions, zeolite Y may be produced. (Union Carbide Zeolite Y, a silica rich variety of zeolite X).<sup>(95,27)</sup>

Example 6. Synthesis of zeolite P<sup>(17)</sup> from raw kaolinite. Raw kaolinite of good purity (25.8g.) is mixed with precipitated silica gel (BDH) (12g.) and sodium hydroxide (reagent grade) (24g.) in water (250 ml.). The charge is agitated in a sealed polypropylene bottle at  $80^\circ$  for 10-20 days.

Example 7. Synthesis of a variety of Gmelinite.<sup>(17)</sup> A solution of 153g. of sodium silicate (18% w/w  $\text{Na}_2\text{O}$ , 36% w/w  $\text{SiO}_2$ ) in 200 ml. of water is prepared. A second solution of 10g. of commercial sodium aluminate (Hopkin and Williams) in 200 ml. water is prepared and heated to  $80^\circ$ . While stirring rapidly, 10g. of gelatine is slowly added to the hot aluminate



solution. When a homogeneous mixture results the silicate solution is slowly added to form a thick gel, which is beaten very vigorously until emulsion results. The resulting mixture is heated for 72 hours in Pyrex bottles at  $100^{\circ}\text{C}$ . After this time the crystals are separated from the mother liquor by filtration, and dried at  $120^{\circ}$ . Entrained organic matter is removed by heating in oxygen at  $350^{\circ}\text{C}$ .

Example 8. <sup>(3)</sup> Synthesis of the zeolite ZK-5 (Mobil Oil Corporation, molecular sieve type ZK-5). A solution of 3.45g. (0.0206 mole  $\text{Na}_2\text{O}$  and 0.0138 mole  $\text{Al}_2\text{O}_3$ ) of sodium aluminate in 10 ml. water was prepared. A solution of the quaternary ammonium silicate (1,4-dimethyl-1,4-diazoniabicyclo [2.2.2]octane Bis(trihydrogen silicate)) was made by dissolving 9.2g. (0.153 mole  $\text{SiO}_2$ ) of silica gel in 111 ml. of a 2.74 N solution (0.156 mole) of 1,4 dimethyl-1,4 diazoniabicyclo [2.2.2] octane hydroxide solution. The two solutions were mixed and the gelatinous precipitate heated at  $95-100^{\circ}$  for 8 days. The solid product was filtered off and calcined at  $550^{\circ}\text{C}$ .

Example 9. <sup>(38,39,80)</sup> Synthesis of the zeolite ZK-4, a silica-rich modification of Union Carbide Zeolite A (Mobil Oil Corporation, molecular sieve type ZK-4). Sodium aluminate 21.5g. (0.126 mole  $\text{Na}_2\text{O}$  and 0.086 mole  $\text{Al}_2\text{O}_3$ ) was dissolved in 250 ml. water. A solution of 20.25g. (0.35 mole  $\text{SiO}_2$ ) of silica gel was prepared by heating with 285 ml. 2.49M (0.71 mole) tetramethylammonium hydroxide solution. The latter solution was filtered, and after heating both solutions to boiling, the silicate was added rapidly to the aluminate with stirring. The resulting precipitate was heated at  $\sim 100^{\circ}\text{C}$  (reflux temperature) for 24 hours.

Example 10. <sup>(34)</sup> Synthesis of "large-port" mordenite (i.e. a mordenite which occludes cyclohexane, as opposed to a "small-port" one which does not). When a charge of composition  $\text{Na}_2\text{O}/\text{Al}_2\text{O}_3/\text{SiO}_2/\text{H}_2\text{O}$  6.3:1:27:61 of raw materials diatomite, sodium aluminate, sodium silicate, sodium hydroxide and water is heated at  $100^{\circ}$  for 168 hours, large port mordenite is produced as a single phase. Many other compositions and conditions may be used.

Example 11. (40,41) Synthesis of Strontium Ferrierite. When aqueous gels of composition  $\text{SrO}$ ,  $\text{Al}_2\text{O}_3$ ,  $n \text{SiO}_2$  ( $7 \leq n \leq 9$ ) compounded from strontium hydroxide, aluminium hydroxide gel and "syton 2X" (silica sol) are autoclaved in stainless steel vessels at  $340-400^\circ$  for about 10 days, crystals of a zeolite which is almost identical with the rare natural zeolite ferrierite, are formed.

The above examples indicate the variety of products which can be obtained from outwardly simple systems. Examples 8, 9 and 11 are slightly more esoteric and show some of the variety which characterizes new developments. The methods given for the preparation of sodalite, A, X and P are superior to those normally used, giving excellent samples suitable for research work. In example 7 an attempt was made to increase the viscosity of the gels. When the gelatine is omitted from the reaction, less crystalline samples are produced.

Present and future work aims at explaining the fundamental processes which account for the variety in this fascinating field of zeolite synthesis.

### SECTION 3.

#### The Properties and Structure of Sodalite.

Natural sodalite has the composition  $6(\text{NaAlSiO}_4) \cdot 2\text{NaCl}$ .<sup>(42)</sup> It crystallizes in the cubic system with one formula unit per unit cell. The unit cell parameter is about  $8.86 \text{ \AA}$ . Some controversy has taken place in the past concerning the space group, whether  $P\bar{4}3m$  or  $P\bar{4}3n$ .<sup>(43)</sup> However, the latest work suggests that the  $8 \text{ Na}^+$  are structurally equivalent, and the point group  $\bar{4}3n$  is to be taken as correct, at least for the particular specimen used by Löns and Schulz whose paper<sup>(44)</sup> forms the basis of this discussion. By application of modern methods, these authors refined the structure postulated by Pauling<sup>(45)</sup>. Table 3.1 gives the coordinates and other data based on refinement in space group  $P\bar{4}3n$  to weighted and unweighted R factors of 0.077 and 0.082. The specimen had a Si/Al ratio of 1:1 and a cell parameter  $a_0 = 8.870 \pm 0.004 \text{ \AA}$ .

In order to understand the molecular geometry corresponding to the data of Table 3.1, we take a Cl ion at (0,0,0) as an origin and draw a stick bond representation of the structure by joining Si and Al atoms. To do this the ORTEP thermal ellipsoid plot programme<sup>(46)</sup> was used, and was kindly supplied by its author, Dr. Carrol K. Johnson of Oak Ridge National Laboratory. ORTEP is an ingenious and sophisticated Fortran program which generates, from crystallographic data such as those in Table 3.1, a set of instructions which are written onto magnetic tape. This tape is used to drive an off-line x-y plotter, such as a Calcomp machine to produce accurately scaled perspective drawings of crystal structures. Fig. 3.1 shows such a drawing of the chloride ion environment in a single sodalite cage. The atoms have been given arbitrary small dimensions so as to better expose the geometry, and the sodium ions have been joined to show how the  $\text{Cl}^-$  ion is situated at the centre of a tetrahedron formed by them. The full sodalite structure is better seen when the building units are represented as solid octahedra as in Fig. 3.2. Here, a central unit shares one of its 8 six-ring faces with each of 8 other units. The sodalite structure consists, therefore

Table 3.1Crystallographic Data for Sodalite. Space Group  $P\bar{4}3n$ .

| <u>Atom</u> | <u>Position</u> | <u>Parameters</u>   | <u>Isotropic Temperature Factor</u> |
|-------------|-----------------|---|-------------------------------------|
| 2 Cl        | 2(a)            | 0 0 0   | $1.90 \pm 0.04$                     |
| 8 Na        | 8(e)            | x x x $x = 0.1777 \pm 0.0004$   | $1.49 \pm 0.04$                     |
| 6 Si        | 6(d)            | $1, 0, \frac{1}{2}$   | $0.35 \pm 0.04$                     |
| 6 Al        | 6(c)            | $1, \frac{1}{2}, 0$   | $0.80 \pm 0.07$                     |
| 24 O        | 24(i)           | x y z $x = 0.1401 \pm 0.0004$<br>$y = 0.4385 \pm 0.0003$<br>$z = 0.1487 \pm 0.0004$ | $0.89 \pm 0.02$                     |

Distances and Angles.SiO<sub>4</sub> tetrahedra

|      |                                    |
|------|------------------------------------|
| Si-O | $1.628 \pm 0.004 \text{ \AA}^0$    |
| O-O  | $2.629 \pm 0.008, 2.714 \pm 0.008$ |

AlO<sub>4</sub> tetrahedra

|        |   |
|--------|---|
| Al-O   | $1.728 \pm 0.004 \text{ \AA}^0$         |
| O-O    | $2.806 \pm 0.008,$<br>$2.855 \pm 0.008$ |
| O-Al-O | $108.5^0, 111.3$                        |

|         |                                 |
|---------|---------------------------------|
| Si-O-Al | $138.3^0$                       |
| Na-Cl   | $2.730 \pm 0.004 \text{ \AA}^0$ |
| Na-O    | $2.351 \pm 0.008$               |

of unique octahedral cages having restricted windows which link them to give an isotropic channel system. The cages normally contain anions trapped during formation, such as  $\text{Cl}^-$ , and these are nicely coordinated by cations, making for a symmetric and stable structure. When the anions have been removed, partly or completely, and replaced by water, sodalite behaves as a condensed zeolite. It undergoes exchange with small ions such as  $\text{Li}^+$ ,  $\text{Na}^+$ ,  $\text{K}^+$ ,<sup>(47)</sup> and exhibits a high capacity. It will also sorb water, ammonia and alkali metal vapours,<sup>(48,49)</sup> after suitable activation.

In the zeolite laboratory sodalite is recognised by its x-ray powder photographs and its low water content ( $< 14$  wt.%). The calculated powder lines for sodalite are given in Table 3.2. These are based on space group  $\text{P}\bar{4}3\text{n}$ , with  $a_0 = 8.88 \text{ \AA}$ .

In mineralogy various sodalites in which the  $\text{Cl}^-$  inclusion is replaced by other anions are given different names, such as Nosean, Häuyne and Lazurite.<sup>(42)</sup> Sodalite in which other elements replace Al and Si in the tetrahedral framework are known.<sup>(42)</sup> For example in the mineral Danalite Be replaces Al, and various replacements by Ge, and Ga have been made in the laboratory. The replacement of Al by Fe is suspected, but not yet conclusively demonstrated.<sup>(18)</sup>

Further comments on the structures and properties of various sodalites will be made when the need arises.

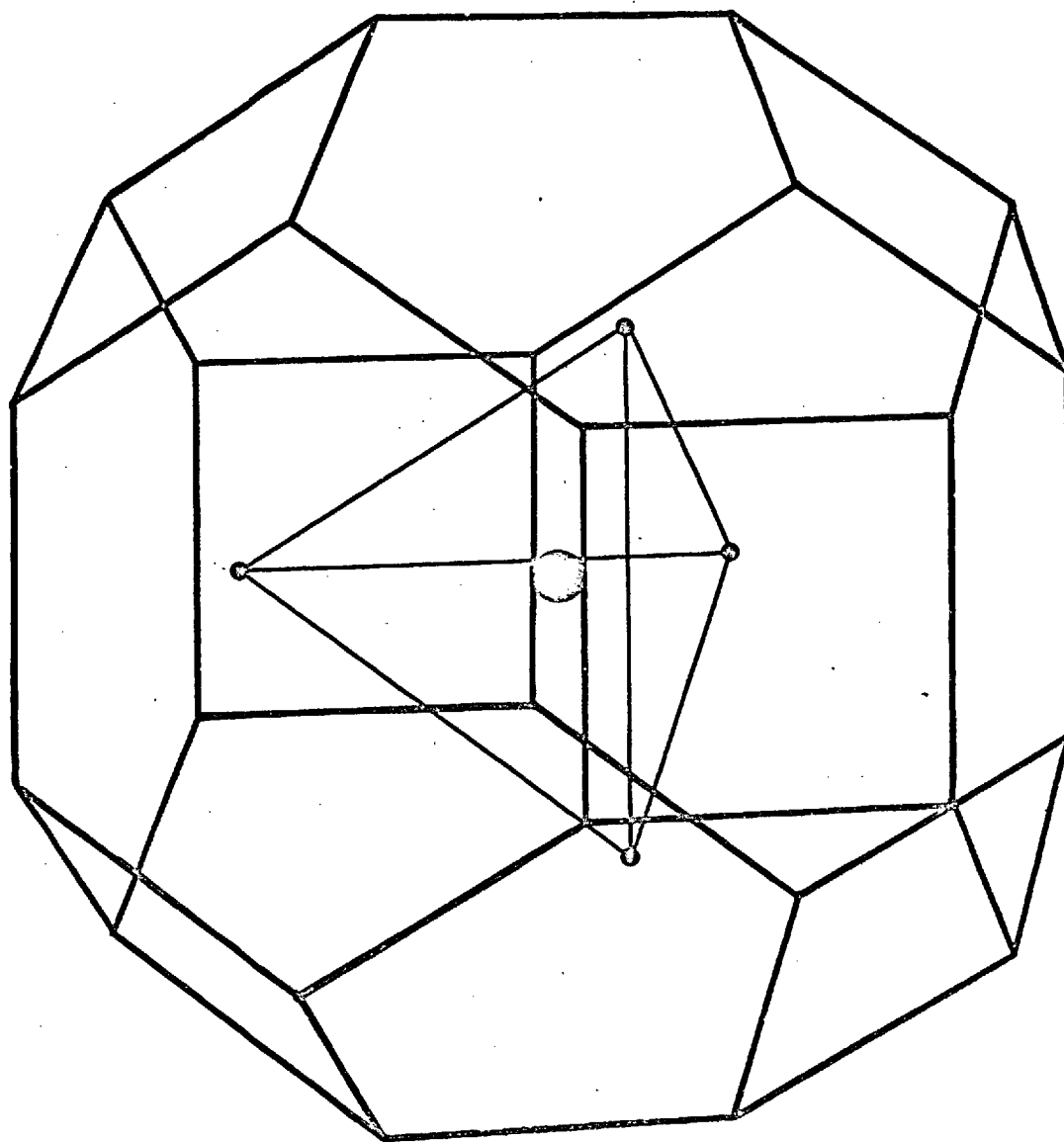


Figure 3.1 Truncated octahedron or "sodalite cage" found in sodalite and molecular sieves A and X. Tetrahedral disposition of  $\text{Na}^+$  ions about central  $\text{Cl}^-$  ion in natural sodalite shown.

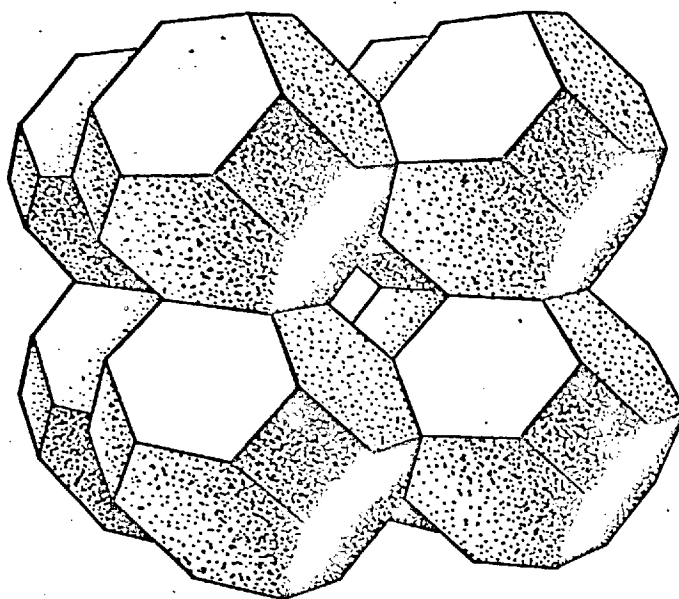


Figure 3.2 Line drawing of sodalite structure.

Table 3.2d-spacings for sodalite

$$a_0 = 8.88 \text{ \AA} \quad \text{space group } \bar{P}43n$$

$$\text{cell volume} = 700.23 \text{ \AA}^3$$

| H | K | L |    | D     |
|---|---|---|----|-------|
| 1 | 0 | 0 | NG | 8.880 |
| 1 | 1 | 0 |    | 6.279 |
| 1 | 1 | 1 | NG | 5.126 |
| 2 | 0 | 0 |    | 4.440 |
| 2 | 1 | 0 |    | 3.971 |
| 2 | 1 | 1 |    | 3.625 |
| 2 | 2 | 0 |    | 3.139 |
| 3 | 0 | 0 | NG | 2.960 |
| 2 | 2 | 1 | NG | 2.960 |
| 3 | 1 | 0 |    | 2.808 |
| 3 | 1 | 1 | NG | 2.677 |
| 2 | 2 | 2 |    | 2.563 |
| 3 | 2 | 0 |    | 2.462 |
| 3 | 2 | 1 |    | 2.373 |
| 4 | 0 | 0 |    | 2.220 |
| 3 | 2 | 2 | NG | 2.153 |
| 4 | 1 | 0 |    | 2.153 |
| 3 | 3 | 0 |    | 2.093 |
| 4 | 1 | 1 |    | 2.093 |
| 3 | 3 | 1 | NG | 2.037 |

Note: The symbols associated with indices in this and other tables designate the kind of condition within the particular space group which causes the annotated reflection to be extinguished. Such symbols are explained more fully in specialized works. See for example refs. (50) and (51).



### The Properties and Structure of Cancrinite.

The following discussion will be based on a recent paper by Jarchow,<sup>(52)</sup> who determined the composition of a natural specimen by x-ray methods as  $6(\text{NaAlSiO}_4) \cdot \text{CaCO}_3 \cdot 2\text{H}_2\text{O}$ . The chemically determined composition was  $(\text{Al} + \text{Si} = 12) \text{Na}_{6.3} \text{Si}_{6.4} \text{Al}_{6.0} \text{O}_{24} \cdot \text{Ca}_{0.91} \text{Fe}_{0.06} (\text{CO}_3)_{1.47} \cdot (\text{H}_2\text{O})_{2.47}$ . Cancrinite crystallizes in the hexagonal system. Jarchow refined his structure in space group  $P6_3$  to a final R factor for observed reflections of 0.089. The specimen had the cell parameters  $a = 12.75 \text{ \AA} \pm 0.02$  and  $c = 5.14 \text{ \AA} \pm 0.03$ . The coordinates and other data are collected in Table 3.3. From these data the ORTEP drawing of Fig. 3.3 was made. The alumino silicate framework of cancrinite is built from the 11-hedral cages which are joined as shown in Fig. 3.3. In the zeolite field these units are called cancrinite cages, and are found in other natural and synthetic zeolites, for example in erionite, offretite and Union Carbide zeolite L.<sup>(53)</sup> In cancrinite the arrangement of these cages about the threefold axis forms a wide channel system parallel to  $\underline{c}$ , as shown in Fig. 3.4. Cations are situated in the 6-rings which open onto this channel, and anions and water molecules take up suitable positions in the channel during synthesis. In natural specimens, cations and sometimes water molecules are found in the cages, but no anions. Part of the present work shows that in synthetic specimens anions are also present in the cancrinite cages. This will be further discussed in section 4. Cancrinite is an example of a zeolite whose characteristic properties have been more or less annulled by salt molecules blocking the intracrystalline pores. The main channel system of approximate diameter  $6.2 \text{ \AA}$ , together with the protruding cations, provides a kind of female threaded cavity which firmly holds ions such as  $\text{CO}_3^{2-}$ ,  $\text{CrO}_4^{2-}$  and so on, so that they cannot be washed out. However, under certain conditions ion exchanges can be made with small cations,<sup>(47)</sup> and synthetic basic cancrinites,<sup>(54)</sup> in which  $\text{OH}^-$  is the anion present, can be extracted to produce a cancrinite hydrate which shows sorptive properties.<sup>(55)</sup> Cancrinite, like sodalite, has a high ion-exchange capacity. In the zeolite laboratory, cancrinite is recognised by its x-ray powder pattern, and its low water content ( $< 14 \text{ wt. \%}$ ). The calculated powder lines for cancrinite are given for reference in Table 3.4. These are based on space group  $P6_3$  and Jarchow's parameters.

Table 3.3

Structural Parameters of Cancrinite.

| Atom                 | Number of atoms per unit cell (x-ray data) | x ( $\sigma_x$ )        | y ( $\sigma_y$ )        | z ( $\sigma_z$ )               | Temperature factor B ( $\sigma^2 B$ ) |
|----------------------|--|-------------------------|-------------------------|--------------------------------|---------------------------------------|
| A $\lambda$          | 6  | 0,0750<br>(0,002)       | 0,4124<br>(0,002)       | 0,7500<br>(0,008)              | 0,73 <sub>8</sub><br>(0,06)           |
| Si                   | 6  | 0,3272<br>(0,0002)      | 0,4101<br>(0,0002)      | 0,750 <sub>8</sub><br>(0,0008) | 0,74 <sub>1</sub><br>(0,06)           |
| Na <sub>2</sub> (Ca) | 6  | 0,1232<br>(0,0004)      | 0,2486<br>(0,0004)      | 0,2920<br>(0,0014)             | 1,74 <sub>3</sub><br>(0,14)           |
| Na <sub>1</sub> (Ca) | 2  | 0,666 <sub>7</sub><br>- | 0,333 <sub>3</sub><br>- | 0,1440<br>(0,0028)             | 2,54<br>(0,18)                        |
| O <sub>1</sub>       | 6  | 0,2039<br>(0,0007)      | 0,4045<br>(0,0007)      | 0,6589<br>(0,0022)             | 1,38<br>(0,14)                        |
| O <sub>2</sub>       | 6  | 0,1141<br>(0,0008)      | 0,5623<br>(0,0008)      | 0,7229<br>(0,0023)             | 1,60<br>(0,15)                        |
| O <sub>3</sub>       | 6  | 0,0269<br>(0,0007)      | 0,3485<br>(0,0007)      | 0,0619<br>(0,0020)             | 1,06<br>(0,14)                        |
| O <sub>4</sub>       | 6  | 0,3150<br>(0,0008)      | 0,3587<br>(0,0008)      | 0,0407<br>(0,0022)             | 1,53<br>(0,15)                        |
| C                    | ~1   | 0,0<br>-                | 0,0<br>-                | 0,6835<br>(0,010)              | 2,21<br>(0,90)                        |
| O <sub>5</sub>       | ~3   | 0,0584<br>(0,0016)      | 0,1200<br>(0,0016)      | 0,6857<br>(0,0042)             | 2,45<br>(0,43)                        |
| H <sub>2</sub> O     | ~2   | 0,6150<br>(0,0038)      | 0,3130<br>(0,0050)      | 0,6492<br>(0,014)              | 3,80<br>(1,6)                         |

Table 3.3 (contd.)

Interatomic Distances.

|  |   |
|--|---|
| <p>in <math>AlO_4</math> Tetrahedra.</p> <p><math>Al(1)-O(1) = 1,76_1 \overset{0}{A}</math><br/> <math>-O(2) = 1,72_4 \overset{0}{A}</math><br/> <math>-O(3') = 1,76_4 \overset{0}{A}</math><br/> <math>-O(4'') = 1,76_4 \overset{0}{A}</math></p>   | <p>in <math>SiO_4</math> Tetrahedra.</p> <p><math>Si(1)-O(1) = 1,60_0 \overset{0}{A}</math><br/> <math>-O(2) = 1,65_1 \overset{0}{A}</math><br/> <math>-O(3'') = 1,61_2 \overset{0}{A}</math><br/> <math>-O(4''') = 1,60_3 \overset{0}{A}</math></p>  |
| <p>mean <math>1,75_3 \overset{0}{A} \pm 0,01</math></p> <p><math>O(1)-O(2) = 2,78_9 \overset{0}{A}</math><br/> <math>-O(3') = 2,87_9 \overset{0}{A}</math><br/> <math>-O(4'') = 2,83_7 \overset{0}{A}</math><br/> <math>O(2)-O(3') = 2,92_5 \overset{0}{A}</math><br/> <math>-O(4'') = 2,92_1 \overset{0}{A}</math><br/> <math>O(3')-O(4'') = 2,79_0 \overset{0}{A}</math></p> | <p>mean <math>1,61_7 \overset{0}{A} \pm 0,01</math></p> <p><math>O(1')-O(2) = 2,60_9 \overset{0}{A}</math><br/> <math>-O(3'') = 2,59_3 \overset{0}{A}</math><br/> <math>-O(4''') = 2,62_8 \overset{0}{A}</math><br/> <math>O(2)-O(3'') = 2,67_2 \overset{0}{A}</math><br/> <math>-O(4''') = 2,70_8 \overset{0}{A}</math><br/> <math>O(3'')-O(4''') = 2,58_2 \overset{0}{A}</math></p> |
| <p>mean <math>2,85_7 \overset{0}{A} \pm 0,02</math></p>  | <p>mean <math>2,63_2 \overset{0}{A} \pm 0,02</math></p>   |

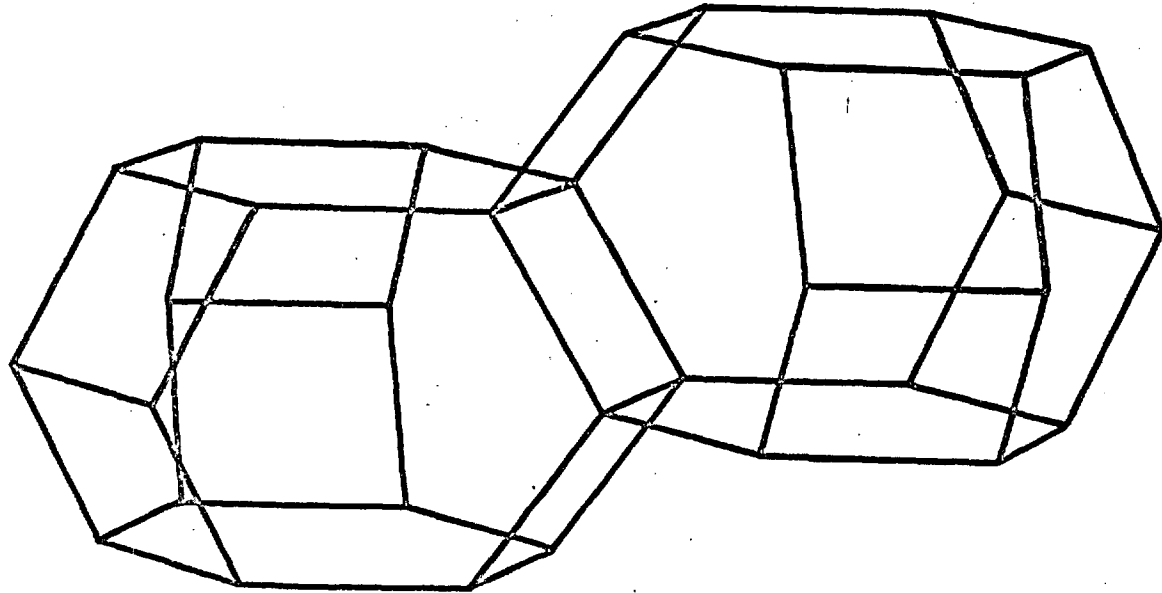


Figure 3.3 Showing method of linkage of "cancrinite cages" in cancrinite.

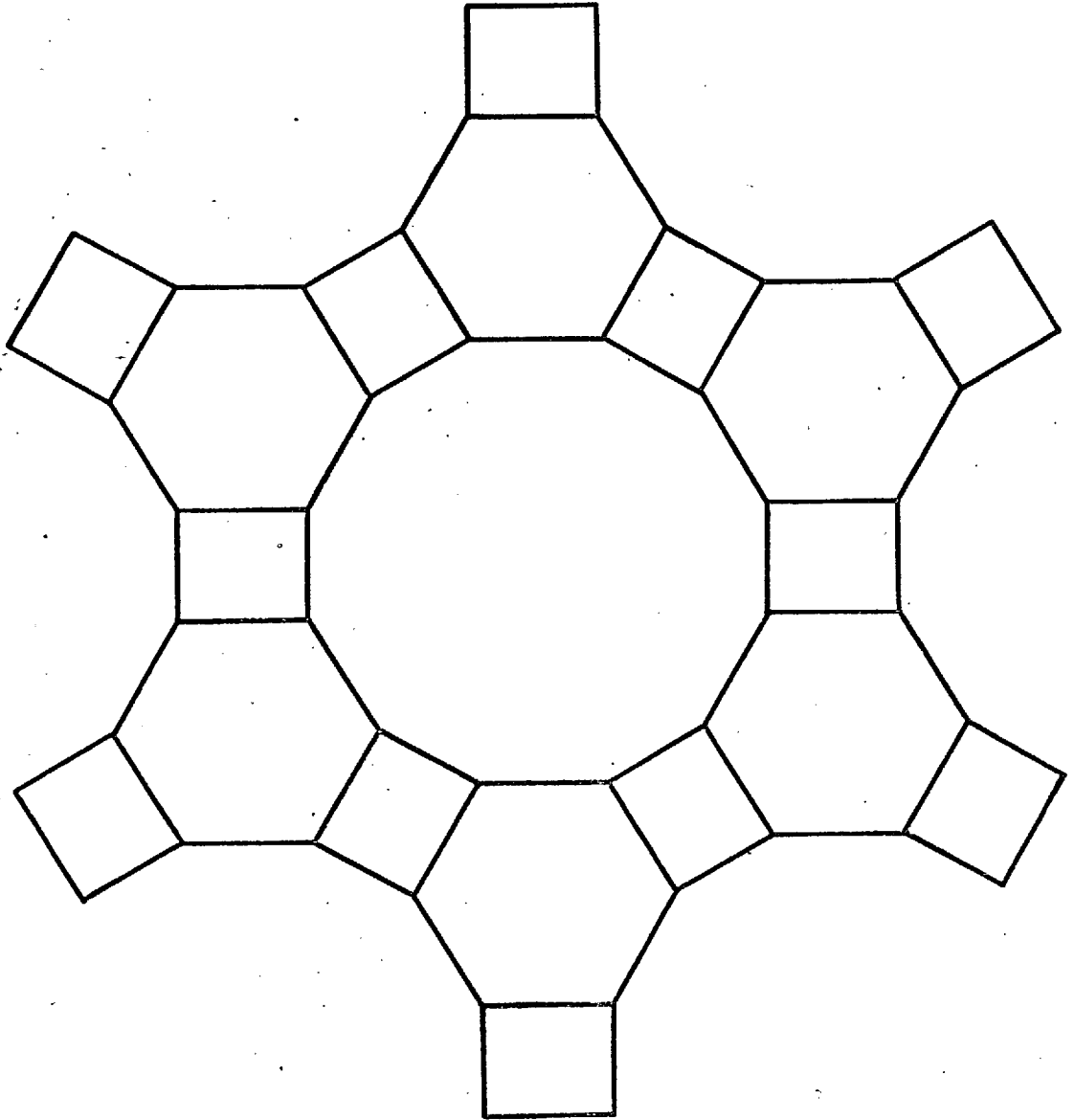


Figure 3.4 View down  $6_3$  axis of cancrinite structure showing main channel surrounded by cancrinite cages. (schematic).

Table 3.4d-spacings for cancrinite.
 $a = 12.75 \text{ \AA}, \quad c = 5.14 \text{ \AA}$  space group  $P6_3$ 
 $\text{cell volume} = 723.63 \text{ \AA}^3$ 

| H | K | L    | D      |
|---|---|------|--------|
| 1 | 0 | 0    | 11.041 |
| 1 | 1 | 0    | 6.375  |
| 2 | 0 | 0    | 5.520  |
| 0 | 0 | 1 2S | 5.140  |
| 1 | 0 | 1    | 4.659  |
| 2 | 1 | 0    | 4.173  |
| 1 | 1 | 1    | 4.001  |
| 2 | 0 | 1    | 3.762  |
| 3 | 0 | 0    | 3.680  |
| 2 | 1 | 1    | 3.239  |
| 2 | 2 | 0    | 3.187  |
| 3 | 1 | 0    | 3.062  |
| 3 | 0 | 1    | 2.992  |
| 4 | 0 | 0    | 2.760  |
| 2 | 2 | 1    | 2.708  |
| 3 | 1 | 1    | 2.630  |
| 0 | 0 | 2    | 2.570  |
| 3 | 2 | 0    | 2.533  |
| 1 | 0 | 2    | 2.503  |
| 4 | 0 | 1    | 2.431  |
| 4 | 1 | 0    | 2.409  |
| 1 | 1 | 2    | 2.383  |
| 2 | 0 | 2    | 2.329  |
| 3 | 2 | 1    | 2.272  |
| 5 | 0 | 0    | 2.208  |
| 2 | 1 | 2    | 2.188  |
| 4 | 1 | 1    | 2.181  |
| 3 | 3 | 0    | 2.125  |
| 3 | 0 | 2    | 2.107  |

### Stacking Faults and Hypothetical Frameworks.

Examination of the cancrinite structure and comparison with that of sodalite shows that a layer of sodalite framework may be built onto the cancrinite framework in the c direction, and the cancrinite framework afterwards continued without apparent ill effects. Such an intergrowth is known as a stacking fault, and in this case it closes the cancrinite channel with a six-ring. The existence of stacking faults has sometimes been<sup>n</sup> postulated to explain observed sorption capacities which are smaller than the theoretical values expected for an open known structure. Mordenite is a possible case, although differences of opinion exist on this particular example. <sup>(34,56)</sup> One may detect even occasional stacking faults by electron diffraction methods. When stacking faults are frequent and strictly maintained we may be justified in assuming that the resulting crystal has a unique structure and is therefore a new compound.

The cancrinite case will be taken as a hypothetical example. If every layer of cancrinite, along the c direction is followed by a layer of sodalite, we have a structure which is a sort of hybrid between the two, and can imagine various degrees of hybridization, between the pure end members. In fact a model can be readily built of the 1:1 structure, and its symmetry and approximate cell parameters can be estimated. One might be tempted to compute the d-spacings of such a hypothetical lattice and expect it to appear one day as a product of some laboratory experiment. This line of reasoning is perfectly valid, and it is indeed possible to compute expected powder patterns for various degrees of regular faulting, and to specify those reflections in the pure end members which should be strongly indicative of the presence of such faults. But to base one's argument on models alone can lead to serious errors. That a new structure can be built from model tetrahedra is no proof that such a structure could ever be synthesized or that it deserves a place amongst 'respectable' hypothetical structures. Apart from statistical considerations which are not in favour of the strict maintenance of complicated progressions, other factors such as the suitable and satisfactory extension of a postulated unit cell in three dimensions must be considered. During this extension, bond

distances and angles must remain within reasonable numerical limits, so that considerable strain does not result. For these reasons most "hypothetical structures" which are appearing in the literature at an increasing rate, must either be rejected or accepted with several provisos. Remembering the recent synthesis of the remarkable compound cubane,<sup>(57)</sup> in organic chemistry, and the elucidation of the complex structure of the zeolite paulingite,<sup>(58)</sup> we should perhaps mesh our net finely, and accept these hypothetical zeolites until they have been synthesized, or rejected on good structural principles.

One good way of deciding whether a hypothetical structure designated H is acceptable is as follows. We examine a model of H and try to elucidate its symmetry and the approximate parameters of its unit cell. By recourse to the literature, we see that in tetrahedral framework aluminosilicates  $Al-O_4$  and  $Si-O_4$  bonds have lengths which are relatively constant and these measures depend on the  $Si/Al$  ratio in a given structure.<sup>(59)</sup> The same applies to other distances and angles of the structure. By constructing various suitable functions of these known measures and of the trial atomic coordinates of our new structure H, we can, by the method of least squares, refine the trial coordinates to give proper distances and angles. A suitable refinement assures us that H, with the final computed trial coordinates, and chosen symmetry, represents a structure which at least does not violate the known laws of crystallography in this area. Non-refinement means that H cannot be properly built without breaking these rules - for example by allowing bond lengths to go outside the known range and to take up hitherto unobserved values. The computer program DLS<sup>(60)</sup> performs these calculations. If DLS can satisfactorily deal with our problem the refined trial coordinates and cell parameters can be used to compute powder lines and fourier maps which may reasonably be held to represent the new structure. Such structures may be called true hypothetical structures to distinguish them from the host of possible hypothetical structures which may be constructed with imagination and a few model tetrahedra in a matter of minutes.



## SECTION 4.

### Indexing of X-ray Powder Patterns.

Of fundamental importance in this area is the collection of accurate data, without which no meaningful conclusions can be reached. Graphical methods (61) for indexing the complex patterns characteristic of zeolites are inadequate and may lead to serious errors. To be preferred are the analytical methods described below, which have been tested on aluminosilicate patterns, and have been entirely successful when the data were sufficiently precise. They have only failed when the latter were uncertain or manifestly incorrect. The procedure assumes access to a fast digital computer suited to scientific calculation, for example an IBM7094, (28) with Fortran IV compilers and punched card equipment, and is conveniently divided into sections.

#### Theory. (61)

Let the reciprocal cell dimensions of a general cell in reciprocal space be  $a^*$ ,  $b^*$ ,  $c^*$ ,  $\alpha^*$ ,  $\beta^*$  and  $\gamma^*$ . If the miller indices of crystal planes are  $h$ ,  $k$  and  $l$ , it may be shown that the expression

$$Q_{hkl} = h^2 a^{*2} + k^2 b^{*2} + l^2 c^{*2} + 2 h k a^* b^* \cos \gamma^* + 2 k l b^* c^* \cos \alpha^* + 2 h l c^* a^* \cos \beta^* \quad (1)$$

relates these quantities to a measure  $Q_{hkl}$ , which is itself related to the spacings  $d_{hkl}$  of the crystal planes by the equation

$$Q_{hkl} = \frac{1}{d_{hkl}^2} \quad (2)$$

By virtue of Bragg's law we also have

$$Q_{hkl} = \frac{4 \sin^2 \theta_{hkl}}{\lambda^2} \quad (3)$$

where  $\lambda$  is the wavelength of x-rays. Since indexing corresponds to finding

quantities on the RHS of (1) which satisfy an observed list of  $Q_{hkl}$ 's, it is natural to transform experimental  $d_{hkl}$ 's or  $\theta_{hkl}$ 's to  $Q_{hkl}$ 's before further manipulation.

#### Collection of Accurate Data.

The powder pattern is most conveniently recorded on a strip of photographic film, along with the separate pattern of a recommended internal standard, <sup>(51)</sup> such as that of lead nitrate. This is conveniently done with the usual Guinier-deWolff camera, an instrument capable of recording four separate patterns on the same piece of film. The preparation of samples is very important, and is well known and documented. <sup>(61)</sup> The processed film should exhibit sharp black lines on a clear background. Assuming that the equipment is excellent and the camera is in alignment, fuzzy, broad and indistinct diffraction lines are normally due to impure, badly crystallized compounds and not to small particle size as is often claimed, especially in the patent literature. By means of an internal standard, the multiple film technique may be used to overexpose strong lines so as to better observe weak ones.

The positions of the arcs relative to a zero mark are then measured in mm for sample and standard. This is preferably done with a magnifying vernier instrument, several kinds of which are available commercially. The zero mark and each arc should be measured as accurately as possible several times, and the results averaged. An experimental error is also recorded for each observation. For the Guinier-deWolff camera, if  $\tau_0$  represents the position of the zero mark, and  $\tau_1$  the position of an arc, then  $(\tau_1 - \tau_0)$  in mm corresponds to the position of the arc in degrees of  $4\theta$ . Using the wavelength of x-rays,  $d$ -values can be computed.

#### Example.

For synthetic zeolite ZK-5, <sup>(97)</sup> the first arc (at low angles) is 13.369 mm from the zero mark, hence  $4\theta = 13.369$ , and since the radiation was copper  $K\alpha$  of  $\lambda = 1.5418 \text{ \AA}$  we derive  $d_{(110)} = 13.223 \text{ \AA}$ .

### Correction of Data.

Assuming the collection of accurate data for sample and standard, as outlined above, for a phase which by all tests appears to be single, distinct and well-crystallized, the data reduction can be commenced. The method now divides into two, according as the compound is known or unknown.

#### Case when Compound is Known.

It is commonly required to index a compound whose structural features are known. For example, in the present work it was required to index many specimens of sodalite and cancrinite, and to determine accurate cell parameters. In this case approximate cell parameters are used to compute  $d$ -values, indices and  $Q$ -values according to eqns. (1) and (3). This is done using the program APOL.<sup>(50)</sup> A list of these measures similar to those in Table 3.2 is produced, and the calculated list of  $4\theta$  is compared with the experimental list, and trial indices are assigned, taking into account the fact that, as yet, the experimental list is uncorrected for film shrinkage, etc.

The computed measure ( $4\theta$  or other variable) for the internal standard is next generated by APOL using precision cell parameter data from the literature.<sup>(51)</sup> The observed lists of  $4\theta$  (or other variable) for the sample and standard, plus the calculated list for the standard, and the trial indices and cell parameters for the sample are then given as data on punched cards to the program LCLSQ.<sup>(62,63)</sup> For accurate work, which is the only kind acceptable at this stage, the experimental errors in observed variables for sample and standard must also be supplied. This program first approximates to a correction function by means of a least squares polynomial of order up to 10, by computing the differences between the observed and calculated standard values. To ensure that this correction function behaves correctly over the entire range of observed variable, it is plotted out on the IBM 1460 line printer, as part of the result.

The observed variable for the sample is then corrected against the standard data by means of the polynomial function. The result is a corrected list of  $4\theta$  (or other variable) which represents the most plausible (least-squares) values of the observations, taking into account experimental errors. It should be

stated, that for the Guinier cameras in use in this laboratory, d-values far from  $\sim 3 \text{ \AA}$  are subject to appreciable corrections, resulting from film shrinkage and errors of measurement.

LCLSQ then performs a full-matrix least-squares refinement of the trial cell parameters, using the corrected list of observations, resulting in a list of refined d-values and accurate cell parameters.

While  $4\theta$  was the variable discussed, both APOL and LCLSQ have been designed to work in terms of other variables such as d,  $2\theta$  and Q. For example, if using automatic diffractometer chart output,  $2\theta$  would normally be a more convenient choice. The programs mentioned will deal with any crystal symmetry

#### Case When Compound is Unknown.

In this case the indices are as yet unknown, so the same procedure is followed as above, omitting the preliminary assignment. A shortened version of LCLSQ is used to produce a corrected list of experimental Q-values. Tests are first made on this list to determine whether the crystals are isometric, tetragonal or hexagonal. For the isometric system eqn. (1) becomes

$$\begin{aligned} Q_{hkl} &= (h^2 + k^2 + l^2) a^*{}^2 \\ &= N_c a^*{}^2 \end{aligned} \quad (4)$$

where  $N_c$  can be represented by the sum of three squares, eg.  $Q_{100} = a^*{}^2$ ,  $Q_{110} = 2a^*{}^2$ . In direct lattice terms this equation becomes

$$d_{hkl} \sqrt{[h^2 + k^2 + l^2]} = a_0 \quad (5)$$

Indexing on the cubic system corresponds to finding solutions of (4) or (5), but with certain conditions. Clearly, if the edge of the unit cube  $a_0$  is taken sufficiently large and many lines are regarded as being "absent" from an observed list, then any set of lines may be "indexed" on the cubic system, since the solutions of (5) read like a table of square roots. Thus errors may,

and do, arise.

As an example of these difficulties, consider the d-spacings given in Table 4.1. These data have been indexed on a cubic cell of edge  $15.85 \text{ \AA}$ . It should be realized, however, that good arithmetic agreement such as that shown in the table is a necessary but insufficient condition for satisfactory indexing. Symmetry conditions must also be considered. The method of indexing in the table precludes a body-centred lattice ( $h + k + l = 2n$ ), and a face-centred lattice ( $h, k, l$  unmixed). The crystals must therefore be primitive, with all reflections present. That being so, 84 reflections should be observed over the range of d-values quoted. Even when generous allowance is made for weak and possibly unobserved reflections, 70 lines are absent without reason. The conclusion is that the crystals are not cubic.

Table 4.1

| $d_{(hkl)}^0 \text{ \AA}$ | hkl | $h^2 + k^2 + l^2$ | a.A <sup>0</sup><br>calculated |
|---------------------------|-----|-------------------|--------------------------------|
| 5.60                      | 220 | 8                 | 15.85                          |
| 4.81                      | 311 | 11                | 15.86                          |
| 4.39                      | 320 | 13                | 15.84                          |
| 4.23                      | 321 | 14                | (15.81)                        |
| 3.38                      | 332 | 22                | 15.85                          |
| 3.17                      | 500 | 25                | 15.85                          |
| 2.80                      | 440 | 32                | 15.84                          |
| 2.65                      | 600 | 36                | (15.89)                        |
| 2.52                      | 620 | 40                | 15.87                          |
| 2.24                      | 710 | 50                | 15.84                          |
| 2.16                      | 721 | 54                | 15.85                          |
| 1.99                      | 800 | 64                | 15.85                          |
| 1.68                      | 944 | 97                | 15.85                          |
| 1.58                      | 755 | 99                | 15.85                          |
|                           |     | mean              | 15.85                          |

This example serves to point out important considerations, such as systematic absences, and the necessity of accurate data in indexing procedures.

If the attempt to index on the cubic system has failed, tests for tetragonal and hexagonal symmetry are made. Eqn. (1) reduces to simple forms for these systems in reciprocal space, and a list of all possible differences between Q-values in the observed list can be used to advantage, following Azaroff and Buerger.<sup>(61)</sup> The methods of these authors have been computerized and are currently in use in this laboratory.<sup>(64)</sup> A combination of the above methods may also be used to index orthorhombic crystals.

If, as often happens, these methods fail it is either because the sample data are incomplete or inaccurate, or the crystals have a lower symmetry. At this point a decision must be taken, whether one has sufficient confidence in the quality of the sample and reflection data, to proceed to the Ito<sup>(65,61)</sup> method for indexing crystals of monoclinic or triclinic symmetry. These calculations are lengthy and complex, and may consume much time for little or no return. Research in the United States<sup>(66,67,68)</sup> has shown that in a few years mathematical and computer techniques will be available to deal with this problem, but at present it is uncertain whether the complex powder data characteristic of zeolites will be handled effectively, even by these methods.

A list of X-ray d-spacings is not a unique identification.

While dealing with x-ray powder methods, another important point needs to be raised. In this and allied work, a great deal of confidence must be placed in the x-ray powder diffraction pattern of a crystalline species as a means of identification. But while the positions of diffraction lines on the film determine the size of the unit cell (this being the smallest geometrical unit which when produced in the three dimensions, produces the entire crystal), and the distances between the various atomic planes in this cell, the intensities of these lines determine the arrangement of scattering matter within the cell.

The diffracted intensity  $I_{hkl}$  is related to a quantity  $F_{hkl}$  by the relation

$$I_{hkl} = I_0 \frac{cm}{\mu} F_{hkl}^2 V L_p \quad (6)$$

$$\text{where } F_{hkl} = \sum_j f_j e^{\frac{2\pi i (kx_j + hy_j + lz_j)}{d}} \quad (7)$$

the summation being over all atoms in the cell.

$F_{hkl}$  is called the structure factor, and it depends on the scattering power  $f$  of atoms in the unit cell, and their positional coordinates  $x, y, z$ . In (6)  $I_0$  is the direct x-ray beam intensity,  $c$  is a constant which has the same value for all reflections recorded on one photograph,  $m$  is the multiplicity of reflecting planes - the number of planes in a crystal which are symmetrically equivalent -  $\mu$  is a linear absorption coefficient,  $V$  is the total volume of the diffracting crystals.  $L_p$  is the Lorentz-polarization factor which is  $\frac{1 + \cos^2 2\theta}{\sin^2 \theta \cos \theta}$ .

Specialized treatments of these matters are found in standard works, (61, 98) but for our purposes we can see from (6) and (7) that a list of d-spacings without accurately measured intensities, does not serve uniquely to identify a crystalline powder. For it is perfectly possible to have two different structures which give the same d-spacings; or we may have two or more aluminosilicate crystals with the same framework structure, but with different cation or inclusion structures. Two striking examples will be offered. The intensities of powder lines in the patterns of Na-X and La-X are very different, while the positions of the lines are nearly identical. This is mainly due to the very different scattering powers  $f$  (or form factors) of sodium and lanthanum, which affect the  $I_{hkl}$  as shown in (6) and (7). The sodalite inclusion compounds to be discussed in this work afford a second example. The positions of the lines are nearly identical, allowing for small changes in cell size, but the intensities  $I_{hkl}$  of lines are very different for different inclusions, because the  $F_{hkl}$  are different. The intensities bespeak the unique arrangement of the included anions and cations, and in any particular case may be used to determine this arrangement.

For these reasons, literature claims to the preparation of new zeolites based on a few inaccurate d-spacings ("main spacings", so called) and intensities which are visually estimated, or indeed not quoted at all, are highly suspect. Some authors and inventors have already realized this, and in a field of extremely vigorous and often unscrupulous competition have become increasingly sophisticated in their patent claims. In a recent claim <sup>(96)</sup> a synthetic faujasite molecular sieve catalyst is said to be characterized inter alia by an electron density of 1-2 per  $\text{Å}^3$  at a particular framework position! While such a claim could be strongly criticized it at least shows that future progress will be based on crystal structure analysis to an increasing degree.

#### Determination of Aluminosilicate Structures by Powder Methods.

Since nearly all synthetic zeolites and allied compounds of scientific and industrial interest are available as microcrystalline powders, structural work in this area must be based on intensity data collected by powder methods. A reasonably accurate knowledge of crystal parameters is necessary to most other studies in ion-exchange, sorption, salt entrainment and catalysis. This powder crystallography of zeolitic materials has been neglected because it is full of difficulties, and even if they are overcome, the resulting information is often uncertain.

Detailed procedures will not be discussed here. They may be found for example in the work of Villiger, <sup>(71)</sup> who has shown that careful methods and patience can yield worthwhile results. Some brief comments and methods are given below.

#### Problems peculiar to the powder method.

The great disadvantage of the powder method lies in the limited amount of reflection data which can be collected, and their accuracy. A typical aluminosilicate pattern (photograph or diffractometer trace) may yield only 80 measurable lines or observations. This leads to serious errors when fourier series are terminated, and produces information which is correspondingly inaccurate and misleading. For example it commonly leads to the



appearance of "atoms" in fourier maps which are not atoms at all, but noise. Careful measurement of intensities is also difficult. Particular attention must be paid to the collection of data.

Problems peculiar to the determination of structures of porous crystals.

The non-framework material in porous crystals, water, cations and salt inclusions is normally disordered and non-stoichiometric, and is particularly subject to thermal motion. Variable cation and inclusion locations are also common. These phenomena make it very difficult, if not impossible, to determine just those structural parameters of greatest interest. Even when a successful structural refinement has been achieved it is often impossible to say with certainty exactly what is the inclusion and cation structure. To some extent these difficulties are lessened by collecting data at high temperatures on outgassed structures, but in practical cases one does not have such idealized conditions, and this method is of more use in framework determination. In any case, such things as cation locations may vary considerably with temperature

Villiger<sup>(71)</sup> has discussed the different problems encountered in inclusion determination as the sizes of intracrystalline pores are increased relative to the sizes of the guest molecules or ions. It appears from this work that by judicious choice of inclusion types, additional information may be found, but again, in practical cases, such a choice may not be available.

Determination of an unknown aluminosilicate framework structure.

Meier<sup>(72,73)</sup> and others have discussed the known building units in zeolites and allied compounds, and have catalogued all natural and synthetic zeolites into various structurally related groups. Smith and Bailey<sup>(59)</sup> and others have noted and catalogued the relatively constant Si-O and Al-O bond lengths in (Si, Al)-O<sub>4</sub> tetrahedra in these structures. Barrer<sup>(30)</sup> and others have catalogued zeolitic crystals on the basis of their pore sizes as determined by sorption experiments. Additional information relating to ion-exchange and ion-sieve phenomena, and salt inclusion during synthesis is available for many crystalline powdered zeolites whose structures are unknown. All this information is available to help those skilled in the art to propose frameworks for

unknown compounds which are compatible with the chemical composition, density and x-ray data. In recent years a number of structures have been determined by these methods.

An important advance has been made by Meier and Villiger<sup>(60)</sup>, who showed that in tetrahedral framework structures of this kind, the number of crystallographically independent interatomic distances (which are reasonably well known in advance) exceeds the number of coordinates to be determined. Therefore, given an initial trial solution, for example read from a model, it is possible to compute coordinates by the method of least squares adjustment, i.e. by "D-refinement", where D, the interatomic distance is a function only of the atomic coordinates involved, and the unit cell constants. These authors have developed a computer programme, DLS, which performs the calculations, and have noted that whenever D-refinement has not proceeded, either the trial structure or the assumed symmetry has been incorrect. An example of the use of this method is found in the determination of the structure of synthetic zeolite L.<sup>(53)</sup> Here, the inadequacy of an earlier proposal for the L structure<sup>(27)</sup> was clearly shown by this method.

#### Determination of the inclusion structure by powder methods.

It is often necessary to locate the positions of cations and included anions and molecules within an aluminosilicate lattice whose structural features are known in advance, having been determined by methods already outlined, or well established in the literature. The difficulties associated with powder data make this task almost as tedious as a full structure determination, and in practice, a full determination and refinement are necessary conditions if meaningful results are required. Partial refinement may give helpful qualitative information, but experience has shown that it is very qualitative indeed.

The following is an extremely brief account of the general approach. The problem is to find an arrangement of atoms which will produce the observed set of intensities of powder lines,  $I_{hkl}$ , subject to geometric cell factors, density, chemical composition and other considerations. If we rewrite eqn. (6) as

$$I_{hkl} = \left\{ I_0 \frac{c}{\mu} V \right\} L_{p.m} F_{hkl}^2 \quad (8)$$

the term in braces is called the scale factor, and under certain experimental conditions may be regarded as an unknown constant which has to be determined. The Lorentz-polarization factor  $L_p$  and multiplicity  $m$  are computed in multiplication, and trial structure factors  $F_{hkl}$  are formed.  $F_{hkl}$  also contains in addition to dependencies noted in eqn. (7) terms which allow for the temperature motion of atoms, and the occupancy factor, which determines the amount of scattering material (electrons) at a given location. In a word, the coordinates, temperature factors and occupancy of atoms are varied so that the intensities calculated according to eqn. (8) are brought into substantial agreement with those observed. More details may be found elsewhere. <sup>(92)</sup>

Determination of <sup>a</sup>Anion positions in cancrinite with imbibed  $Na_2CrO_4$  and  $Na_2MoO_4$ .

Since this work was undertaken only to attempt to help explain effects observed in the synthesis experiments, it will be recorded with extreme brevity. Two well-crystallized specimens were chosen, of chromate and molybdate cancrinite. The unit cells were determined, from the indexed powder patterns, according to the methods outlined, to give

|         |             |            |             |                                  |
|---------|-------------|------------|-------------|----------------------------------|
| (CCANC) | $Na_2CrO_4$ | cancrinite | $a = 12.72$ | $c = 5.19 \overset{0}{\text{Å}}$ |
| (MCANC) | $Na_2MoO_4$ | cancrinite | $a = 12.75$ | $c = 5.19 \overset{0}{\text{Å}}$ |

Intensities were gathered, using a diffractometer with chart output, and were measured by counting squares of about 80 powder lines ( $0 \leq 2\theta \leq 80^\circ$ ). The  $L_p$  and multiplicity were computed and the data punched onto cards. The symmetry was taken in both cases as  $P6_3$ , following Jarchow, <sup>(52)</sup> although the albeit weak appearance of  $00l$  lines ( $l$  odd) demonstrated that the inclusion had already slightly destroyed elements of symmetry. Initial framework coordinates were also taken from Jarchow, and scattering factors from standard sources <sup>(51)</sup> and ref. 102. Calculations were made using Fortran IV programmes which are referred to by their names in Roman capitals in the text. Initial

structure factor calculations\* were made using PFOU,<sup>(75)</sup> a modification of ORFLS.<sup>(74)</sup> Initial R values based on intensities, defined by

$$R(I) = \frac{\sum | I_{\text{obs}} - I_{\text{calc}} |}{\sum I_{\text{obs}}} \quad (9)$$

were around 0.9 for both structures, attesting to the great influence the inclusions have upon the intensities of powder lines. Magnetic tapes written by PFOU were used to drive the fourier synthesis programme of the X-RAY SYSTEM.<sup>(76)</sup> The first fourier sections showed outstandingly large peaks in the cancrinite cages of both structures, as well as a complicated mixture of peaks in and near the wide channel. These cage peaks which were attributed to  $\text{CrO}_4^{2-}$  and  $\text{MoO}_4^{2-}$  persisted throughout the work, and it was interesting to note that they always indicated the presence of more included anions on this location, rather than in the channel. Attempts were next made to assign the various peaks observed, to atoms. The following procedure was used. Inclusion atoms were put in with large temperature factors ( $6 \text{ \AA}^2$ ), and occupancies as indicated by the fourier maps. Numerous combinations were used and structure factors were computed for each, using PFOU. After each such calculation, the interatomic distances for all atoms in the asymmetric unit

---

\* Footnotes. The author acknowledges a debt to his colleague Mr. Hans Villiger, who expended considerable effort during 1967 in rewriting some of the computer programmes used to enable powder data to be handled, and also compiled and debugged them. This essential work, which is not usually counted as research output, is a trial understood only by those who have had to deal with the exacting requirements of data processing and computing, mixed with human fallibility, and a variety of computers with different compilers and other systems software. During this work it became necessary to rewrite several programmes in the updated Fortran IV language and to make major reconstructions of routine computing methods for powder work. This work resulted in a system of x-ray powder crystallography for the IBM 7094, which contains all programmes necessary to the complete structural determination of aluminosilicate crystals from powder data, and operates from a programme master magnetic tape. This was done with Mr. H. Villiger, who has also described the system in more detail.<sup>(71)</sup> The programmes are designated by names in Roman capitals in the text

were generated using a programme designated FSHIFT. By trial and error, the R factors were lowered, and such progress was allowed, provided the framework-inclusion interatomic distances did not become too short. After a number of such structure factor calculations, the best one was chosen to make a new fourier map. The map was evaluated by carefully examining the forms of peaks in observed and calculated maps, in the three crystallographic directions, and estimating backshifts in coordinates required to bring the calculated peaks into coincidence with the observed peaks. These shifts were then added in multiples (eg. 1 x shift, 2 x shift, etc.) to the fourier coordinates by the programme FSHIFT, which then computed interatomic distances and punched onto cards several sets of trial coordinates for further structure factor runs. Provided the distances were acceptable, each of these sets of shifted coordinates were used to compute new R values, after occupancies had been varied in accord with the fourier maps. New atoms, as indicated by the fourier maps, were also added. The most reasonable set of data was then used to make a new fourier synthesis, as before, and the complete cycle repeated many times. When the  $R(F)$  (eqn. 10) reaches 0.2-0.3, least squares refinement of parameter is usually attempted, to complete the structure determination.

### Results.

By application of the above methods the  $R(F)$  values (eqn. 10) of both structures were brought to  $\sim 0.35$ , but no further lowering was found possible. At this point framework interatomic distances were reasonable, the framework atoms having moved slightly from Jarchow's coordinates. This framework "breathing" during different inclusion processes is normal. The framework - non-framework distances were also reasonable, and fourier peaks tentatively assigned to sodium ions and chromium and molybdenum atoms were chemically sensible. Some difficulty was experienced in interpreting weak peaks near the heavy atoms. These were visible and were put in as oxygen atoms so as to form tetrahedral  $CrO_4^{2-}$  and  $MoO_4^{2-}$  ions, but there seemed to be a severe disturbance in the fourier maps in the vicinity of chromium and molybdenum atoms, and this point has not yet been resolved.

Experience with the powder method has shown<sup>(53,71)</sup> that unless  $R(F)$  values

around 0.2 are reached,  $R(F)$  being defined as

$$R(F) = \frac{\sum || F_{obs} | - | sF_{calc} ||}{\sum F_{obs}} \quad (10)$$

where  $F$  are the structure amplitudes and  $s$  is the scale factor (eqn. 8), then least-squares refinement cannot be expected to work. However, since no further lowering of  $R(F)$  from around 0.3 could be brought about by fourier refinement, least-squares refinement was attempted. It resulted in improbable framework distances. The work was temporarily stopped here because it was rapidly becoming a full-time problem in crystallography. It is hoped to continue it at a later date. The final state of the structure determination, despite its incompleteness, allows the reasonably certain conclusion that the samples contained imbibed salt both in the channels and cancrinite cages. A similar conclusion, based on a complete refinement of a  $\text{NaNO}_3$  rich cancrinite structure, <sup>(71)</sup> was reached.

SECTION 5.The Kaolinite Raw Material.

The clay mineral kaolinite was used as a source of silicon and aluminium in the alkali-aluminosilicate syntheses to be described. Two batches were used, the analyses of which are given in Table 5.1.

Table 5.1Chemical Composition of Kaolinite Starting Materials.

|                                | <u>Batch A.</u> | <u>Batch B.</u> |
|--------------------------------|-----------------|-----------------|
| SiO <sub>2</sub>               | 45.10%          |                 |
| Al <sub>2</sub> O <sub>3</sub> | 38.57           |                 |
| Fe <sub>2</sub> O <sub>3</sub> | 0.46            |                 |
| TiO <sub>2</sub>               | 1.75            |                 |
| CaO                            | 0.10            |                 |
| MgO                            | 0.03            |                 |
| K <sub>2</sub> O               | 0.08            | 0.95%           |
| Na <sub>2</sub> O              | 0.18            | 0.26%           |
| Ignition Loss.                 | 13.67           |                 |
|                                | <hr/>           |                 |
|                                | 99.94%          |                 |
|                                | <hr/>           |                 |

For batch A, neglecting the TiO<sub>2</sub>, and oxides present to an extent less than 1%, and assuming the loss on ignition to be due to constitutional water, these figures indicate a composition Al<sub>2</sub>O<sub>3</sub>.2SiO<sub>2</sub>.2H<sub>2</sub>O. Differential thermal analyses (D.T.A.) and thermogravimetric analyses (Th.G.A.) which show a single exotherm at 600 °C and a corresponding loss of around 13.5 wt.% support this formula. Since these materials were to be used in all subsequent work, it was necessary to know how to identify unreacted kaolinite in a

mixture of products, and to know the precise nature of the main impurities present, since these could have an effect upon phenomena observed.

The first problem was overcome by making a series of Guinier photographs of the kaolinite, some of which were overexposed. In the few cases when the reactant kaolinite was mixed with products in substantial amounts, a simple visual comparison of photographs was sufficient to identify it. In more subtle circumstances, optical and electron microscopic studies were made. It was often possible to see the flaky platelets of kaolinite, which were sometimes even hexagonal in outline, by these means. Occasionally an identifying electron diffraction pattern could also be obtained. The second problem, that of impurities, was handled as follows. Samples of both batches were heated to 80 °C in aqueous syrupy sodium hydroxide for 7 days in polypropylene bottles. The mixtures were filtered hot on sintered glass, and the very small amounts of solids remaining on the filters were collected and examined by x-rays. Most, if not all of the kaolinite had by these means been put into solution.

The powder patterns of the residues were identified as those of hydrous titanium dioxide (from sample A) and muscovite (from sample B). Thus we have at once, an explanation of the high potassium content of sample B and of two hitherto unidentifiable reflections in the kaolinite batch B powder pattern at 10.017 and 3.329 Å, which must be the 001 and 003 mica lines. We are now in a position to identify the starting material and its impurities or alkaline degradation products, in subsequent preparations.

The calculated d-spacings for low angle reflections of kaolinite, anatase and muscovite are given for reference in Tables 5.2, 5.3 and 5.4.

#### Standard Reaction Compositions.

For the synthesis experiments a "standard reaction composition" was used so that correlations between different preparations could be easily made. The standard composition was as follows:



|                  |            |
|------------------|------------|
| kaolinite        | 2.0 g.     |
| NaOH             | 32 g.      |
| H <sub>2</sub> O | 200 ml.    |
| salt             | ~0.1 mole. |

These components were added to screw-top polypropylene bottles of capacity 250 mls. Severe agitation was maintained during the heating at 80° by means of an electrically rotated plate fixed inside an air oven. In the experiments used to determine the salt inclusion isotherms, the products after reaction were as far as possible subjected to identical washing procedures. The general experimental methods used have already been described.

Sodalites and cancrinites obtained under these conditions were excellent specimens. The reactions were clean, and proceeded in high yield. The crystalline powders were readily filtered and washed and were highly suitable for study by the usual methods of zeolite chemistry. Descriptions of some of these phases will now be given.

Table 5.2d-spacings for kaolinite.

$a = 5.15$ ,  $b = 8.95$ ,  $c = 7.37 \text{ \AA}$ ,  $\alpha = 91.8^\circ$ ,  $\beta = 104.8^\circ$ ,  $\gamma = 90.0^\circ$   
 cell volume  $328.26 \text{ \AA}^3$ .

| H  | K  | L  | D     |
|----|----|----|-------|
| 0  | 1  | 0  | 8.945 |
| 0  | 0  | 1  | 7.121 |
| 0  | -1 | 1  | 5.662 |
| 0  | 1  | 1  | 5.485 |
| 1  | 0  | 0  | 4.979 |
| -1 | 0  | 1  | 4.680 |
| 0  | 2  | 0  | 4.472 |
| -1 | 1  | 0  | 4.365 |
| 1  | 1  | 0  | 4.335 |
| 1  | 1  | -1 | 4.170 |
| -1 | 1  | 1  | 4.124 |
| 0  | -2 | 1  | 3.844 |
| 0  | 2  | 1  | 3.733 |
| 1  | 0  | 1  | 3.664 |
| 0  | 0  | 2  | 3.560 |
| 1  | -1 | 1  | 3.418 |
| 1  | 1  | 1  | 3.364 |
| 0  | -1 | 2  | 3.345 |
| -1 | 2  | 0  | 3.341 |
| -1 | 0  | 2  | 3.326 |
| 1  | 2  | 0  | 3.313 |
| 0  | 1  | 2  | 3.272 |
| 1  | 2  | 1  | 3.255 |
| -1 | 2  | 1  | 3.212 |
| 1  | 1  | -2 | 3.143 |
| -1 | 1  | 2  | 3.092 |

Table 5.3

d-spacings for muscovite.

$a = 5.19$ ,  $b = 9.04$ ,  $c = 20.08 \text{ \AA}$ ,  $\alpha = \gamma = 90.0^\circ$ ,  $\beta = 95.5^\circ$ .  
 space group C2C, cell volume  $937.77 \text{ \AA}^3$ .

| H  | K | L |    | D      |
|----|---|---|----|--------|
| 0  | 0 | 1 | CG | 19.987 |
| 0  | 0 | 2 |    | 9.993  |
| 0  | 1 | 0 | CL | 9.040  |
| 0  | 1 | 1 | CL | 8.236  |
| 0  | 1 | 2 | CL | 6.704  |
| 0  | 0 | 3 | CG | 6.662  |
| 0  | 1 | 3 | CL | 5.363  |
| 1  | 0 | 0 | CL | 5.166  |
| -1 | 0 | 1 | CL | 5.122  |
| 0  | 0 | 4 |    | 4.996  |
| 1  | 0 | 1 | CL | 4.889  |
| -1 | 0 | 2 | CL | 4.779  |
| 0  | 2 | 0 |    | 4.520  |
| 1  | 1 | 0 |    | 4.485  |
| -1 | 1 | 1 |    | 4.456  |
| 1  | 0 | 2 | CL | 4.419  |
| 0  | 2 | 1 |    | 4.408  |
| 0  | 1 | 4 | CL | 4.373  |
| 1  | 1 | 1 |    | 4.300  |
| -1 | 0 | 3 | CL | 4.286  |
| -1 | 1 | 2 |    | 4.225  |
| 0  | 2 | 2 |    | 4.118  |
| 0  | 0 | 5 | CG | 3.997  |
| 1  | 1 | 2 |    | 3.970  |
| 1  | 0 | 3 | CL | 3.905  |

Table 5.4

d-spacings for anatase (hydrated  $\text{TiO}_2$ )

$a = 3.78$ ,  $c = 9.57 \text{ \AA}$ , space group I  $4/a$

cell volume  $135.88 \text{ \AA}^3$ .

| H | K | L |    | D     |
|---|---|---|----|-------|
| 0 | 0 | 1 | IL | 9.510 |
| 0 | 0 | 2 |    | 4.755 |
| 1 | 0 | 0 | IL | 3.780 |
| 1 | 0 | 1 |    | 3.512 |
| 0 | 0 | 3 | IL | 3.170 |
| 1 | 0 | 2 | IL | 2.959 |
| 1 | 1 | 0 | AG | 2.672 |
| 1 | 1 | 1 | IL | 2.573 |
| 1 | 0 | 3 |    | 2.428 |
| 0 | 0 | 4 |    | 2.377 |
| 1 | 1 | 2 |    | 2.330 |
| 1 | 1 | 3 | IL | 2.043 |
| 1 | 0 | 4 | IL | 2.010 |
| 0 | 0 | 5 | IL | 1.902 |
| 2 | 0 | 0 |    | 1.890 |
| 2 | 0 | 1 | IL | 1.853 |
| 1 | 1 | 4 |    | 1.776 |
| 2 | 0 | 2 |    | 1.756 |
| 1 | 0 | 5 |    | 1.699 |
| 2 | 1 | 0 | IL | 1.690 |
| 2 | 1 | 1 |    | 1.664 |
| 2 | 0 | 3 | IL | 1.623 |
| 2 | 1 | 2 | IL | 1.592 |
| 0 | 0 | 6 |    | 1.585 |

Reaction of kaolinite with aqueous sodium hydroxide.

Solutions containing excess of sodium hydroxide were chosen so as to produce sodalites containing imbibed NaOH + H<sub>2</sub>O ("basic" sodalites<sup>(54)</sup>). It is noted that Zhdanov's zeolite Zh<sup>(77)</sup> is also a basic sodalite. These compounds are represented by the general formula 6(NaAlSiO<sub>4</sub>), xH<sub>2</sub>O, yNaOH. The values of x and y were altered by varying the concentration of NaOH in reaction mixtures of otherwise constant composition (Fig. 5.1). The yield of crystals from a fixed weight of kaolinite diminished as the concentration of alkali increased, so that eventually in very strong solutions (>30M) all the aluminium and silicon remained in solution. The yield of basic sodalite and the solubility of the crystals at 80° are shown in Fig. 5.1 in relation to the concentration of sodium hydroxide.

The cubic unit cell edge of the basic sodalites increased with increased content of NaOH. Maximum loadings of alkali leading to virtually water-free preparations, are best obtained at higher temperatures. Such a preparation (made at 160°) was treated with purified dry chlorine at 150° and a substantial decrease in unit-cell edge was observed, together with the formation of extracrystalline NaCl. Thus intracrystalline sodium hydroxide migrated out of the crystals and reacted with the chlorine. Similar changes in unit-cell are observed when basic sodalites are continuously extracted in a soxhlet apparatus.<sup>(55)</sup> These "washed out" sodalites behave like condensed zeolites, and have some interesting properties. Some of these will be discussed later in this section.

When kaolinite was autoclaved with 300% excess\* aqueous sodium hydroxide at 390-420°, basic cancrinite,<sup>(54)</sup> 6(NaAlSiO<sub>4</sub>), xH<sub>2</sub>O, yNaOH, was formed. However, at low temperatures it appears to be impossible to grow cancrinites directly from raw kaolinite in the sodium system, except in presence of certain salts (next paragraph). Cancrinite may however be grown from metakaolinite in the Li/Na system at 80°C.<sup>(78)</sup>

\* i.e. above the framework requirement for Na<sup>+</sup>.

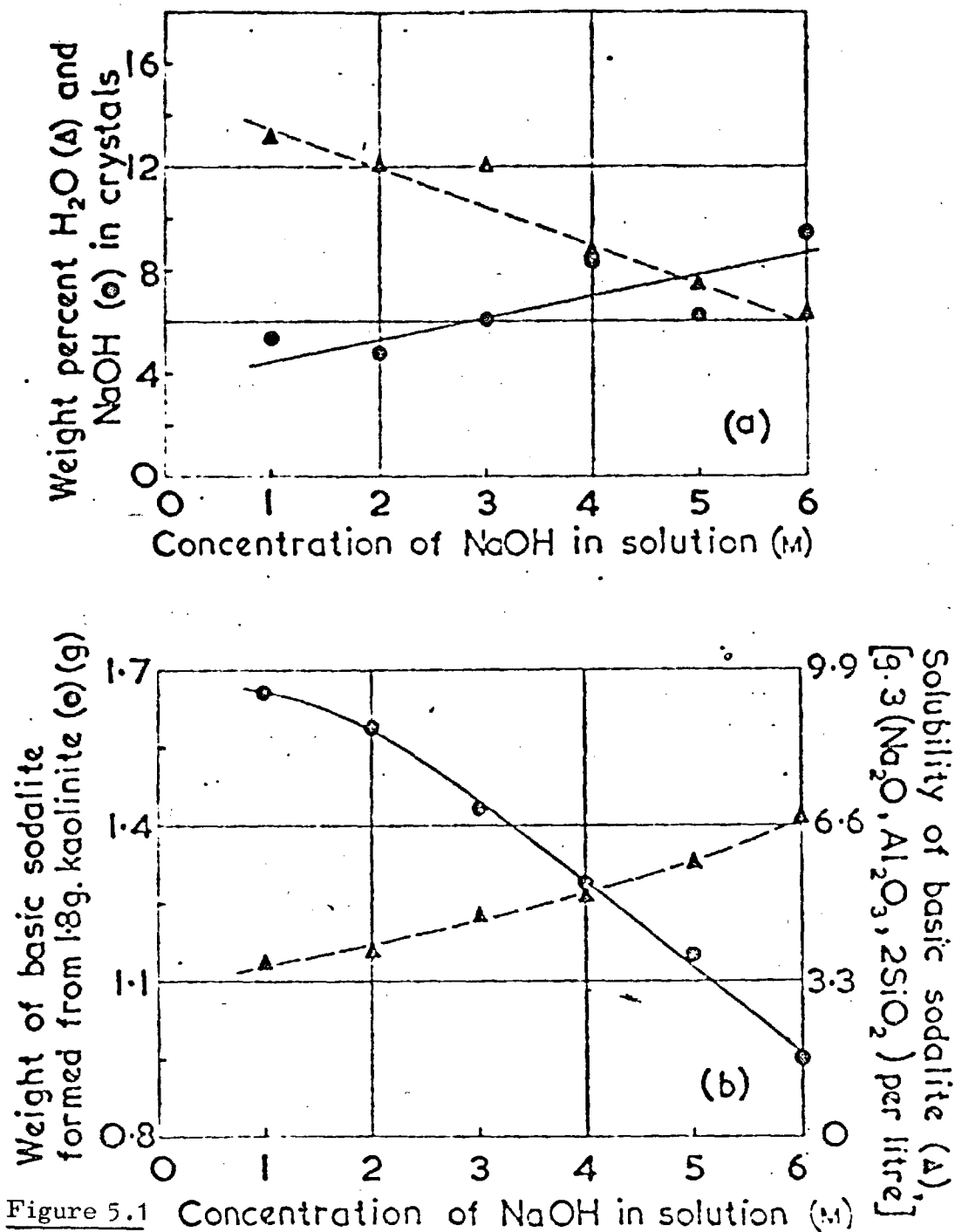


Figure 5.1 Concentration of NaOH in solution (M)

(a) Dependence of water (A) and sodium hydroxide (O) contents of basic sodalites upon concentration of sodium hydroxide in synthesis solution; 80°; (b) dependence of yield of anhydrous and salt-free sodalite (O), and solubility of basic sodalite (A), upon sodium hydroxide concentration in synthesis solution at 80°

### Reaction of kaolinite with aqueous alkaline salt solutions.

In presence of solutions of sodium hydroxide plus alkali stable sodium salts kaolinite recrystallised at  $80^{\circ}$  to sodalites and cancrinites containing a wide range of intercalated salts (Table 5.5). Under the conditions indicated in the Table, with one separately considered exception, the phases appeared in yields which were usually nearly quantitative. The encapsulated salts could not be released except by decomposing the silicates with mineral acids. The zeolitic water was removed continuously on heating at temperatures rising to  $400^{\circ}$ , as shown in DTA and thermogravimetric runs.

The properties of some individual salt rich sodalites and cancrinites will now be discussed in such a way as to bring out as far as possible general trends, and to highlight the most important features, such as thermal stability, individual crystallographic features, and chemical properties of potential usefulness.

#### (a) Sodalites with imbibed sodium halides.

The salt inclusion isotherms for NaCl and NaBr are shown in Figs. 5.2 and 5.3. It is seen that under these mild conditions of synthesis the completely anhydrous forms  $6(\text{NaAlSi}_3\text{O}_8)$  are not obtained. This would correspond with 11.2 and 19.6 wt.% NaCl and NaBr respectively. The maximum uptake here is apparently limited by the solubility of NaX in the reaction mixture, which is not very high.

Samples of sodalite made in the presence of NaF normally had unusually high water contents ( $\sim 12\%$ ) attesting to the fact that if NaF was initially imbibed it was washed out during working up. These specimens behaved as "washed out" basic sodalites. This is an important observation, which has extensions in molecular sieve synthesis.

The halide-rich specimens gave good x-ray powder photographs which yielded for the series Cl<sup>-</sup>, Br<sup>-</sup>, I<sup>-</sup> the unit cell parameters 8.82, 8.88 and 8.96 Å. These specimens dehydrated smoothly when heated in the thermogravimetric apparatus slowly from  $20^{\circ}$  to  $400^{\circ}\text{C}$  and were thermally quite stable. Breakdown occurred only on prolonged heating at  $1000^{\circ}\text{C}$ , resulting

Table 5.5.

Some Reactions of Kaolinite with NaOH and Sodium Salts.

(Reactions of 2g Kaolinite with 200 mls. NaOH(4M) Solution + Na salts  
(10g. unless otherwise stated) at 80°C for 5 days)

| Product         | Reaction Composition.           | Imbided Salt *                                | Remarks  |
|-----------------|---------------------------------|---|--|
| <u>Sodalite</u> | no added salt                   | NaOH  |  |
|                 | NaCl                            | NaCl  |  |
|                 | NaBr                            | NaBr  |  |
|                 | NaI                             | NaI   |  |
|                 | NaF                             | NaOH (small amount)                           | no evidence for intracrystalline NaF.                            |
|                 | NaClO <sub>3</sub>              | NaClO <sub>3</sub>                            |  |
|                 | NaClO <sub>4</sub>              | NaClO <sub>4</sub>                            | pale blue crystals, complex reaction, but sulphur salts imbided. |
|                 | Na <sub>2</sub> SO <sub>3</sub> | Na <sub>2</sub> SO <sub>3</sub>               |  |
|                 | Na <sub>2</sub> S               | Na <sub>2</sub> S(?)                          |  |
|                 | Na <sub>2</sub> CO <sub>3</sub> | Na <sub>2</sub> CO <sub>3</sub> , NaOH        |  |
|                 | Na <sub>2</sub> WO <sub>4</sub> | Na <sub>2</sub> WO <sub>4</sub>               |  |
|                 | Na <sub>3</sub> PO <sub>4</sub> | Na <sub>3</sub> PO <sub>4</sub>               |  |
| Sodium Formate  |                                 | HCO <sub>2</sub> Na                           |  |
| Sodium Acetate  |                                 | CH <sub>3</sub> CO <sub>2</sub> Na            |  |
| Sodium Oxalate  |                                 | C <sub>2</sub> O <sub>4</sub> Na <sub>2</sub> |  |



Table 5.5 (contd.)

| Product           | Reaction Composition.  | Imbibed Salt*  | Remarks   |
|-------------------|--|--|---|
| <u>Cancrinite</u> | $\text{Na}_2\text{SO}_4$   | $\text{Na}_2\text{SO}_4$   | { pale yellow<br>crystals.                          |
|                   | $\text{Na}_2\text{SeO}_4$  | $\text{Na}_2\text{SeO}_4$  |   |
|                   | $\text{Na}_2\text{CrO}_4$  | $\text{Na}_2\text{CrO}_4$  |   |
|                   | $\text{Na}_2\text{MoO}_4$  | $\text{Na}_2\text{MoO}_4$  | { pale brown<br>crystals admixed<br>with species H. |
|                   | $2\text{g. Na}_2\text{Fe}^{\text{VI}}\text{O}_4 + 12\text{M NaOH}$                                     | Fe(III)<br>compound  |   |
|                   | $\text{Na}_3\text{VO}_4$<br>$\text{NaMnO}_4$ (large xs)<br>$\text{NaNO}_3$                             | $\text{Na}_3\text{VO}_4$<br>$\text{NaMnO}_4 + \text{Na}_2\text{MnO}_4(?)$<br>$\text{NaNO}_3$ |   |
|                   | $\text{Cu}(\text{NH}_3)_4\text{SO}_4$ in presence<br>of xs $(\text{NH}_3)$ aq.                         | $\text{Cu}(\text{NH}_3)_4\text{SO}_4$<br>$\text{Na}_2\text{SO}_4$                            | { pale blue/grey<br>crystals.                       |
| <u>Species H</u>  | $2\text{g. Na}_2\text{Fe}^{\text{VI}}\text{O}_4$ in 30 mls.<br>10M NaOH + 2g.<br>silica (precipitated) |  | { admixed with<br>material amorphous<br>to X-rays.  |

\* In general NaOH was also imbibed in small varying amounts. In addition all the products contained zeolitic water.

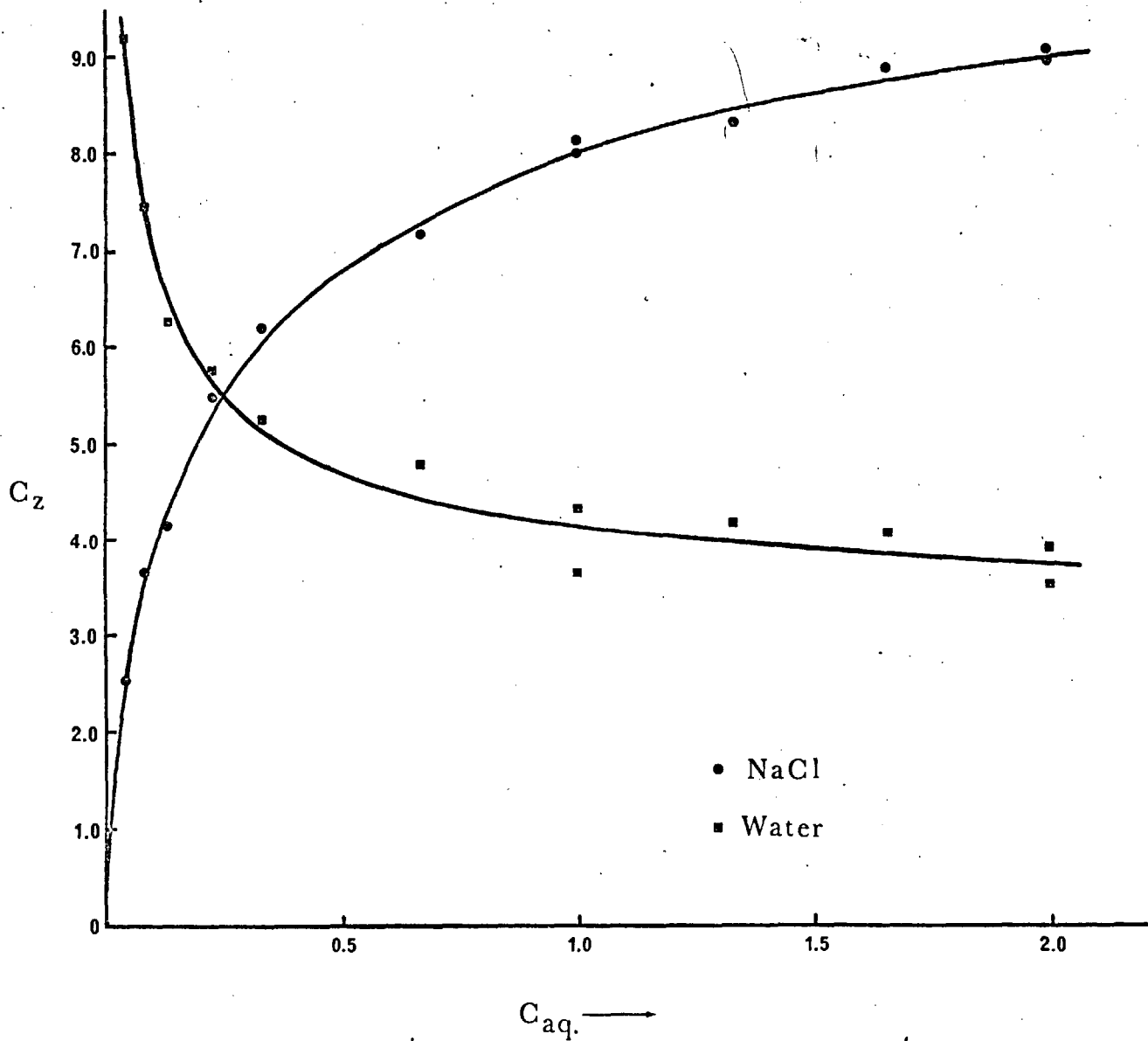


Figure 5.2 Imbibition of NaCl/H<sub>2</sub>O by sodalite.  $C_z$ : wt.% NaCl/H<sub>2</sub>O in crystals;  $C_{aq}$ : conc<sup>n</sup> NaCl (moles Kg<sup>-1</sup> H<sub>2</sub>O) in synthesis solution. NaOH concentration 4 moles Kg<sup>-1</sup> H<sub>2</sub>O. 0.90°C

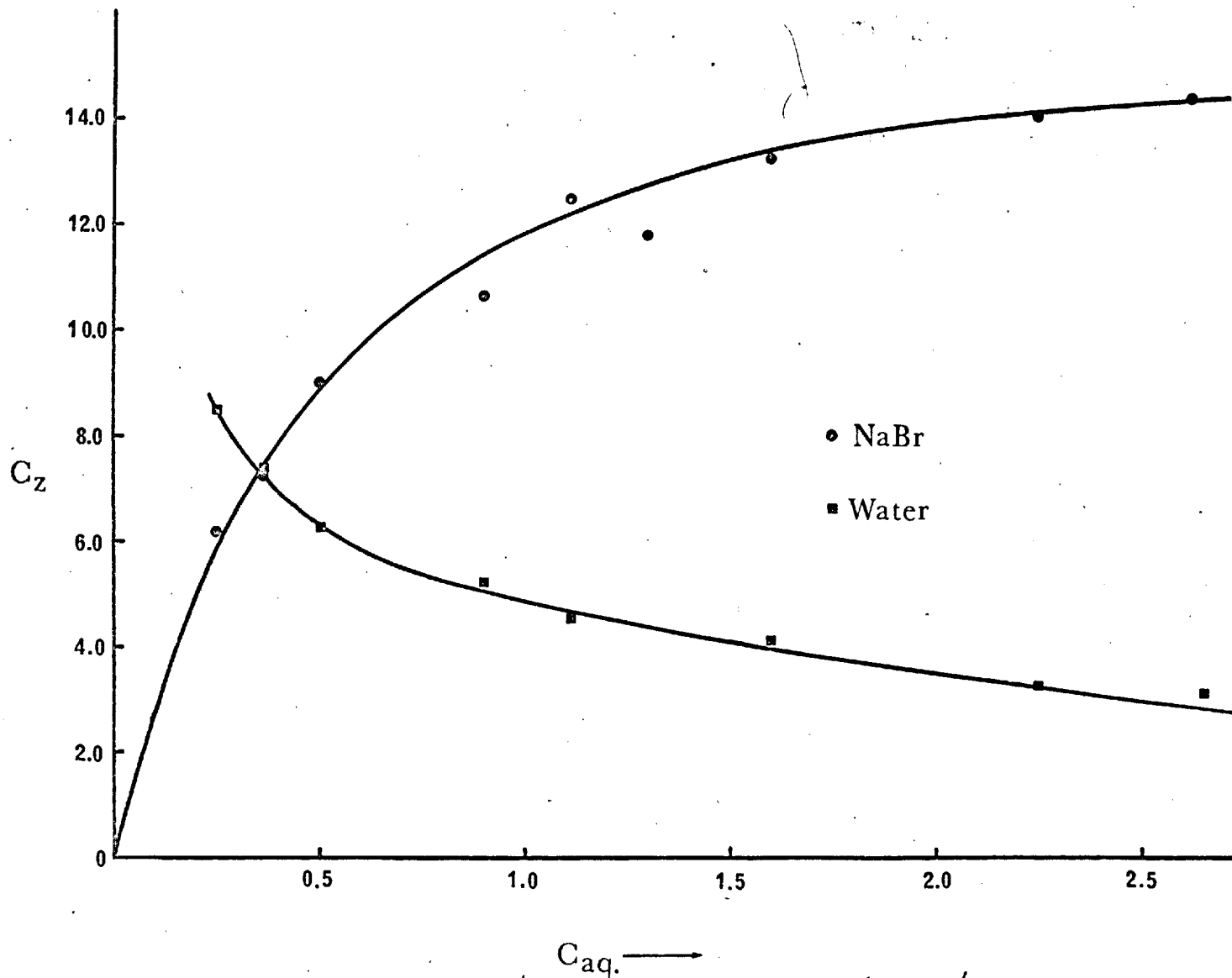
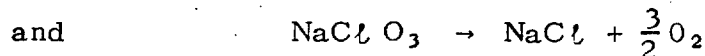
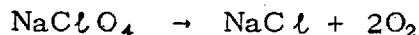


Figure 5.3 Imbibition of NaBr/H<sub>2</sub>O by sodalite.  $C_z$ : wt.% NaBr/H<sub>2</sub>O in crystals,  $C_{aq.}$  conc<sup>n.</sup> NaBr in synthesis solution. NaOH conc<sup>n.</sup> 4 moles K<sup>-1</sup> H<sub>2</sub>O. 80 °C.

in evaporation of NaX which, in amount, was usually the same as that found by chemical analysis. Recrystallization to the condensed phase nepheline ( $\text{NaAlSiO}_4$ ) ultimately took place.

(b) Sodalites with imbibed sodium perchlorate and sodium chlorate.

These salts have the inclusion isotherms shown in Figs. 5.4 and 5.5. The ideal compositions  $6(\text{NaAlSiO}_4) \cdot 2 \text{NaClO}_{3/4}$  are not actually attained, but the highest loadings show that they are closely approached. The effect on crystal quality of inclusions of  $\text{ClO}_4^-$  and  $\text{ClO}_3^-$  was quite remarkable. Perchlorate ions in particular produced beautifully crystalline samples of sodalite which gave unusually excellent x-ray powder photographs with sharp well-defined lines. The unit cell edges of these specimens clearly varied with salt loading. For example an inclusion of 0.86 wt.%  $\text{NaClO}_4$  had  $a_0 = 8.86 \text{ \AA}$  while a loading of 20.93 wt.% had  $a_0 = 9.01 \text{ \AA}$ . These samples dehydrated smoothly when slowly heated in a thermobalance from  $20^\circ$  to  $400^\circ$ . Further heating initiated the thermal decompositions



which went strictly according to these equations, as evidenced from the weight of  $\text{O}_2$  removed, and analysis of NaCl in the residues. The reactions were most rapid around  $650^\circ\text{C}$ . It was interesting to observe that at this temperature the ignition products were in fact sodalites with imbibed NaCl, and behaved as described in (a) above upon further heating. The release of oxygen at  $650^\circ\text{C}$  was studied for  $\text{NaClO}_4$ -sodalite by quickly bringing a sample into the thermobalance furnace zone at this temperature. The near linearity of oxygen evolution found with the square root of time bespeaks the diffusion-controlled process. Thus these systems offer unusual possibilities for such diffusion studies.

(c) Sodalite with imbibed sodium carbonate.

Sodium carbonate imbibition was accompanied by water and sodium hydroxide in larger relative amounts than in the cases with other salts. At  $80^\circ$  it was not possible to achieve a higher salt loading at the expense of these components,

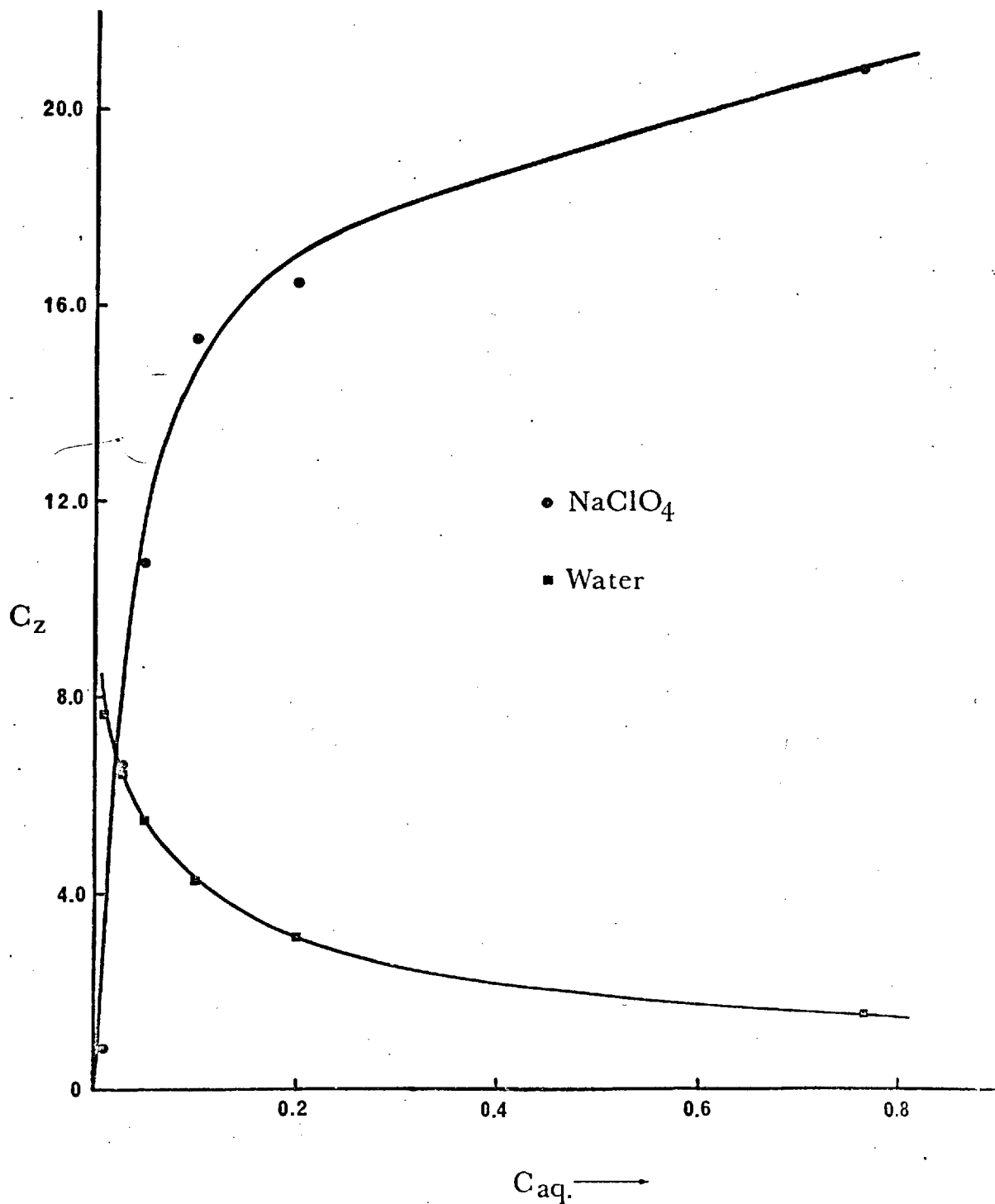


Figure 5.4, Imbibition of  $\text{NaClO}_4/\text{H}_2\text{O}$  by sodalite.  $C_z$ :wt.%  $\text{NaClO}_4/\text{H}_2\text{O}$  in crystals;  $C_{\text{aq}}$  conc<sup>n</sup>.  $\text{NaClO}_4$  in synthesis soln. moles  $\text{Kg}^{-1}\text{H}_2\text{O}$ .  $\text{NaOH}$  conc<sup>n</sup>. .4 moles  $\text{Kg}^{-1}\text{H}_2\text{O}$ . 80 °C.

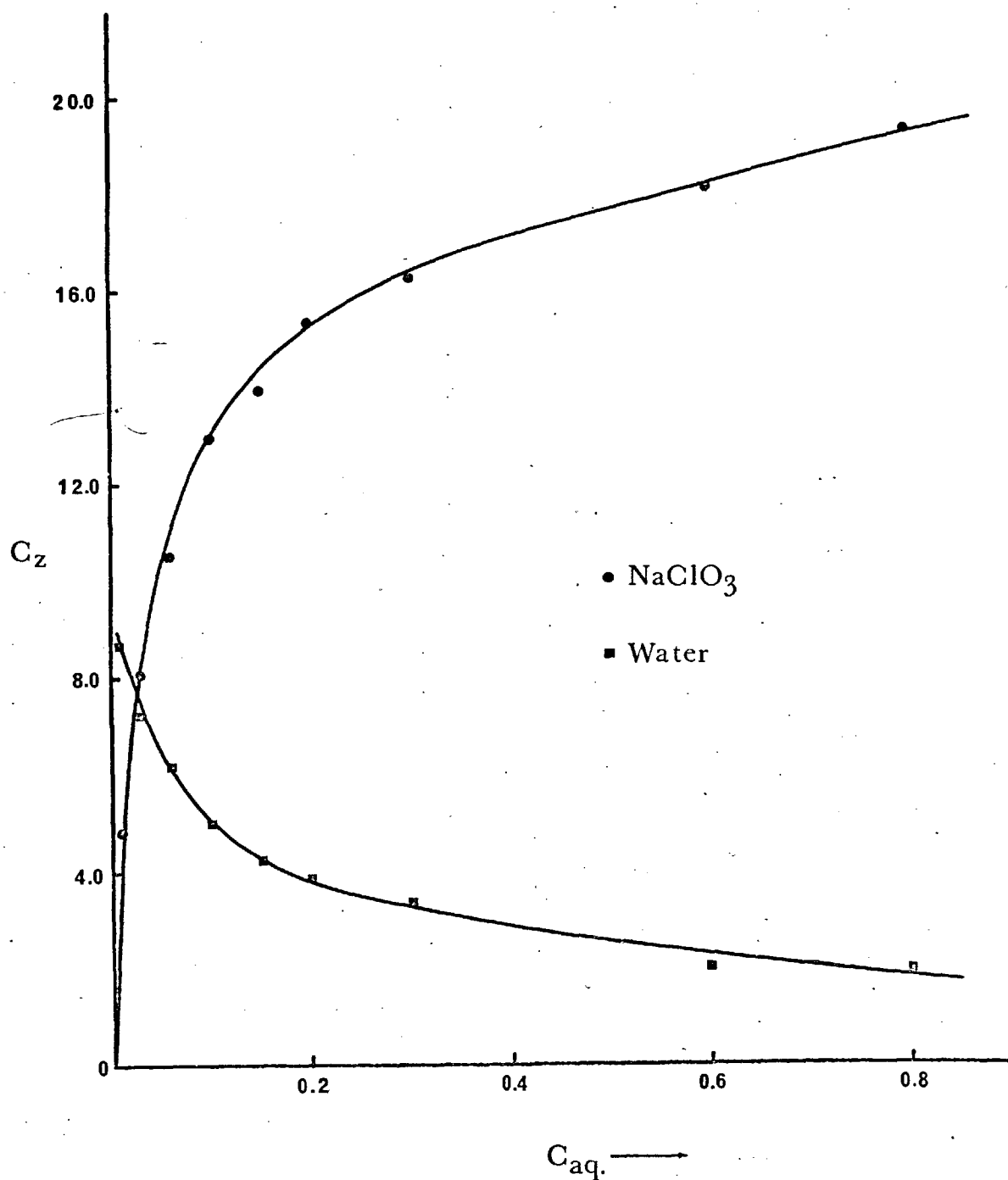


Figure 5.5 Imbibition of  $\text{NaClO}_3/\text{H}_2\text{O}$  by sodalite.  $C_z$ : wt. %  $\text{NaClO}_3/\text{H}_2\text{O}$  in crystals;  $C_{\text{aq.}}$  conc<sup>n</sup>.  $\text{NaClO}_3$  in synthesis soln. moles  $\text{Kg}^{-1}\text{H}_2\text{O}$ . Concentration  $\text{NaOH}$  4 moles  $\text{Kg}^{-1}\text{H}_2\text{O}$ .  $80^\circ\text{C}$ .

as shown by Fig. 5.6. This unusual behaviour is reflected in the x-ray powder data: the inclusion is here evidently incompatible with the symmetry and/or the size of cavities in the sodalite framework and a superstructure results (Table 5.6). Many powder reflections appear which can be indexed on a cell with twice the usual sodalite parameter. In this case the whole pattern was initially indexed on a cubic cell with parameter  $17.80 \text{ \AA}$ . Least squares refinement of this quantity gave  $a_0 = 17.799 \text{ \AA}$ . The superstructure naturally should become less distinct as the salt loading decreases, as was observed for the specimens used to construct Fig. 5.6. The order in this structure now extends over two cages - as if one cage and its inclusion affected its neighbour. The present samples were thermally unstable, and after loss of zeolitic water before  $400^\circ$ , dehydration of NaOH and decomposition of  $\text{Na}_2\text{CO}_3$  followed, ultimately leading to crystal collapse and formation of nepheline.

(d) Sodalite isolated from a system with added  $\text{Na}_2\text{S}$ .

Addition of  $\text{Na}_2\text{S}$  to the standard reaction mixture produced unusual effects. The resulting blue-grey crystals were separated from a yellow mother liquor and shown to contain imbibed sulphur compounds, as follows. A sample was placed in a quartz tube between glass wool pads and slowly heated to  $200^\circ\text{C}$  in a stream of  $\text{Cl}_2$ . A sulphurous oil was condensed in the cool zone above the specimen, and x-ray examination of the latter showed the presence of extra-crystalline  $\text{NaCl}$ . The experiment was repeated with a fresh specimen, but using  $\text{O}_2$  and heating to  $500^\circ\text{C}$ . No condensable residues were observed, but the crystals turned pink, and this colour remained on cooling. Thermogravimetric analysis in air showed that after loss of zeolitic water at low temperature there was actually a gain in weight. The crystalline residue thereafter was stable to  $1000^\circ\text{C}$ , but at high temperature the unit-cell edge was larger than at room temperature. Thus, the sequence of reactions is essentially clear. Sulphide or hydrosulphide ions were initially imbibed and these could be subsequently oxidised to thermally stable  $\text{SO}_4^{2-}$  or  $\text{SO}_3^{2-}$  ions inside the crystals; these account for the gain in weight, the unusual thermal stability of the product, and the increase in unit-cell edge. The production of coloured specimens in this area is not well understood and is currently being investigated by several groups.

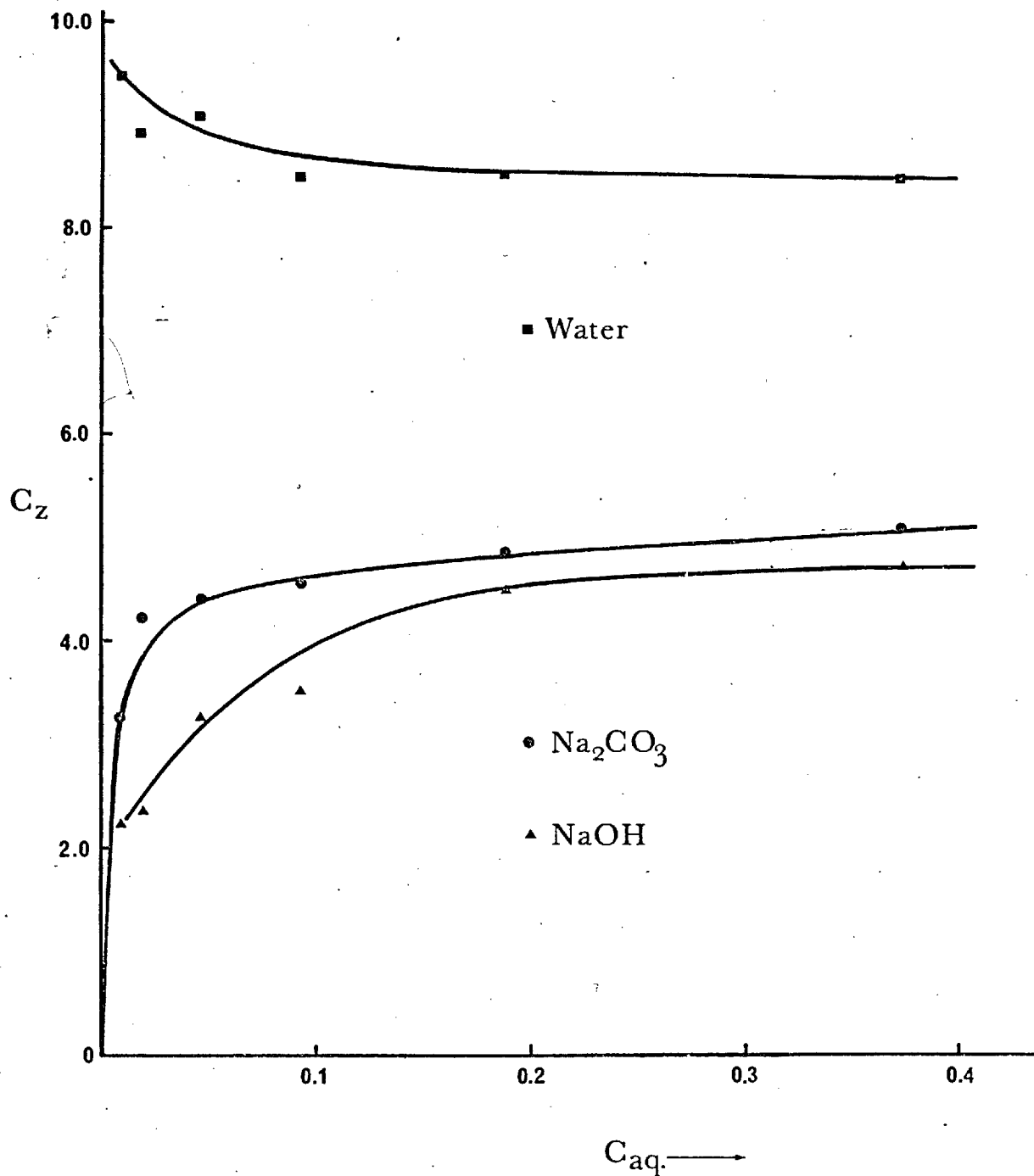


Figure 5.6 Imbibition of  $\text{Na}_2\text{CO}_3/\text{NaOH}/\text{H}_2\text{O}$  by sodalite.  $C_z$ : wt.%  $\text{Na}_2\text{CO}_3/\text{NaOH}/\text{H}_2\text{O}$  in crystals;  $C_{aq}$ : conc<sup>n</sup>  $\text{Na}_2\text{CO}_3$  in synthesis solution. Moles  $\text{Kg}^{-1}$   $\text{H}_2\text{O}$ .  $\text{NaOH}$  conc<sup>n</sup>. 4 moles  $\text{Kg}^{-1}$   $\text{H}_2\text{O}$ .  $80^\circ\text{C}$ .



Table 5.6

Sodium carbonate sodalite - observed and calculated powder lines.

$$a_0 = 17.799 \pm 0.007 \text{ \AA}.$$

| H | K | L | $D_{(\text{obs})}$ | $D_{(\text{calc})}$ |
|---|---|---|--------------------|---------------------|
| 1 | 1 | 1 | 10.163             | 10.276              |
| 2 | 2 | 0 | 6.256              | 6.293               |
| 3 | 1 | 1 | 5.304              | 5.366               |
| 2 | 2 | 2 | 5.115              | 5.138               |
| 4 | 0 | 0 | 4.441              | 4.449               |
| 3 | 3 | 1 | 4.080              | 4.083               |
| 4 | 2 | 0 | 3.968              | 3.980               |
| 4 | 2 | 2 | 3.631              | 3.633               |
| 5 | 1 | 0 | 3.495              | 3.490               |
| 5 | 1 | 1 | 3.433              | 3.425               |
| 4 | 4 | 0 | 3.149              | 3.146               |
| 5 | 3 | 1 | 3.029              | 3.008               |
| 6 | 0 | 0 | 2.980              | 2.966               |
| 6 | 2 | 0 | 2.814              | 2.814               |
| 5 | 3 | 3 | 2.723              | 2.714               |
| 6 | 2 | 2 | 2.690              | 2.683               |
| 4 | 4 | 4 | 2.578              | 2.569               |
| 7 | 1 | 1 | 2.497              | 2.492               |
| 6 | 4 | 2 | 2.387              | 2.378               |
| 7 | 3 | 1 | 2.319              | 2.317               |
| 6 | 4 | 4 | 2.160              | 2.158               |
| 6 | 6 | 0 | 2.103              | 2.097               |
| 8 | 3 | 1 | 2.062              | 2.069               |
| 8 | 3 | 2 | 2.025              | 2.028               |
| 8 | 4 | 0 | 1.991              | 1.990               |
| 8 | 3 | 3 | 1.962              | 1.965               |

(e) Sodalite with imbibed sodium tungstate and phosphate.

(i)  $\text{Na}_2\text{WO}_4$ . A typical specimen contained up to 11% zeolitic water, which is an unusually large water content. The tungstate loading, and hence the thermal stability, was correspondingly lower, and by  $930^\circ$  the well crystallized sodalite had begun to recrystallize to nepheline.

(ii)  $\text{Na}_3\text{PO}_4$ . Similar behaviour was shown by the phosphatic sodalites prepared at  $80^\circ$ . A water content around 9% was usual.

Under hydrothermal conditions  $\text{Na}_3\text{PO}_4$  undergoes extensive hydrolysis and is capable of generating the high pH necessary to kaolinite recrystallization reactions. A series of high temperature reactions were made to illustrate this. In these experiments cancrinite, rather than sodalite, was formed. Table 5.7 shows the products obtained from various reaction compositions, and it is clear that as the ratio of moles  $\text{Na}_3\text{PO}_4$  to moles kaolinite is lowered, eventually the main product changes from cancrinite to the condensed zeolite <sup>analcite,</sup> and finally, there is insufficient hydrolyzable phosphate present to decompose all the kaolinite, some of which remains after the reaction. These results confirm and extend the earlier studies of Barrer and Marshall. <sup>(79)</sup> Another series of crystallizations is recorded in Table 5.8. Here the effect of extra sodium hydroxide and a higher temperature is examined. The most interesting feature of these results is the first appearance of the layer silicate paragonite, at the higher temperature, in less alkaline systems. If the  $\text{Na}_3\text{PO}_4$  is replaced by a non-hydrolyzable salt such as  $\text{NaCl}$ , at temperatures of  $395^\circ$  good yields of well-formed paragonite are found. Table 5.9, for example gives a list of charges which produced paragonite alone. The high temperature experiments show that hydrolyzable salts can be used to supply  $\text{OH}^-$  for the zeolitization process. In the field of zeolite synthesis a balance must be struck between the temperature and base concentration. Highly basic systems at all temperatures favour relatively condensed zeolites, eg. sodalite and analcite or cancrinite, while at high temperatures and low basicities, clay mineral formation is favoured.

In order to produce the very open framework structures which are suitable for molecular sieving and catalysis, low base concentration and low temperatures

Table 5.7Reactions of kaolinite with  $\text{Na}_3\text{PO}_4$  solutions

(Conditions as indicated, 0.5 g. kaolinite plus 7 ml. water.)

| $n$ { moles $\text{Na}_3\text{PO}_4$ per }<br>{ mole kaolinite. } | crystalline product .  | conditions.    |
|---|--|----------------|
| 7.4 to 2.2  | phosphatic cancrinite  | 3 days, 290°C. |
| 2.0 to 0.8  | mixtures of phosphatic*<br>cancrinite with analcite.                           | 3 days, 290°C. |
| 0.7 to 0.2  | mixtures of phosphatic<br>cancrinite with analcite and<br>unreacted kaolinite. | 3 days, 335°C. |

\* analcite becoming predominant as  $n$  lowered.

Table 5.8

Effect of additional NaOH on products from kaolinite/Na<sub>3</sub>PO<sub>4</sub> system

(Conditions as indicated, 0.5 g. kaolinite plus 7 ml. water. 5 day reactions at 395 °C.)

| $n \left\{ \begin{array}{l} \text{moles Na}_3\text{PO}_4 \\ \text{per mole kaolinite} \end{array} \right\}$ | moles NaOH added $\times 10^4$ | product *          |
|---|--------------------------------|--------------------|
| 0.11  | -                              | K + (A) + C + P    |
| 0.11  | 4                              | as above           |
| 0.11  | 8                              | (A) + P            |
| 0.29  | 8                              | (A) + C            |
| 0.11  | 12                             | (A) + P            |
| 0.11  | 16                             | (A) + C + traces P |
| 0.11  | 20                             | as above           |
| 1.54  | -                              | (A) + C            |
| -   | 28                             | (A) + P            |

\* K = unreacted kaolinite, A = analcite, C = phosphatic cancrinite,  
P = paragonite; brackets enclose predominant product.

Table 5.9.Synthesis of Paragonite at 395 °C, from kaolinite.

(Conditions as indicated, 0.5 g. kaolinite, 3 day reactions).

| Vol. NaCl soln.<br>satd. at 25°.(ml.) | Vol. 0.4 M<br>NaOH (ml.) | Vol. water (ml.) |
|---------------------------------------|--------------------------|------------------|
| 7                                     | -                        | -                |
| 6                                     | -                        | 1                |
| 5                                     | -                        | 2                |
| 4                                     | -                        | 3                |
| 3                                     | -                        | 4                |
| 2                                     | -                        | 5                |
| 1                                     | -                        | 6                |
| 3                                     | 4                        | -                |
| 5                                     | 2                        | -                |

have to date been more successful, although lately more variety has been found by using template molecules,<sup>(3)</sup> and Barrer and Denny's method<sup>(80)</sup> of artificially increasing the Si/Al ratio in the products by using tetra-alkyl ammonium hydroxide bases.

(f) Sodalite with imbibed Na<sub>2</sub>SO<sub>3</sub>

These specimens were exceptionally thermally stable, and after a typical zeolitic dehydration of around 7% water, no further changes were noted. Slight weight gains around 600 °C were sometimes observed which bespeak the formation of some sulphate. It is interesting that this intracrystalline reaction involving diffusion of oxygen and subsequent lattice expansion, is evidently not prevented by encapsulation.

(g) Sodalite with imbibed organic salts.

Addition of sodium formate, acetate or oxalate to the standard reaction mixture produced sodalites whose properties demonstrated that these salts were indeed encapsulated.

(i) NaHCO<sub>2</sub>. These samples showed a strong infra-red absorption at 1610 cm<sup>-1</sup> which was attributed to the  $-\text{C} \begin{array}{l} \nearrow \text{O} \\ \searrow \end{array}$  function, and on heating this peak disappears between 500 ° and 600 °. In this region, an inflammable gas or mixture of gases was transpired, probably CO and H<sub>2</sub> from the formate decomposition. On further heating, nepheline was formed. Typical samples also contained around 5% zeolitic water which was removed by 400 °, i.e. before decomposition of the imbibed species.

(ii) NaCH<sub>3</sub>CO<sub>2</sub>. Similar behaviour was observed. An infra-red absorption around 1596 cm<sup>-1</sup> was assigned to  $-\text{C} \begin{array}{l} \nearrow \text{O} \\ \searrow \end{array}$  and was removed by heating at 650 °C. The decomposition produced inflammable vapours and some coking was noticed. When slowly heated under vacuum, one sample lost 4% zeolitic water below 400 °C, and at higher temperatures a colourless involatile oil and some acetone were isolated in a cold trap. At 930 ° the crystals had begun the transformation to nepheline.

(iii) Na<sub>2</sub>C<sub>2</sub>O<sub>4</sub>. The thermal decomposition of this phase began at lower temperatures and could not be separated by thermogravimetric methods from the zeolitic

dehydration. It behaved entirely similarly to the other organo-sodalites.

(h) Other sodalite inclusion compounds.

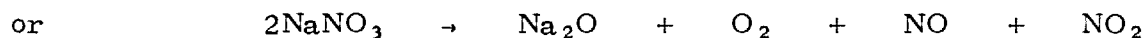
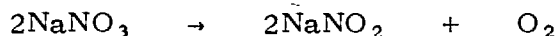
The sodalites with imbibed anions whose properties were discussed above are by no means the only ones obtainable by this method. Many other inorganic inclusions were isolated, together with some organic types. These, together with the above, make the scope of the imbibition process very wide, and the products often have physical and chemical properties of great interest, and potential usefulness.

(i) Cancrinites with imbibed  $\text{Na}_2\text{SO}_4$ ,  $\text{Na}_2\text{SeO}_4$ ,  $\text{Na}_2\text{CrO}_4$ ,  $\text{Na}_2\text{MoO}_4$ ,  $\text{Na}_3\text{VO}_4$  and  $\text{NaMnO}_4$ .

Addition of these salts to the standard reaction mixture produced cancrinites. The crystals were coloured when the anion was, for example chromate and permanganate cancrinites were yellow and red respectively. All contained variable amounts of zeolitic water which could be removed by slow heating up to  $400^\circ$ . When the imbibed salt was thermally stable, eg.  $\text{Na}_2\text{SO}_4$ ,  $\text{Na}_2\text{SeO}_4$ ,  $\text{Na}_2\text{CrO}_4$  and  $\text{Na}_2\text{MoO}_4$ , this stability was conferred upon the aluminosilicate lattice; otherwise on heating, complex intracrystalline decompositions took place which were followed by lattice collapse at high temperatures. The crystals with imbibed  $\text{Na}_2\text{SO}_4$  were exceptionally thermally stable, and could be heated to  $1000^\circ$  without lattice decomposition.

(j) Cancrinites with imbibed  $\text{NaNO}_3$ .

These compounds were especially interesting, since the imbibed nitrate ions could be decomposed thermally according to the equations:



A wet chemical determination of  $\text{NO}_3^-$  using nitron reagent<sup>(71)</sup> confirmed that the  $\text{NO}_3^-$  estimated from the high temperature weight loss according to these

equations was correct.

Close inspection of the thermogravimetric traces in the decomposition range indicated that a two-step process was in progress, which might be explained if the  $\text{NO}_3^-$  ions occupied not only the channels of the aluminosilicate framework, but also the small cavities (see section 3). Infra-red evidence also suggested two different sites, since in the N-O stretch region ( $\sim 800 \text{ cm}^{-1}$ ) two sharp but slightly separated absorptions were noted. It should be theoretically possible to pack exactly two nitrate ions into each unit cell of cancrinite,<sup>(71)</sup> and experiments were made to do this. The composition  $6(\text{NaAlSiO}_4) \cdot 2\text{NaNO}_3$  requires  $\sim 16.6 \text{ wt.}\%$   $\text{NaNO}_3$ . Table 5.10 shows imbibition compositions of several synthetic cancrinites made under different conditions. It is seen that under these conditions, this ideal composition is closely approached. Another observation of some importance was recorded. When small but increasing amounts of  $\text{NaNO}_3$  were added to the standard mixture of 2 g. kaolinite in 200 mls. 4M  $\text{NaOH}$ , the crystalline product changed from sodalite to cancrinite. Table 5.11 gives these data. Sodium chromate also possessed this property, and data for this system are likewise given in the table.



Table 5.10

Compositions of Cancrinites with Imbided  $\text{NaNO}_3$ .

| Sample No. | Wt.% $\text{H}_2\text{O}$ | Wt.% $\text{NaNO}_3$ | Synthesis Conditions  |
|------------|---------------------------|----------------------|---|
| 340-F1     | 3.02                      | 14.02                | 0.1-7.0 M $\text{Kg}^{-1}\text{H}_2\text{ONaNO}_3$<br>100% XS NaOH 80 °C.                             |
| 368-F8     | 2.75                      | 14.60                |   |
| 369-F9     | 4.08                      | 13.05                |   |
| 370-F10    | 4.03                      | 14.23                |   |
| 371-F11    | 2.34                      | 14.30                |   |
| 373-K14    | 3.98                      | 13.42                | 2 - 14 M $\text{Kg}^{-1}\text{H}_2\text{ONaNO}_3$<br>100% XS NaOH 190 °C.<br>under autogeneous pressu |
| 374-K15    | 3.53                      | 13.90                |   |
| 375-K18    | 3.48                      | 15.53                |   |
| 376-K13    | 4.42                      | 13.34                |   |
| 377-L14    | 3.99                      | 14.04                |   |
| 378-K15    | 3.98                      | 13.92                |   |
| 379-K18    | 2.38                      | 14.52                |   |
| 363-K13    | 0.40                      | 15.55                | Saturated $\text{NaNO}_3$<br>0-100% XS NaOH<br>420 °C.<br>and autogeneous pressur                     |
| 364-K14    | 0.60                      | 14.97                |   |
| 365-K15    | 0.20                      | 14.33                |   |
| 366-K18    | not detected              | 15.79                |   |

Table 5.11

Effect of  $\text{NaNO}_3$  and  $\text{Na}_2\text{CrO}_4$  on reaction products.

(Conditions as indicated, 2.0 g. kaolinite, 200 ml. 4 moles /Kg  $\text{H}_2\text{O}$  NaOH at  $80^\circ$ .)

| Concentration of added salt (moles $\text{Kg}^{-1} \text{H}_2\text{O}$ ) |                           | product                               |
|--|---------------------------|---------------------------------------|
| $\text{NaNO}_3$  | $\text{Na}_2\text{CrO}_4$ |                                       |
| 0.0023   | 0.0308                    | Sodalite.                             |
| 0.0039<br>0.007<br>0.013<br>0.066<br>0.99                                | 0.0617<br>0.1543          | Mixtures of sodalite and cancrinite*. |
| 2.0  | 0.309<br>0.617<br>1.235   | Cancrinite.                           |

\* Cancrinite becoming predominant as salt concentration increases.

(k) Other cancrinite inclusion complexes.

The compounds listed above are, again, merely representative of a great many which were actually prepared, using a variety of salts. Interesting and complex reactions could be observed with some salts, two of which are described.

(i) Formation of cancrinite with  $\text{Cu}(\text{NH}_3)_4\text{SO}_4$  imbibition.

This compound is obtained when 100 mls. of concentrated  $\text{Cu}(\text{NH}_3)_4\text{SO}_4/\text{NH}_3$  solution is mixed with 2 g. kaolinite in 100 mls. 4M NaOH, and the charge heated in a sealed vessel at 80 °C for 5 days.

The blue crystals of cancrinite were admixed with small amounts of copper oxide formed by dehydration of the hydroxide in a minor side reaction. These particles were large and could be separated from the bulk by hand picking. DTA, thermogravimetric and chemical tests showed that  $\text{Cu}(\text{NH}_3)_4^{2+}$  cations were present in the crystals, as well as  $\text{SO}_4^{2-}$  ions. When heated, a mixture of water and ammonia was released and the residue was thereafter stable on heating to 1000 °. This stability was no doubt due to the intracrystalline mixture of sulphate ions; this behaviour closely parallels that found with the  $\text{Na}_2\text{SO}_4$  cancrinites and  $\text{Na}_2\text{SO}_3$  sodalites, which has already been discussed. A small contraction in the unit cell parameters was observed during the heating cycle. It proved possible to reduce the intracrystalline copper to the metal by heating in a stream of hydrogen at 500 °C. The blue crystals turned pink and certain superstructural lines in the powder photograph were removed during this treatment. Heating at temperatures much above 500 °, or at 500 ° for prolonged periods caused the powder lines of metallic copper to appear, thus demonstrating migration and aggregation, outside the crystals, of copper atoms.

(ii) Formation of cancrinite in the presence of  $\text{Na}_2\text{Fe}^{\text{VI}}\text{O}_4$ .

This species was prepared from kaolinite and a 5M NaOH solution of sodium ferrate ( $\text{NaFe}^{\text{VI}}\text{O}_4$ ) made by the chlorine oxidation method. (81) The Mössbauer spectrum\* of this cancrinite at room temperature establishes that

---

\* I am indebted to my colleague Joe Morice for Mössbauer measurements.

the iron is in oxidation state (III). The quadrupole splitting of  $0.63 \pm 0.05$  mm.  $\text{sec}^{-1}$  and the isomer shift of  $+ 0.30 \pm 0.05$  mm.  $\text{sec}^{-1}$  (relative to iron metal), indicate some covalent bonding of iron, for example, to oxygen. These observations are further supported by the ESR spectrum at room temperature, which showed a strong absorption at  $g \doteq 2.0$ . Analysis gave a Si/Al ratio of 1.06 indicating that no aluminium in the framework has been replaced by iron. Thermogravimetric investigations showed a weight loss of 7.7% below  $500^\circ\text{C}$ , characteristic of zeolitic water, and a high temperature loss of 7.3% which was most rapid at  $750^\circ\text{C}$ . The product after ignition to constant weight at  $1000^\circ\text{C}$  was shown by x-ray powder photography and Mössbauer spectroscopy to be a mixture of nepheline and  $\alpha - \text{Fe}_2\text{O}_3$ . These observations are consistent with the imbibition of iron compounds which must be at least partly in the oxidation state III. It is interesting that even in such a highly reactive system as the present one, the feldspathoid crystallization takes place with no apparent ill-effects, and with simultaneous imbibition of suitable species from solution.

#### Species H.

Species H appeared in minor yield together with the iron-bearing cancrinite discussed above. It crystallized as beautiful, perfectly formed 0.1 mm tetrahedra coloured pale-green to pale red brown. It was soluble with some effervescence in dilute HCl and could be made in the absence of aluminium but was never observed in the absence of silicon. Side-reactions made it impossible to get a pure sample suitable for analysis. H was cubic, with a unit cell edge of  $9.50 \text{ \AA}$  and systematic absences in its x-ray powder pattern (Table 5.12) suggested that it was probably body-centred. On this basis H could not be identified with any known compound. It is possible that H is a sodalite-type compound in which part of the framework aluminium has been replaced by iron. The  $\text{Fe}(\text{III})\text{-O}$  bond-length for tetrahedral coordination is  $1.86 \text{ \AA}$  (cf.  $\text{Al}(\text{III})\text{-O}$ ,  $1.75 \text{ \AA}$ ) and a simple calculation shows that replacement of all Al by Fe in a sodalite framework should result in an increase in unit-cell edge to about  $9.7 \text{ \AA}$  (cf.  $9.5 \text{ \AA}$  observed). Halstead and Moore<sup>(82)</sup> have described a compound  $3\text{CaO}$ ,  $3\text{Al}_2\text{O}_3$ ,  $\text{CaSO}_4$  having an

Table 5.12.

d-spacings of species H

| $d(\text{\AA})$ obs. | $d(\text{\AA})$ calc. <sub>0</sub><br>( $a_0 = 9.50 \text{ \AA}$ ) | I  | hkl     |
|----------------------|--|----|---------|
| 6.74                 | 6.718  | s  | 110     |
| 4.75                 | 4.750  | m  | 200     |
| 3.89                 | 3.878  | s  | 211     |
| 3.36 <sub>5</sub>    | 3.359  | w  | 220     |
| 3.00 <sub>0</sub>    | 3.004  | w  | 310     |
| 2.74 <sub>5</sub>    | 2.742  | vs | 222     |
| 2.540                | 2.539  | s  | 321     |
| 2.375                | 2.375  | m  | 400     |
| 2.240                | 2.239  | m  | 411,330 |
| 2.122                | 2.124  | m  | 420     |
| 1.935                | 1.939  | w  | 422     |
| 1.860                | 1.863  | w  | 510,431 |
| 1.735                | 1.734  | w  | 521     |
| 1.680                | 1.679  | s  | 440     |
| 1.630                | 1.629  | s  | 530,433 |
| 1.583                | 1.583  | m  | 600,442 |
| 1.540                | 1.541  | m  | 611,532 |
| 1.430                | 1.432  | m  | 622     |
| 1.400                | 1.401  | w  | 631     |
| 1.372                | 1.371  | w  | 444     |

x-ray powder pattern resembling that of sodalite-nosean feldspathoids and a body-centred cubic unit-cell with an edge of 9.195 Å. The authors consider their compound to be derived from such feldspathoids by replacement of all Si by Al and all Na by Ca. This would not accord with Lowenstein's rule<sup>(83)</sup> if the tetrahedral framework of the feldspathoids were retained.

(1) Importance of Structure Determination to Understand Results.

In the past it has always been assumed without good evidence that in natural cancrinites, the imbibed  $\text{CO}_3^{2-}$  is contained only by the framework channels as described in section 3. Jarchow's work confirmed this, and showed that the only occupants of the small cavities were sodium ions. Such a scheme does not accord with the experimental observations for these synthetic cancrinites, and unless the salt enters the small cages during formation they are not explained. For this reason solution of the crystal structures of basic cancrinite,<sup>(71)</sup>  $\text{NaNO}_3$ -cancrinite<sup>(71)</sup>,  $\text{Na}_2\text{CrO}_4$  and  $\text{Na}_2\text{MoO}_4$  cancrinite were undertaken in this laboratory. The results for the last two specimens were discussed in section 4, and we now assume the result found there, that the anion can enter both parts of the cancrinite structure.

The crossover phenomenon illustrated in Table 5.11 made it impossible to obtain the standard wide range salt inclusion isotherms for cancrinites; however, some interesting effects were observed when mixtures of salt were used in the syntheses.

(m) Crystallizations in the presence of mixed salts.

As has been described above, certain salts, for instance  $\text{NaClO}_4$ , strongly promote sodalite formation, whereas others, eg.  $\text{Na}_2\text{MoO}_4$ , equally readily produce the cancrinite structure. It is of immediate interest to know what happens when mixtures of the various salts are used.

Table 5.13 gives the results for a number of key mixtures. In each case 0.1 moles of each salt was added to the standard mixture. From these experiments we can get an idea of the relative "efficiency" of structural promotion of particular anions.

Table 5.13

Crystallizations in the presence of mixtures of salts.

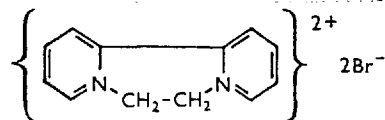
(Conditions as indicated, 2.0 g. kaolinite, 200 ml. 4 moles  $\text{Kg}^{-1}$   $\text{H}_2\text{O}$  NaOH, 80°; 0.10 moles of each salt present).

| Anions present                       | Product (predominant phase marked*)    |
|--------------------------------------|--|
| $\text{Cl}^-/\text{CrO}_4^{2-}$      | <u>Sodalite</u> * + traces cancrinite. |
| $\text{Cl}^-/\text{NO}_3^-$          | <u>Cancrinite</u> * + traces sodalite. |
| $\text{Cl}^-/\text{MoO}_4^{2-}$      | <u>Sodalite</u> * + traces cancrinite. |
| $\text{Br}^-/\text{CrO}_4^{2-}$      | Sodalite + traces cancrinite.          |
| $\text{Br}^-/\text{NO}_3^-$          | <u>Sodalite</u> * + traces cancrinite. |
| $\text{Br}^-/\text{MoO}_4^{2-}$      | <u>Sodalite</u> * + traces cancrinite. |
| $\text{Cl}^-/\text{CrO}_4^{2-}$      | Sodalite                               |
| $\text{Cl}^-/\text{NO}_3^-$          | <u>Sodalite</u> * + traces cancrinite. |
| $\text{Cl}^-/\text{MoO}_4^{2-}$      | <u>Sodalite</u> * + traces cancrinite. |
| $\text{WO}_4^{2-}/\text{CrO}_4^{2-}$ | <u>Cancrinite</u>                      |
| $\text{WO}_4^{2-}/\text{NO}_3^-$     | <u>Cancrinite</u>                      |
| $\text{WO}_4^{2-}/\text{MoO}_4^{2-}$ | <u>Sodalite</u>                        |
| $\text{CO}_3^{2-}/\text{CrO}_4^{2-}$ | Sodalite                               |
| $\text{CO}_3^{2-}/\text{NO}_3^-$     | Sodalite                               |
| $\text{CO}_3^{2-}/\text{MoO}_4^{2-}$ | <u>Sodalite</u> * + traces cancrinite. |
| $\text{ClO}_3^-/\text{CrO}_4^{2-}$   | Sodalite                               |
| $\text{ClO}_3^-/\text{NO}_3^-$       | <u>Sodalite</u> * + cancrinite.        |
| $\text{ClO}_3^-/\text{MoO}_4^{2-}$   | Sodalite                               |
| $\text{NO}_3^-/\text{CrO}_4^{2-}$    | Cancrinite                             |
| $\text{NO}_3^-/\text{MoO}_4^{2-}$    | Cancrinite                             |

The most powerful promoters of the sodalite structure under these conditions are undoubtedly  $\text{Br}^-$ ,  $\text{ClO}_4^-$ ,  $\text{ClO}_3^-$  and  $\text{CO}_3^{2-}$ , while  $\text{NO}_3^-$  is shown to be a powerful aid to cancrinite formation. In the experiments with mixed salts, single phases rarely appear, so that each salt makes its own contribution, as far as possible independently of the other component in the mixture. The products still contain imbibed salts as before.

Another question of importance arises in these connections. So far we have only considered salts whose physical dimensions enable them to be trapped by the aluminosilicate framework cavities. One might legitimately ask what happens when large salt molecules, too big to be encapsulated by these sodalite and cancrinite structures, are added to the reaction mixtures. Some preliminary experiments were made along these lines using organic salts such as sodium phenate, sodium nitromethane and sodium benzoate. In these experiments sodalite formation was observed. Assuming negligible alkaline degradation of the organic substrates, it can be further assumed that no inclusion took place. However, the products showed unusual characteristics, for example water sorption and thermal behaviour, and expansion or contraction of the aluminosilicate lattice. This evidence leads us to postulate that changes in the Si/Al ratio of the product were taking place. This is of considerable interest and merits further investigation.

Sometimes it was possible to observe the influence of surfactants on kaolinite recrystallization. Thus addition of diquat dibromide



to a reaction mixture which would otherwise produce basic sodalite, almost completely inhibited the reaction. This compound rapidly flocculated the kaolinite and appeared to render it less soluble in alkali. These results are in accord with the observations of Knight and Tomlinson, who studied the adsorption of a similar compound, "paraquat", on mineral soils. <sup>(86)</sup> However, even after the delayed destruction of the kaolinite (evidenced by the loss of x-ray diffraction properties) no subsequent crystallization of any product took place.



### Kinetics of Formation of Sodalite from Kaolinite.

Kinetic studies of aluminosilicate crystallizations are rare. This is probably due to the fact that systems of interest are alkaline and highly corrosive so that normal experimental procedures are not readily applicable. Nevertheless, the small amount of work done under these difficult conditions has yielded interesting results. Kerr,<sup>(99)</sup> in a notable series of experiments, the record of which incidentally underlines the experimental difficulties ("one pump failed at this point"), studied the kinetics of formation of zeolite A, from amorphous aluminosilicate feedstock. He found that the results could be explained by assuming that this feedstock dissolved in sodium hydroxide solution to form a soluble active species, which then nucleated to form zeolite A. The reaction was first order with respect to the quantity of crystalline zeolite present, and was also characterized by an induction period, which could be eliminated by seeding. The extent of reaction was followed by quantitative x-ray powder photography, and by volumetric gas sorption.

Domine and Quobex<sup>(101)</sup> also used volumetric gas sorption to determine the rate of formation of mordenite from aluminosilicate gels. These authors again found an induction period, which increased as the pH of the mother liquor was lowered. The results, in general, are in accord with those of Kerr.

Barrer, Cole and Sticher<sup>(18)</sup> studied the rate of formation of synthetic zeolite I from raw kaolinite and KOH solutions. In this work, Sticher found that after an induction period, zeolite I was formed rapidly. Before this rapid formation, however, the kaolinite was rendered almost completely amorphous, and this amorphous material had a chemical composition similar to that of the zeolite ultimately formed.

In the present work, the opportunity presented itself of following the kinetics of sodalite formation, by analyzing the solid phase for imbibed salt at various times.

### Experimental.

Since sodalite with imbibed  $\text{NaCl} \cdot \text{O}_4$  eliminates oxygen quantitatively at

650<sup>o</sup>, long after zeolitic water has been driven off, a careful thermogravimetric analysis of samples taken during reaction may provide as a kinetic variable, the weight of O<sub>2</sub> evolved as a function of time, by equal portions of the reaction mixture. Twenty grams of kaolinite were rapidly stirred in a litre of N NaClO<sub>4</sub>, which was also 1 N with respect to NaOH, at reflux temperature (~105<sup>o</sup>C). Equal samples of the mixture were taken by syringe each hour, dried at 120<sup>o</sup>C, and subjected to thermogravimetric analysis on a Stanton TR/1 instrument. The heating rate was 4<sup>o</sup>C. min<sup>-1</sup>. Gel and zeolitic water was removed by 400<sup>o</sup>, and samples were held at 550<sup>o</sup>C for 20 minutes to remove hydroxyl water before continuing to 650<sup>o</sup>C. The quantity of O<sub>2</sub> evolved was measured. X-ray powder photography was also used to examine samples.

### Results.

The x-ray patterns showed that the kaolinite was appreciably attacked by NaOH during the first two hours of reaction. Sodalite began to appear after four hours, and then grew rapidly, exhibiting sharp diffraction patterns after five hours. The results strongly suggest, but do not prove, that much of the crystalline kaolinite is gelatinized and brought into solution before any sodalite appears. The thermogravimetric data are in complete accord with the x-ray data. They are shown in Fig. 5.7. An initial induction period is followed by rapid crystallization and the reaction is complete in about twelve hours.

The four experimental studies quoted argue convincingly for the following pattern of zeolite crystallization.

- (a) Kaolinite is gelatinized by strong alkaline solutions of KOH and NaOH to form an amorphous solid of composition sometimes similar to that of the final crystalline product. In the case of experiments with gels, this initial gelatinization is not required.
- (b) The amorphous aluminosilicate is then solubilized, Al and Si going into solution in approximately the same mole ratio as that in the substrate; this process will be faster as the base concentration is increased. Steps (a) and (b) account for the main part of the induction period.
- (c) The reactive soluble species crystallize from true solution when an equilibrium concentration has been reached, producing the final zeolite.

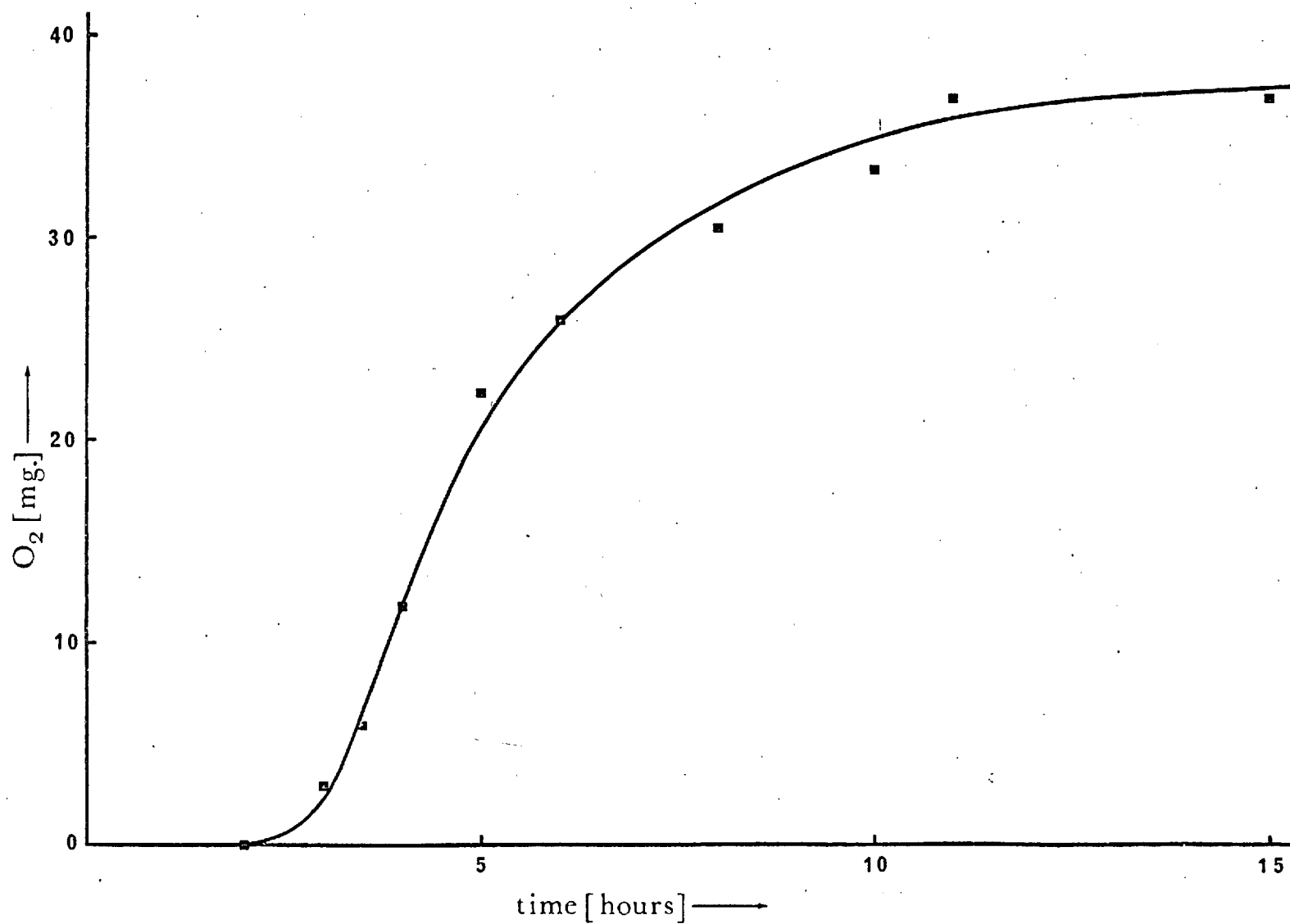


Figure 5.7 Rate of formation of Sodalite with Imbibed NaCl O<sub>4</sub>.

Recent experiments of Sticher<sup>(100)</sup> prove beyond doubt that this reaction scheme is true for raw kaolinite crystallizations. The reaction mechanisms, with emphasis on the role of additional salts, will be discussed further in section 6.

### Discussion.

The synthesis of sodalite and cancrinite appears first to have been investigated by Lemberg<sup>(84)</sup> and Thugutt<sup>(85)</sup>. Although no x-ray data were available in the early years of this work, these authors synthesized a great many phases at elevated temperatures, which, according to analytical and optical data, were probably feldspathoids. In modern work there have been occasional reports of their formation, usually as side products during the synthesis of other phases of more immediate interest,<sup>(87)</sup> and also as minor phases in boiler residues.<sup>(88)</sup> During early experiments on hydrothermal synthesis of aluminosilicates Barrer and White<sup>(48)54</sup> reported "basic" sodalites and cancrinites, in which the imbedded NaCl and Na<sub>2</sub>CO<sub>3</sub> found in natural specimens, is replaced by NaOH. Later work, which was more concerned with the growth of open pore structures, has always consciously moved away from feldspathoid crystallization fields, and these phases were considered to be contaminants. Since sodalite and cancrinite have structural and characteristic elements in common with the standard molecular sieve zeolites A and X, we might expect investigations on these simpler condensed compounds to yield information of general interest. This has proved to be so.

### Stoichiometry.

The stoichiometric observations on salt inclusion already noted are in harmony with the well-known idealized compositions  $6(\text{NaAlSiO}_4) \cdot 2$  salt, found in natural specimens of sodalite and cancrinite. This composition is approached with difficulty in the laboratory at 80°, but at modest temperatures above this figure, virtually anhydrous specimens can be made. Nor is the inclusion limited to anions. Meier and Barlöcher<sup>(89)</sup> have made a sodalite with exactly 2 tetramethyl ammonium ions per unit cell, i.e. one per cage, with no other cations and virtually no water. Naturally, in this case there must be a deviation from a 1:1 Si/Al ratio, which need not occur with anion entrainment. It is

interesting to note here that neutral atoms such as argon may be encapsulated in "washed out" sodalite.<sup>(90)</sup> Also Barrer and Cole<sup>(49)</sup> showed that two sodium atoms could be introduced into a sodalite cage and that, after removal of one of these atoms, an electron remained in the tetrahedral hole formed when the sodium ion took up a crystallographic framework position. Sodalite therefore is a model framework compound in these respects, its cubo-octahedral cages being capable of trapping electrons, neutral molecules, anions and cations. The water contents of synthetic sodalites are of great interest. In earlier work the ideal water contents of partly salt-filled sodalites have been in doubt. It is now clear from the salt inclusion experiments, that as the salt and NaOH loading is decreased, the water contents of the specimens approach 14-15 wt.% which requires exactly 8 water molecules per unit cell, or 4 per cage. In large pore zeolites water does not normally take up fixed structural positions and usually appears as disordered clusters to x-ray examination. However, in the present structure this probably would not be the case, and an x-ray or neutron diffraction examination should throw interesting light on packing problems in the cubooctahedral cavity, which would be of use elsewhere.

Although the evidence for its imbibition was normally slight, NaOH is a component of the synthesis solution, and must be considered a potential candidate for encapsulation. The experimental evidence leads to the conclusion that most other salts are more selectively imbibed than NaOH. In the systems investigated  $\text{Na}_2\text{CO}_3$  was an exception and these experiments have been separately discussed. On the other hand, when sodalites are crystallized without additional salts,  $\text{OH}^-$  ions are merely in competition with  $\text{H}_2\text{O}$ , and are readily imbibed. It is interesting that even in very concentrated NaOH solutions, there is at low temperature nowhere near the  $\text{OH}^-$  imbibition observed with the more selective anions. This situation changes of course as the temperature and pressure are increased.

A suitable formulation of the unit cell contents of the present compounds is therefore  $6(\text{NaAlSiO}_4) \times \text{salt}$ ,  $y \text{ NaOH}$ ,  $z \text{ H}_2\text{O}$ , provided the added salts have not altered the  $\text{Si}/\text{Al}$  ratio during synthesis. We derive equations for

the coefficients  $x$ ,  $y$ ,  $z$  as follows. If  $A$ ,  $B$  and  $C$  represent the experimentally determined wt.% salt, NaOH and  $H_2O$  we have

$$x = 852 A / \text{m.wt. salt } x (100 - A - B - C)$$

$$y = 852 B / 40 x (100 - A - B - C)$$

$$z = 852 C / 18 x (100 - A - B - C)$$

Computations using these equations are rapidly handled by digital computer. Normally the coefficient  $y$  is small, and using the analytical data given in the inclusion isotherms some space-filling relationships for the sodalite cages can be given. For example, one perchlorate or chlorate ion is equivalent to four water molecules, and in the NaOH system ( $x=0$ ), and two NaOH ion pairs (or  $OH^-$ ) are equivalent to four  $H_2O$  molecules. Some extensions to this line of argument can be made. In analytical practice it is easy to determine salts and water in the silicates, but difficult to determine NaOH. However, by using the analytical data for salt and water, the space-filling relationships can be assumed and an estimation of the NaOH content made. This data fitting is best done by computer. As has already been stated, low figures are expected for the salt- or water-rich specimens, and are indeed found by this method.

Most of the discussion has so far centred on sodalite, but the greater general part also applies to cancrinite. Unfortunately, no salt could be found which would produce cancrinite over its entire range of concentration at  $80^0-100^0$ , so that the quantitative isotherm data over the entire range are not yet available. When cancrinite first appears free of sodalite, for example in the  $NaNO_3$  system, the salt loading is already quite high (Table 5.11). The partial isotherm from this point on is virtually linear with  $NaNO_3$  concentration in solution, and a change in temperature at constant composition shifts the isotherm line only to slightly higher loadings.

#### Thermal Stability.

The question of thermal stability is an important one. A porous crystal which is stuffed full of a thermally stable salt should be more stable than its

empty counterpart, and the experiments are in accord with this view. Condensed framework aluminosilicate structures are also more stable than open ones. But then we have the interesting extension, that open structures containing sodalite and cancrinite cavities, should be more thermally stable if these cavities are filled with the correct thermally stable filler salt, ion or molecule. Consider the synthetic zeolite A,<sup>(91)</sup> which can be thought of as being built from sodalite cages, linked through cubes (or 4-rings) as shown in Fig. 5.8. To stabilize this structure we could synthesize it with  $\text{Cl}^-$  ions in the sodalite cages, and pack  $\text{K}^+$  or  $\text{Na}^+$  ions into the cubes, using a melt ion-sieve process or a gas of K or Na. By generally "tightening up" the framework in this way, we should achieve a more stable structure. Since the general consensus of evidence supports the view that these smaller building units are not responsible in an important way for the adsorption and catalytic properties of the sieves, no loss has been made. In fact by pushing cations out of these smaller cavities into the larger ones, a gain in usefulness may be achieved. Similar arguments apply in principle to synthetic zeolite X<sup>(92)</sup> (sodalite cages and hexagonal prisms) Fig. 5.9, and sieve L (cancrinite cages and hexagonal prisms).<sup>(53)</sup>

On the basis of the DTA, thermogravimetric and x-ray data, the sodalites and cancrinites can be classed according to their thermal stability. This is done in Table 5.14.

The best thermal fillers are  $\text{Na}_2\text{SO}_3$  and  $\text{Na}_2\text{SO}_4$ , while the halides are quite effective. Salts such as  $\text{NaClO}_4$  which are useful in synthesis on account of their low associative inclinations can be afterwards degraded to the thermally stable halides, and these perform the same function. Also, since the large oxygenated anions are more readily taken up by the frameworks than for example the halides, a better filling may be achieved, and the method is superior. Many extensions and modifications are immediately apparent.

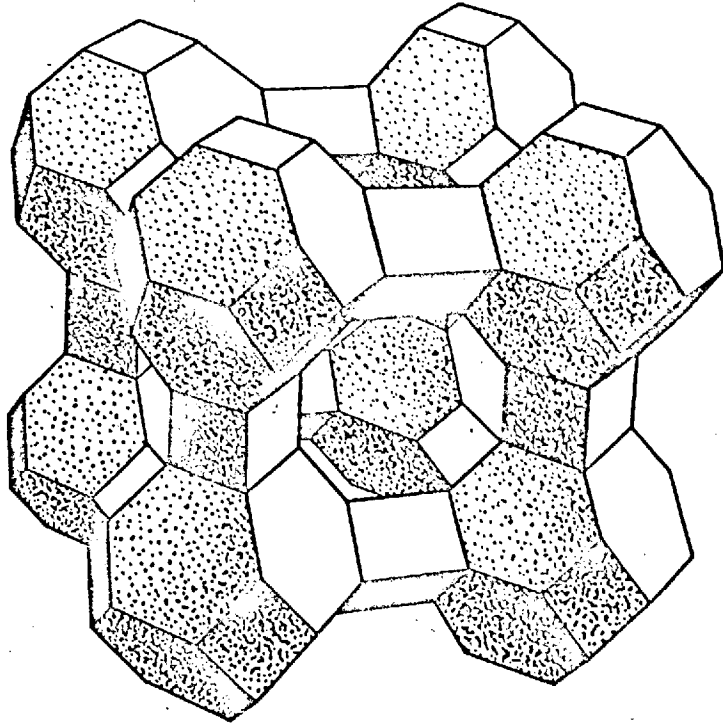


Figure 5.8 Line drawing of zeolite type A structure.



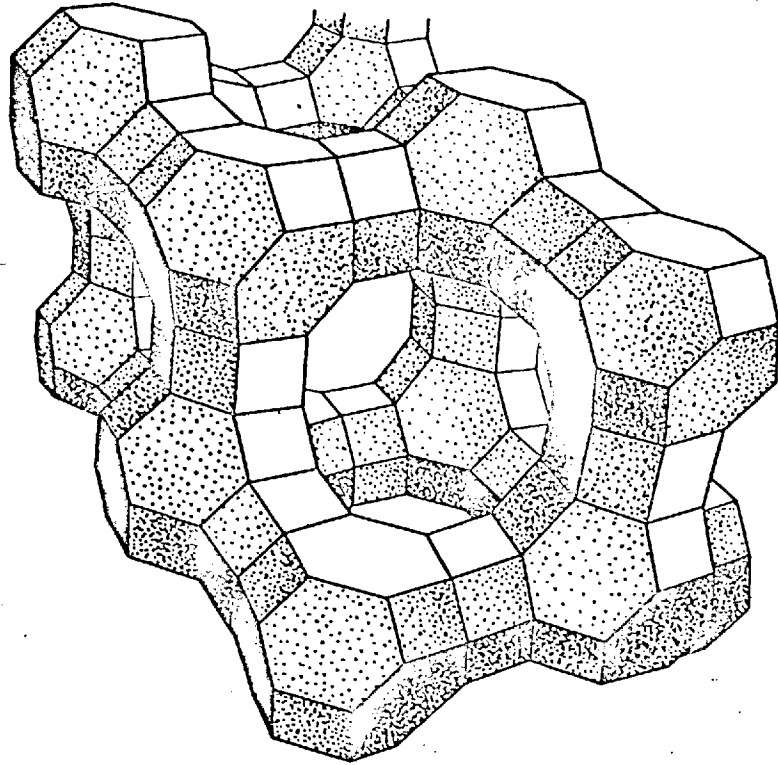


Figure 5.9 Line drawing of faujasite structure.

Table 5.14

Thermal Stability of various Sodalites and Cancrinites with imbibed salts.

|                               | <u>Sodalites</u>  | <u>Cancrinites</u>  |
|-------------------------------|---|---|
| <u>Class I</u><br>very stable | $\text{Na}_2\text{SO}_3$  | $\text{Na}_2\text{SO}_4$  |
| <u>Class II</u><br>stable     | $\text{NaCl}$<br>$\text{NaBr}$<br>$\text{NaI}$  | $\text{Na}_2\text{SeO}_4$   |
| <u>Class III</u><br>unstable  | $\text{NaOH}$<br>$\text{NaCH}_3\text{CO}_2$<br>$\text{Na}_2\text{CO}_3$<br>$\text{NaHCO}_2$<br>$\text{Na}_2\text{C}_2\text{O}_4$<br>$\text{Na}_2\text{WO}_4^*$<br>$\text{Na}_3\text{PO}_4^*$<br>$\text{NaClO}_3^\dagger$<br>$\text{NaClO}_4^\dagger$<br>$\text{Na}_2\text{S}$ | $\text{NaOH}$<br>$\text{Na}_2\text{CrO}_4$<br>$\text{NaNO}_3$<br>$\text{Na}_2\text{MoO}_4$<br>$\text{Na}_2\text{FeO}_4(?)$<br>$\text{NaMnO}_4$<br>$\text{Na}_3\text{VO}_4$<br>$\text{Na}_2\text{TeO}_4$ |

\* probably unstable because of the low salt loadings obtained at 80°.

† release  $\text{O}_2$  and form  $\text{NaCl}$ , then revert to Class II.

### Chemical Reactivity of Encapsulated Species.

A number of examples have already been given of chemical reactions undergone by anions trapped in sodalite and cancrinite frameworks. In most cases the framework acted merely as a porous matrix supporting the reacting molecules. It is interesting to note that in these systems, particularly with the sodalites, the opportunity presents itself of studying the reactivity of isolated single molecules. The most usual reaction observed was thermal decomposition involving the release of small molecules such as  $H_2O$ ,  $O_2$ ,  $CO$  and so on.

Encapsulation appeared slightly to stabilize the trapped species. For example  $NaClO_4$  when heated in air, begins to decompose at about  $520^\circ C$ . When trapped inside sodalite, onset of decomposition is delayed until about  $620^\circ C$ . Similar results were found for other species. Other kinds of reactions are also possible. These involve diffusion of trapped species out of the crystals, or diffusion of reactants into the crystals. The reactions of various sodalites with chlorine or  $HCl$  at high temperature afford examples of the first kind. When basic sodalite is heated with  $HCl$ , intracrystalline  $Na^+$  migrates out of the crystal and forms  $NaCl$  while <sup>there is</sup> an equivalent migration of  $H^+$  into the crystals to form  $H_2O$  which is subsequently desorbed. <sup>(54)</sup> Similarly, sulphur-bearing sodalites react with chlorine at elevated temperatures to form extracrystalline  $NaCl$ . As examples of the second kind we have reactions of the various compounds with  $H_2$  or sodium vapour at high temperature. When pale yellow sodium chromate cancrinite was outgassed at  $500^\circ$  and exposed to  $Na$  vapour, a colour change to bright green was observed and ESR measurements showed that some of the chromium had been reduced to oxidation states <sup>a</sup> 5 and 3. Similar results were found when outgassed chromate cancrinite was exposed to sodium borohydride solution. It is not known to what extent these reactions take place, whether it is only a surface reaction, or whether substantial intracrystalline reduction has taken place. <sup>(93)</sup> The important feature, however, is that various kinds of chemical alterations can be made on encapsulated species even in these condensed framework structures. In framework structures having building elements in common with sodalite and cancrinite various novel compounds of interest and potential usefulness may be made by these methods.

## SECTION 6.

### Mechanisms of Hydrothermal Crystallizations.

A correct understanding of the mechanisms of some important hydrothermal crystallizations is necessary to any quantitative statistical mechanical and statistical thermodynamic description which might successfully predict the courses of new reactions. Such an understanding is presently non-existent. For this reason, the simplest and commercially the least interesting reaction in zeolite chemistry, namely the formation of sodalite, possibly becomes the most important one. When the types of building unit present during sodalite formation are known, and the reasons for their presence understood, we shall be in a much better position to go on to more complicated systems. We begin by discussing what is actually known about these zeolitization reactions, in terms of sodalite. Virtually every principle laid down will apply to other systems.

There are two low-temperature hydrothermal reactions which give rise to sodalite. One involves the reaction of a pre-existing solid with a basic aqueous solution. The solid is "pre-existing" in the sense that it is to be found in a reagent bottle before the reaction, and not formed therein. The solid may contain all the components needed in the reaction, or it may contain fewer components, the others being present in the solution. The solid may be highly crystalline. For example it may be a natural mineral like kaolinite, or a synthetic mineral like zeolite A. On the other hand it may be a poorly crystalline natural mineral like halloysite, or a glass, like synthetic silica glass powder. The solid may finally be an amorphous mixture compounded in the laboratory, for example heat-treated kaolinite, or oven dried aluminosilicate gel of variable composition. The solution, on the other hand, is nearly always an aqueous alkaline feed consisting of various pure hydroxides or hydrolyzable stock such as carbonate, phosphate and the like. In addition it will contain in dissolved form, those necessary components not present in the solid phase, eg. excess silica, sodium aluminate and possibly additives, such as surfactants, and mineralizers, such as salts. Before commencing the discussion we describe the second reaction system. In this, two or more

solutions are mixed and a gel is formed, which afterwards reacts with excess liquid containing alkali to form zeolite. There are two views currently held about the mechanisms of these reactions.

### Solution Theory.

Supporters of this theory assert that the zeolite grows from true solution, and therefore that the starting material, be it crystalline solid, amorphous solid or gel, goes first into true solution, and afterwards nuclei develop from which the zeolite grows.

One of the most powerful lines of evidence supporting this theory is the observation that one can grow the same zeolite from numerous different reactants in the several systems already described. If the surfaces or crystalline constitutions of these reactants are important as some argue, this variety would be remarkable. But clearly it is the alkaline solution of different components to produce the same basic chemical molecules which is responsible. Kerr<sup>(99)</sup> has argued well for the solution theory. His experiments involved the solution of a synthetic amorphous aluminosilicate feed by suspending on a porous glass disc and pumping hot NaOH solution through it. Crystals of zeolite A were filtered out of the system on a second disc. Kerr states that there is some doubt about the kind of "solution" formed, whether it is true or colloidal; this could be resolved in principle by use of the ultracentrifuge, or light scattering methods. The solution would be deemed true according as these methods initially revealed molecules or low macromolecules, rather than high polymers. The second strong evidence is based on the present experiments using a crystalline kaolinite feed and sodium hydroxide solution. When no added salt is present in the solution, or when it contains NaCl, NaBr, Na<sub>2</sub>WO<sub>4</sub>, etc., sodalite is formed, and OH<sup>-</sup>, Cl<sup>-</sup>, Br<sup>-</sup>, WO<sub>4</sub><sup>-</sup> are imbibed. But when NaNO<sub>3</sub>, Na<sub>2</sub>CrO<sub>4</sub>, Na<sub>2</sub>MoO<sub>4</sub> are present, cancrinite is formed and NO<sub>3</sub><sup>-</sup>, CrO<sub>4</sub><sup>2-</sup>, MoO<sub>4</sub><sup>2-</sup> are imbibed, not only in the channels of the structure but also in the cancrinite cages. Very small quantities of these cancrinite structure promoters are needed and these amounts cannot possibly interact at molecular level with anything but a very small fraction of the kaolinite surface available in the initial stages of the

reaction.

There is a reason why we cannot argue conclusively against the view that the kaolinite surface plays an important role in the mechanisms of these reactions. When ignited kaolinite (i.e. kaolinite which has been heated at  $650^{\circ}$  to constant weight and thereby rendered amorphous to x-rays) is substituted for raw crystalline kaolinite in the NaOH-NaNO<sub>3</sub> and -Na<sub>2</sub>CrO<sub>4</sub> systems already discussed, the product is still cancrinite, and no specific effect of the surface has been demonstrated. Had the experimental case been rested here the solution theory might have been regarded as proven. But when further experiments were made with Na<sub>2</sub>MoO<sub>4</sub> and ignited kaolinite, so,alite, not cancrinite, was formed.

Before trying to resolve this dilemma some new and highly significant experiments due to Sticher<sup>(35,100)</sup> will be reviewed. This author measured the rate of dissolution of raw kaolinite in KOH and NaOH solutions at  $80^{\circ}$ , and examined the reaction using electron microscopy and x-ray powder diffraction.

It was observed that the hexagonal kaolinite platelets were initially attacked around their edges by the alkaline solution, and gelatinized. During this period the concentration of Al and Si in solution was initially negligible, but soon increased sharply, very rapidly reaching a maximum. Then zeolite began to crystallize at a point separated from the dissolving and gelatinous kaolinite by pure solution. The concentrations of Al and Si in solution began to fall off, but then assumed relatively constant values until the kaolinite feed had been exhausted. Zeolite crystallized all the time until the dissolved components tailed off.

These observations are in accord with the kinetic evidence already adduced in support of the solution theory (section 5) and strongly support it. However, the unexpected result with Na<sub>2</sub>MoO<sub>4</sub> and ignited kaolinite does not readily fit into this picture.

### Gel Theory.

The view that aluminosilicate gels crystallize directly to form zeolites without first going into solution appears to be supported by Flanigen and Breck.<sup>(103)</sup> The above discussion on the solution theory shows that at some point in the reaction a gel is present, either initially, or as a result of alkaline attack on crystalline feedstocks. It is entirely reasonable, therefore, to argue that the gel structure is a template for the final zeolite, and that minor structural rearrangement takes place within the gel during this process. There are several reasons why this view is satisfactory. First, aluminosilicate gels do have physical and chemical structure. Zhdanov,<sup>(104)</sup> and Dubin and Polstyanov<sup>(105)</sup> have reached this conclusion on the basis of sorption and other measurements; Wieker<sup>(106)</sup> and co-workers have demonstrated by chemical and x-ray methods the presence of specific structure in aluminosilicate gels which were afterwards heated to produce zeolites. We may also add the observation, well known to experimental zeolite chemists, that the order of mixing and rate of stirring of solutions during gel formation has profound effects upon the nature of the final product, even though gels in question may have the same overall composition. If the gel structure is not important this behaviour remains a mystery.

The gel and solution theories now appear to be complementary and will be combined in a single theory which will explain all the known results.

### A Theory of Growth, with Transport.

In this theory, the gel is regarded as the essential component of the reaction, and it does not matter whether it was initially present or not. The theory assumes that at some stage of the reaction, a structured gel is formed, the structure depending on the method of preparation. It is suggested that a gel formed at the edges of a kaolinite crystal will generally have an essentially different structure from another formed by mixing aluminate and silicate solutions, even if the same system composition is maintained. The structure of this gel is supposed to dictate the nature of the zeolite finally formed, in the following way. Just as a large organic molecule may be cleaved at certain positions to yield smaller fragments, the gel is regarded as being cleaved, by

interaction with alkaline solutions, to form smaller structural units, in solution. Depending on the cleavage conditions, these units will more or less represent the structural features in the original gel. In very severe conditions (eg. very strong alkali) we should expect complete degradation to elementary  $Al(OH)_4^-$  and  $SiO_4^{4-}$  ions, and note that under such conditions relatively simple and often condensed structures such as kaliophilite, and sodalite are formed\*. These structural units are free to undergo transport by diffusion and mixing processes and are susceptible to association with dissolved additives such as salts, and cations, with their hydration shells. The aluminosilicate units envisaged would have high molecular weights, being polymeric, but would by no means be colloidal. They would also have multiple negative charges, balanced by association with cations, but by virtue of induction and polarization effects the cation hydration shells would be expected to associate with suitable anions, and thus the possibility exists of additional anions being able to influence the course of ultimate polymerization to form zeolite. It is well known that the cations present in such systems remarkably influence the products obtained, and very fine changes in mixed cation systems lead to structurally different zeolites. This is attributed entirely to the influence of hydration shells upon solution association.

The nature of these soluble building units is regarded as governing the kind of stacking in the final product. More complex gels formed using organic bases and organosilicates as templates naturally form larger units with the corresponding possibility of producing more novel crystals.

In this work anions are grouped into two classes, one of which is assumed to interact with aluminosilicate groups from gelatinized kaolinite to form cancrinite and the other to form sodalite. The reason why changes are possible from one structure to the other using the same salt, but different conditions - for example using higher temperatures or different starting materials - seems to be related to the initial gel structure as well as to changing equilibria, both

---

\* For example, if kaolinite is treated with molten NaOH, sodalite is formed, and when sodalite is similarly treated, zeolite A is formed. <sup>(93)</sup> At present it is not known whether this is a true molten salt reaction, or merely a room temperature formation during washing of excess NaOH from the crucible samples.



ionic and associative, between the gel and soluble species.

These reactions are obviously complicated, but it does seem that the above speculation accounts more completely for the facts than does the gel or solution theory alone. The conclusion is that future progress will be made by directing more attention to the nature of solutions in zeolite systems. Unfortunately our knowledge of solutions is far behind our knowledge of the solid and gas states.

## SECTION 7.

### Theories of Anion Entrainment.

#### Introduction.

A connection between the Langmuir-type isotherms observed for various salts on sodalite (section 5) and the mechanism of hydrothermal crystallization is now sought. In view of the complexity of these systems, we should not expect any startling success, and at some stage we are bound to make the assumption that a complicated property or combination of properties can be replaced by a constant average value. In numerous instances in physics and chemistry this method leads to useful results, and if it does, we must be grateful for such mercies.

There are presently no theories available which deal particularly with these systems. We therefore start out by considering the conditions for equilibrium between a solution and a solid phase, consisting of porous crystals, in contact with it.

Reference has already been made (sections 3 and 5) to the structural features of several aluminosilicates besides sodalite. In general, these structures are characterized by more than one kind of framework cavity. In the present connection we are interested in cavities which can trap anions during synthesis, and, in general, this can be taken to mean cages whose largest openings are formed by six-rings of (Si, Al)-O<sub>4</sub> tetrahedra. Cages with larger openings are not satisfactory traps, since even though salt may be included in them during synthesis, it is normally washed out afterwards. Experiments have shown that when only part of the structure is capable of trapping anions, similar Langmuir-type isotherms may be obtained for this part, while the rest of the crystal behaves as a normal molecular sieve. Thus, when we speak of available trapping sites we refer either to part of a framework (eg. the sodalite cages in zeolite A), or to an entire framework (eg. sodalite).

Consider a solution which is in equilibrium with a solid phase of porous aluminosilicate crystals, and suppose that a certain number of trapping sites exist in the crystals. If the solution contains  $n$  species which are capable of

being trapped, one molecule at a time, by these sites, we can designate as  $\theta_i$  the fractional occupancy of available sites by the  $i$ -th species. If all the sites are occupied by a single species, we have  $\theta = 1$  for this species. But in cases of practical interest there will normally be several chemical species to be considered. In this case we designate the total occupancy of sites as  $\theta$  and have

$$\theta = \theta_1 + \theta_2 + \theta_3 + \dots + \theta_i + \dots + \theta_n \quad (1)$$

$$\text{or } \theta = \sum_n \theta_i \quad (2)$$

If all possibilities have been included in this summation, including  $\theta$  for any unoccupied sites,  $\theta = 1$ .

Experimentally it is found that the  $\theta_i$  depend on many variables such as the temperature, pressure and composition, so that each  $\theta_i$  is a dependent variable of the  $k$  independent variables  $x_i$ . We have then relations of the type

$$\theta_i = \theta_i(x_1, x_2, x_3, \dots, x_i, \dots, x_k) \quad (3)$$

so that the problem is one of finding functions  $\theta_i$  for the imbibable species subject to extra conditions such as (2). In this work we are interested in those cases where the experimental variable is the concentration of imbibable salt in the external solution, and have considered that the other imbibable species which need to be taken into account are the solvent, water and the sodium hydroxide. Both the latter components are present in considerable excess under the experimental conditions chosen, in amounts which have been deliberately chosen so that the composition of the external solution with respect to them is sensibly constant. Thus we deduce artificially simplified forms of (3), under conditions of constant temperature and pressure.

$$\theta_i = \theta_i(c_s, x_1, x_2, x_3, \dots, x_i, \dots, x_k) \quad (4)$$

where  $c_s$  is the concentration of salt in the external solution, and the  $x_i$  are regarded as fixed constants, some of which are known. For example

in all experiments  $[\text{NaOH}] = 4 \text{ moles Kg}^{-1} \text{ H}_2\text{O}$  and  $[\text{H}_2\text{O}] = 55.5 \text{ moles Kg}^{-1}$ . There will be three expressions like (4), one for each imbibable species we have considered.

### The Donnan Membrane Equilibrium.

Before going on to discuss the trapping of salts per se, it is advantageous to examine the case when salts can freely move between an aqueous solution and a porous crystal in contact with it.

A convenient entry to this problem is the Donnan equilibrium.<sup>(70)</sup> For the equilibrium distribution between two phases  $\alpha$  and  $\beta$  of an electrolyte consisting of  $\nu_+$  cations R and  $\nu_-$  anions X, we may derive the equation

$$\frac{\left(M_R^\beta\right)^{\nu_+} \left(M_X^\beta\right)^{\nu_-} \left(\gamma_{RX}^\beta\right)^{\nu_+ + \nu_-}}{\left(M_R^\alpha\right)^{\nu_+} \left(M_X^\alpha\right)^{\nu_-} \left(\gamma_{RX}^\alpha\right)^{\nu_+ + \nu_-}} = \exp. P \quad (5)$$

Here the  $M_i$  represent the concentrations, and the  $\gamma_i$  the activity coefficients. P is a complex quantity which properly contains osmotic coefficients in the two phases and terms in the ionic volumes of R and X. Under certain conditions, the RHS of (5) may approximate to the value 1, and (5) may then be tested in simple experiments. For example, the simplified form of (5) completely accounts for the distribution across a semi-permeable membrane of certain electrolytes, as Donnan originally showed. However, when solutions are not sufficiently dilute, increasing deviations from ideality are found as foreshadowed by the appearance of the  $\gamma_i$  in (5).

### Application to Porous Crystals.

The ion-exchange behaviour of framework alkali aluminosilicates is due to negative framework charge which must be balanced by the presence of cations according to the law of electroneutrality. The law may be expressed

$$\sum_i Z_i M_i = 0 \quad \text{or} \quad \sum_+ Z_+ M_+ = \sum_- |Z_-| M_- \quad (6)$$

where  $Z_i$  is the (signed) charge number of the  $i$ -th species of ion. If  $Z_f$  is the charge number for a zeolitic framework and  $m_f$  designates the "concentration"

of framework in suitable units, for the inclusion of a single salt RX by this framework (6) becomes

$$Z_f M_f + Z_R M_R^\beta + Z_X M_X^\beta = 0 \quad (7)$$

where the superscript  $\beta$  now refers to the crystalline phase. We note here that, in general, an extra term  $Z_{OH} - M_{OH}^\beta$  (or  $-M_{OH}^\beta$ ) must be added to the LHS of (7) since zeolite synthesis always takes place in alkaline solution, but in order to keep the argument as simple as possible this will not <sup>be</sup> included for the moment.

Introducing (7) into (5) we have

$$\frac{\frac{1}{Z_R} \left( Z_f M_f + Z_X M_X^\beta \right)^{v_+} \left( M_X^\beta \right)^{v_-} \left( \gamma_{RX}^\beta \right)^{v_+ + v_-}}{\left( M_R^\alpha \right)^{v_+} \left( M_X^\alpha \right)^{v_-} \left( \gamma_{RX}^\alpha \right)^{v_+ + v_-}} = \exp. P \quad (8)$$

which is the special form of (5) applicable to zeolites. The superscript  $\alpha$  now refers to the aqueous phase. Equation (8) takes special forms for particular salts. For example, if RX is NaCl or NaClO<sub>4</sub> it becomes (putting  $v_+ = v_- = 1$ ,  $Z_R = +1$ ,  $Z_X = -1$ )

$$\frac{\left( M_X^\beta - Z_f M_f \right) \left( M_X^\beta \right) \left( \gamma_{NaX}^\alpha \right)^2}{\left( M_{Na^+}^\alpha \right) \left( M_{X^-}^\alpha \right) \left( \gamma_{NaX}^\alpha \right)^2} = \exp. P_1 \quad (9)$$

and if RX is Na<sub>2</sub>CO<sub>3</sub>, it becomes (putting  $v_+ = 2$ ,  $v_- = 1$ ,  $Z_R = +1$ ,  $Z_X = -2$ )

$$\frac{\left( 2M_{CO_3}^\beta - Z_f M_f \right)^2 \left( M_{CO_3}^\beta \right) \left( \gamma_{Na_2CO_3}^\beta \right)^3}{\left( M_{Na^+}^\alpha \right)^2 \left( M_{CO_3^{2-}}^\alpha \right) \left( \gamma_{Na_2CO_3}^\alpha \right)^3} = \exp. P_2 \quad (10)$$

Despite the complexity still apparent in (8) and its special forms (9) and (10), they have been shown to hold under certain experimental conditions. If the terms in activity coefficients are removed to the RHS, their quotient in

multiplication with the exponential term may be relatively constant over a range of solution concentrations  $M_{RX}^{\alpha}$ . Barrer and Meier,<sup>(107)</sup> and Barrer and Walker<sup>(108)</sup> applied this argument to systems consisting of porous crystals of the molecular sieve type, in contact with aqueous solutions of various salts. They found that their salt inclusion isotherms, which were all concave towards the axis representing inclusion, were reasonably well explained by this argument. Thus the porous crystal behaves as a permeable membrane, and while individual  $\gamma_i^{\alpha}$  are unknown and may vary considerably, their quotient can be nearly constant.

However, it must be said that under these conditions very small quantities of salt are imbibed, of the order of 3 wt.%, and by no means is the crystalline phase completely filled with salt, even when the external solution is very concentrated.

#### Concept of Langmuir-type sites in sodalite.

In sodalite the possibility of treating the cubooctahedral cages as Langmuir "trapping sites" naturally presents itself. If the course of aluminosilicate crystallization presented in section 6 is accepted, then at a certain point during the reaction we can envisage partly formed sodalite framework units associated with anions we hope to imbibe. At the act of crystallization involving such framework units we can think of a reversible equilibrium with respect to imbibable anions (salt ion-pairs) as follows. At the surface of a crystallite are partly formed cages, each of which <sup>is</sup> are capable of accommodating one halide ion or  $ClO_4^-$  ion, and as polymerization takes place and framework components rain down upon this surface, any particular anion on the surface, or associated with the mobile feed, may either be occluded, or expelled. It is possible to derive expressions for the solid phase activities of included species required by the Donnan formulation, by a kinetic argument which takes into account the different space filling properties of included species.

#### Physical Model for Entrainment by Sodalite.

In the preliminary synthesis experiments with sodalite it was found that each truncated octahedral cage was capable of trapping four molecules of water, or two molecules of sodium hydroxide, or one molecule of salt. These

numbers correspond to unit cell compositions as follows:

$6(\text{NaAlSiO}_4) \cdot 8\text{H}_2\text{O}$  for sodalite hydrate,  $6(\text{NaAlSiO}_4) \cdot 4\text{NaOH}$  for basic sodalite, and  $6(\text{NaAlSiO}_4) \cdot 2\text{NaCl}$  for a sodium chloride sodalite. As previously mentioned, a general composition  $6(\text{NaAlSiO}_4) \cdot x\text{H}_2\text{O}$ ,  $y\text{NaOH}$ ,  $z\text{NaCl}$  applies to intermediate cases in this particular system. It is possible to apply this 4:2:1 ratio to sodalite cages by supposing that only certain kinds of occupancy are possible. For example, if a cage contains two molecules of water, it may also take in a molecule of sodium hydroxide, or may remain only partly occupied. Under these conditions it is clear that one sodalite cage must be assumed to provide four inclusion sites.

Let the occupancy of a cage be denoted by  $N_{xyz}$  where  $x$  ( $0 \leq x \leq 4$ ) denotes the occupancy with respect to water,  $y$  ( $0 \leq y \leq 2$ ) denotes occupancy with respect to sodium hydroxide, and  $z$  ( $0 \leq z \leq 1$ ) denotes occupancy with respect to salt. The  $x$ ,  $y$  and  $z$  may only be integers. Thus  $N_{020}$  represents a cage which contains two molecules of hydroxide, and  $N_{001}$ , one with one molecule of salt. Certain compositions, for example  $N_{201}$ , are invalid due to reasons already given.  $N_{xyz}$  also denotes the number of cages with the subscripted composition. It is easy to see that the only possible compositions are

$$N_{000}, N_{100}, N_{200}, N_{300}, N_{400}, N_{010}, N_{020}, N_{110}, N_{210} \text{ and } N_{001}. \quad (10)$$

We now use equations which are of the Langmuir type, derived by a kinetic balancing of rates of condensation and evaporation of a molecular species. For example, consider a single component case with  $N$  equivalent sorption clusters or centres, each capable of holding  $n$  molecules. At any given concentration of species above the sorbent, we use notation similar to that enunciated above, so that  $N_0$  represents the number of centres unoccupied,  $N_1$  the number singly occupied, and so on.

It is assumed first, that there is no appreciable interaction between sorbed species, which in the sodalite case also means that such interactions between species within each cage are also minimized. This, of course, is an approximation, and will be discussed when the model has been formulated mathematically. Second, an equilibrium sorption process is assumed. The change must be reversible, in the sense that it is a hypothetical passage through equilibrium

states. This assumption is taken as valid since the crystallization process can be thought of as satisfying such a passage. By balancing the rates of condensation and evaporation for the simple one-component sorbate, we have

$$\begin{aligned}
 nk_1cN_0 &= k_2N_1 \\
 (n-1)k_1cN_1 &= 2k_2N_2 \\
 &\vdots \\
 (\overline{n-n-1})k_1cN_{n-1} &= nk_2N_n
 \end{aligned}
 \tag{11}$$

where  $k_1$  and  $k_2$  are kinetic constants and  $c$  is the concentration (or pressure) above the sorbent or trapping surface. If we make the substitution  $r = (k_1/k_2)c$ , so that  $k_1/k_2$  is now an equilibrium constant, relations between the  $N_i$ , and  $N_0$  may be obtained:

$$\begin{aligned}
 N_1 &= nrN_0 \\
 N_2 &= \frac{n(n-1)}{1 \cdot 2} r^2 N_0 \\
 &\vdots \\
 N_n &= \frac{n(n-1) \dots 2 \cdot 1}{1 \cdot 2 \cdot 3 \dots n} r^n N_0
 \end{aligned}
 \tag{12}$$

This argument was first shown by Barrer and Rees<sup>(109)</sup> to lead to Langmuir's isotherm, by considering the number of molecules sorbed divided by the total number of sorption centres. It appears that a generalization of this approach for a mixture of three kinds of molecules is a natural step forward in interpreting the sodalite system.

Returning to the compositions represented by eqn. (10), we may derive a number of equations like the set (11):



$$\begin{array}{ll}
4r_1N_{000} = N_{100} & 2r_1N_{010} = N_{110} \\
3r_1N_{100} = 2N_{200} & r_1N_{110} = 2N_{210} \\
2r_1N_{200} = 3N_{300} & 2r_2N_{000} = N_{010} \\
r_1N_{300} = 4N_{400} & r_2N_{010} = 2N_{020} \\
r_3N_{000} = N_{001} & r_2N_{110} = N_{110}
\end{array} \tag{13}$$

In eqn. (13) the  $r_i$  represent ratios  $(k_1/k_2) c_i$  as before, the term in brackets being the equilibrium constant, except that now we have three such ratios,  $r_1$  corresponding to water,  $r_2$  to sodium hydroxide, and  $r_3$  to salt. It is now possible to express the numbers of each kind of centre, shown in (10), in terms of  $N_{000}$ , the number of sorbate free centres. Only the relations not obvious in set (13) are given:

$$\begin{array}{ll}
N_{200} = \frac{3}{2} r_1 N_{100} = 6r_1^2 N_{000} \\
N_{300} = \frac{2}{3} r_1 N_{200} = 4r_1^3 N_{000} \\
N_{400} = \frac{1}{4} r_1 N_{300} = r_1^4 N_{000} \\
\\
N_{110} = 2 r_1 N_{010} = 4r_1 r_2 N_{000} \\
N_{210} = r_1^2 N_{010} = 2r_1^2 r_2 N_{000} \\
N_{010} = 2r_2 N_{000} \\
N_{020} = \frac{1}{2} r_2 N_{010} = r_2^2 N_{000}
\end{array} \tag{14}$$

Let us now calculate  $N$ , the total number of sorption or "trapping" centres. This is the sum of the ten quantities appearing in (10), and using (13) and (14) it is, in terms of  $N_{000}$  and the  $r_i$ :

$$\begin{aligned}
N &= N_{000} \{ 1 + 4r_1 + 6r_1^2 + 4r_1^3 + r_1^4 + 2r_2 + r_2^2 + 4r_1 r_2 + 2r_1^2 r_2 + r_3 \} \\
&= N_{000} \{ (1 + r_1)^4 + 4r_1 r_2 + 2r_1^2 r_2 + 2r_2 + r_2^2 + r_3 \} \\
&= N_{000} \{ [(1 + r_1)^2 + r_2]^2 + r_3 \}.
\end{aligned} \tag{15}$$

Next, we calculate in a similar manner, the number of molecules of water imbibed,  $N_s^{\text{H}_2\text{O}}$ :

$$\begin{aligned}
N_S^{\text{H}_2\text{O}} &= N_{100} + 2N_{200} + 3N_{300} + 4N_{400} + N_{110} + 2N_{210} \\
&= N_{000} \{ 4r_1 + 12r_1^2 + 12r_1^3 + 4r_1^4 + 4r_1r_2 + 4r_1^2r_2 \} \\
&= 4r_1N_{000} \{ 1 + 3r_1 + 3r_1^2 + r_1^3 + r_2 + r_1r_2 \} \\
&= 4r_1N_{000} \{ [1 + r_1]^3 + r_2 [1 + r_1] \} \\
&= 4r_1(1 + r_1)N_{000} \{ [1 + r_1]^2 + r_2 \}.
\end{aligned} \tag{16}$$

We now define the fraction of total sites occupied by water as  $N_S^{\text{H}_2\text{O}}/4N$  and designate it  $\theta_{\text{H}_2\text{O}}$ . Hence from (15) and (16)

$$\begin{aligned}
\theta_{\text{H}_2\text{O}} &= N_S^{\text{H}_2\text{O}}/4N = \frac{4r_1(1 + r_1)N_{000} \{ [1 + r_1]^2 + r_2 \}}{4N_{000} \{ [(1 + r_1)^2 + r_2]^2 + r_3 \}} \\
\theta_{\text{H}_2\text{O}} &= \frac{r_1(1 + r_1) \{ [1 + r_1]^2 + r_2 \}}{\{ [1 + r_1]^2 + r_2 \}^2 + r_3}.
\end{aligned} \tag{17}$$

By entirely similar arguments, for the alkali-metal hydroxide ROH:

$$\begin{aligned}
N_S^{\text{ROH}} &= N_{010} + 2N_{020} + N_{110} + N_{210} \\
&= N_{000} \{ 2r_2 + 2r_2^2 + 4r_1r_2 + 2r_1^2r_2 \} \\
N_S^{\text{ROH}} &= 2r_2N_{000} \{ [1 + r_1]^2 + r_2 \},
\end{aligned} \tag{18}$$

and accordingly, we define the fraction of total sites occupied by base as  $N_S^{\text{ROH}}/2N$ , and designate it  $\theta_{\text{ROH}}$ . Division of (18) by  $2N$  yields

$$\theta_{\text{ROH}} = N_S^{\text{ROH}}/2N = \frac{r_2 \{ [1 + r_1]^2 + r_2 \}}{\{ [1 + r_1]^2 + r_2 \}^2 + r_3}. \tag{19}$$

Finally, for the general salt RX

$$N_S^{\text{RX}} = N_{001} = r_3N_{000}, \tag{20}$$

$$\theta_{\text{RX}} = N_S^{\text{RX}}/N = \frac{r_3}{\{ [1 + r_1]^2 + r_2 \}^2 + r_3}. \tag{21}$$

By a similar argument, it is possible to find the fraction of unoccupied sites. This is designated  $\theta_0$  and is  $N_S^0 / 4N$ , where

$$N_S^0 = 4N_{000} + 3N_{100} + 2N_{200} + N_{300} + 2N_{010} + N_{110}, \quad (22)$$

$$\text{hence } \theta_0 = \frac{(1+r_1) \{ [1+r_1]^2 + r_2 \}}{\{ [1+r_1]^2 + r_2 \}^2 + r_3}. \quad (23)$$

It is clear that if the treatment is consistent, eqn. (2), namely  $\sum_i \theta_i = 1$ , must hold. This may be shown by summation of (17), (19), (21) and (23). These equations give the fractional occupancy of sites by the three kinds of molecules, in terms of the solid phase activities. These activities, which are, of course, proportional to the  $r_i$ , may be found by the equations

$$r_{\text{H}_2\text{O}} = \theta_{\text{H}_2\text{O}} / (1 - \theta_{\text{H}_2\text{O}} - \theta_{\text{ROH}} - \theta_{\text{RX}}) \quad (24)$$

$$r_{\text{ROH}} = \theta_{\text{ROH}} (1 - \theta_{\text{ROH}} - \theta_{\text{RX}}) / (1 - \theta_{\text{H}_2\text{O}} - \theta_{\text{ROH}} - \theta_{\text{RX}})^2 \quad (25)$$

$$r_{\text{RX}} = \theta_{\text{RX}} (1 - \theta_{\text{RX}}) (1 - \theta_{\text{ROH}} - \theta_{\text{RX}})^2 / (1 - \theta_{\text{H}_2\text{O}} - \theta_{\text{ROH}} - \theta_{\text{RX}})^3 \quad (26)$$

since  $r_i = k_i a_i^\beta$ , where the  $k_i$  are the equilibrium constants and the  $a_i^\beta$  are the solid phase activities. These arguments form the basis for our approach to the sodalite system. It is interesting to note that (24) is a simple Langmuir relation, whereas (25) and (26) are more complicated due to the physical model.

#### Introduction of Solution Variables.

If  $\mu_i$  represents the chemical potential, referred to some standard state, of species  $i$ , and the superscripts  $\alpha$  and  $\beta$  refer to the aqueous phase and the solid crystalline phase respectively, then the equilibrium condition

$$\mu_i^\alpha = \mu_i^\beta \quad (27)$$

implies relations of the kind

$$a_i^\beta = K_i a_i^\alpha \quad (25)$$

As a first approximation, there is no reason why we should not replace the  $r_i$  in the previous formulation by means of the relations

$$r_i = K_i^! a_i^\alpha \quad (26)$$

where the  $K_i^!$  are now superscripted to show that they differ from the  $K_i$ . In addition, we assume that for ROH and H<sub>2</sub>O the product  $K_i^! a_i^\alpha$  is unknown, and replace it by  $R_i$ . On the other hand we replace  $K_{RX}^! a_{RX}^\alpha$  by  $R_{RX} m_{RX}^\alpha$  and specifically include the activity coefficient  $\gamma_{RX}$  in the measure  $R_{RX}$ . These replacements are drastic oversimplifications, but we shall have achieved our object if experimentally useful relations result.

When these substitutions are made into eqns. (17), (19), (21) and (23), we have

$$\theta_{H_2O} = \frac{R_1 (1 + R_1) \{ [1 + R_1]^2 + R_2 \}}{\{ [1 + R_2]^2 + R_2 \}^2 + R_3 m_{RX}^\alpha} \quad (27)$$

$$\theta_{ROH} = \frac{R_2 \{ [1 + R_1]^2 + R_2 \}}{\{ [1 + R_1]^2 + R_2 \}^2 + R_3 m_{RX}^\alpha} \quad (28)$$

$$\theta_{RX} = \frac{R_3 m_{RX}^\alpha}{\{ [1 + R_1]^2 + R_2 \}^2 + R_3 m_{RX}^\alpha} \quad (29)$$

$$\theta_0 = \frac{(1 + R_1) \{ [1 + R_1]^2 + R_2 \}}{\{ [1 + R_1]^2 + R_2 \}^2 + R_3 m_{RX}^\alpha} \quad (30)$$

In eqns. (27) - (30)  $R_1 = R_{H_2O}$ ,  $R_2 = R_{ROH}$ , and  $R_3 = R_{RX}$ , and these are taken to be unknown constants. The above formulation should represent an approximate description of a sodalite system for a salt such as  $NaCl$  which fills one cage consisting of four water sites and two hydroxide sites. The concentrations of alkali-metal hydroxide and water are also assumed to be reasonably constant, while the amount of kaolinite reactant should be small. It is interesting that eqn. (29) (for  $\theta_{RX}$ ) is of the Langmuir type, whereas the other equations are of a different form.

### Interpretations.

When  $m_{RX}^\alpha = 0$  we have a basic sodalite system and if  $\theta_i^0$  represents the fractional occupancy of sites, in this case we have

$$\theta_{H_2O}^0 = R_1 (1 + R_1) / \{ [1 + R_1]^2 + R_2 \} \quad (31)$$

$$\theta_{ROH}^0 = R_2 / \{ [1 + R_1]^2 + R_2 \} \quad (32)$$

$$\theta_0^0 = (1 + R_1) / \{ [1 + R_1]^2 + R_2 \} \quad (33)$$

In a typical basic sodalite crystallization at  $80^\circ C$  where the conditions inherent in the theory were satisfied (i.e.  $m_{RX}^\alpha = 0$ ,  $m_{NaOH}^\alpha = 4m$ ) a unit cell composition around  $6(NaAlSiO_4) \cdot 4.8H_2O, 1.6 NaOH$  was obtained. With 8 sites per cell for water and 4 for sodium hydroxide we have  $\theta_{H_2O}^0 = 0.6$  and  $\theta_{NaOH}^0 = 0.4$ . Due to errors of analysis, the sum of the  $\theta_i^0$  is 1.0, whereas it should actually be very slightly less than one because of a small fraction of unoccupied sites (eqn. 33). Thus, using this information and eqns. (31) and (32) we can get information about the relative magnitude of the  $R_{H_2O}$  and  $R_{ROH}$  for this system. Here  $R_{ROH}$  will be about four times  $R_{H_2O}$ , but we cannot say anything about their individual values, which vary very strongly with  $\theta_0^0$ .

The general three component case is more complicated. A computer programme was written which utilized an IBM.1460 line printer and plotting routine, and several thousand hypothetical isotherms were computed and drawn according to eqns. (27) - (30), using various arbitrary values for the  $R_i$  and running  $m_{RX}^\alpha$  from 0 to 5.0 at intervals of 0.10. The  $R_i$  were then adjusted so that the experimental isotherms for salt and water (section 5) were qualitatively reproduced. During this process it became clear that  $R_{RX}$  must be much larger than either of the other two constants.

In Table 7.1 some numerical values are quoted.

Table 7.1

Some calculated values of  $\theta_i$  according to eqns. (27) - (30).

| $m_{RX}^\alpha$ | $\theta_{H_2O}$ | $\theta_{ROH}$ | $\theta_{RX}$ | $\sum_i \theta_i$ | $R_i$  |
|-----------------|-----------------|----------------|---------------|-------------------|--|
| 0.0             | 0.9016          | 0.0081         | 0.0           | 0.9097            | $R_{H_2O} = 10.0$<br>$R_{ROH} = 1.0$<br>$R_{RX} = 50000$ |
| 0.5             | 0.3364          | 0.0030         | 0.6268        | 0.9662            |  |
| 1.0             | 0.2068          | 0.0019         | 0.7706        | 0.9793            |  |
| 1.5             | 0.1493          | 0.0013         | 0.8344        | 0.9850            |  |
| 2.0             | 0.1168          | 0.0011         | 0.8704        | 0.9883            |  |
| 0.0             | 0.4000          | 0.2000         | 0.0           | 0.6000            | $R_{H_2O} = 1.0$<br>$R_{ROH} = 1.0$<br>$R_{RX} = 99.0$   |
| 0.5             | 0.1342          | 0.0671         | 0.6644        | 0.8657            |  |
| 1.0             | 0.0806          | 0.0403         | 0.7983        | 0.9192            |  |
| 1.5             | 0.0576          | 0.0288         | 0.8559        | 0.9423            |  |
| 2.0             | 0.0448          | 0.0224         | 0.8879        | 0.9551            |  |

In Fig. 7.1 some representative plots of eqns. (27)-(30) have been reproduced, for various values of the  $R_i$ .

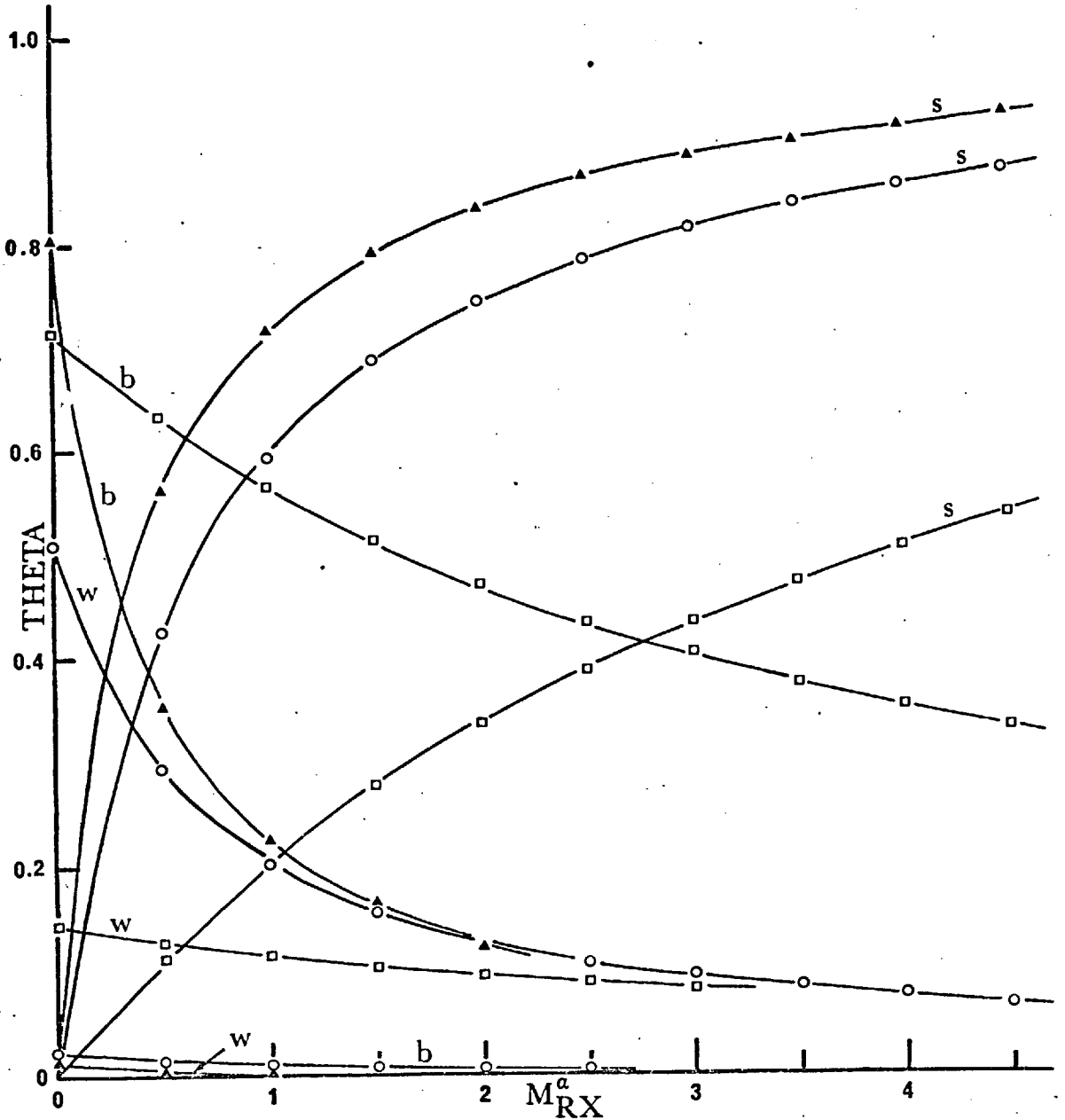


Figure 7.1 Some calculated isotherms according to equations (27)-(29):

|   | RS | RB  | RW  |
|---|----|-----|-----|
| ▲ | 99 | 5   | 0.1 |
| ○ | 30 | 0.1 | 1.1 |
| □ | 50 | 10  | 1   |

These figures show that, qualitatively, the experimental observations may be accounted for by means of this formulation. Before discussing the matter further, a criticism should be made. In this work we are dealing with equations of the kind

$$\theta = \frac{Ac}{B + Dc} \quad \text{or} \quad \theta = \frac{A}{B + Dc} \quad (34)$$

where A, B and D are constants, and c is a variable. These Langmuir type equations, and various modifications of them, are widely used to fit sorption and adsorption data, but it is clear that from a mathematical point of view they may be unsatisfactory. To illustrate this, any set of experimental data for such a Langmuir type adsorption may be taken from the literature together with the equation which is supposed to represent it. By using the proper mathematical procedure given in Appendix 1 a least squares curve is laid through the experimental points by adjusting the constants in the equation, and the error of approximation is compared with weighted residuals for each point. It will be found, in many cases, that it is impossible to fit the data for any values of the constants. Agreement in this context is a mathematical attribute not a visual one, and also implies approximately equal numbers of positive and negative residuals.

While this criticism, when it is valid, negates theoretical superstructure built upon false agreement, it is in no way intended to undermine the practical usefulness of equations like (34). A second related criticism of such equations will be evident. This relates to "parameter insensitivity", that is to say, for certain values of the parameters, the dependent variable is sometimes insensitive to variations in the independent variable. Empirical equations of the kind (34) are of course designed to have this quality. Unfortunately, both these, and similar equations with a theoretical basis, may be unsatisfactory from the point of view of an investigator who wishes to substantiate them by fitting his experimental data.



Question whether the salt inclusionisotherms are accounted for by this formulation.

The problem now is to find values of the  $R_i$  which account for the observations. The first step in this direction is designed to show whether this is possible at all. A calculated set of  $\theta_{RX}$  were made using (29) with  $R_{RX} = 20$ ,  $R_{ROH} = 10$  and  $R_{H_2O} = 1$ , and  $m_{RX}^\alpha$  was run from 0.1 to 5.0 at intervals of 0.1. It is clear that if we cannot work backwards from this accurate list of  $\theta_{RX}$  and  $m_{RX}^\alpha$  to find the  $R_i$  there will be little point in going on to the experimental list which is subject to errors of observation, and the possibility that in these cases the  $R_i$  may not be constants. By application of the methods given in Appendix 1, 833 sets of trial  $R_i$  were calculated using a searching density of 0.2, and  $10 \leq R_{RX} \leq 30$ ,  $5 \leq R_{ROH} \leq 15$ , and  $0.1 \leq R_{H_2O} \leq 2.0$ . The agreement factor for the best set of parameters was  $0.2197 \times 10^{-3}$ , with  $R_{RX} = 10.00$ ,  $R_{ROH} = 8.64$  and  $R_{H_2O} = 0.12$ . No individual weighted residual exceeded  $0.2944 \times 10^{-3}$ , i.e. the calculated  $\theta_{RX}$  using these  $R_i$  agree with the original list to three decimal places. This agreement seems to be excellent, but nevertheless the  $R_i$  differ substantially from the true values, and demonstrate that this system of equations is insensitive to variations in the  $R_i$ . In a second experiment a higher searching density was selected, 0.1, and 2688 sets of  $R_i$  were generated. The best agreement factor was  $0.4227 \times 10^{-4}$  for  $R_{RX} = 11.00$ ,  $R_{ROH} = 8.85$  and  $R_{H_2O} = 0.23$ . In no case did an individual weighted residual exceed  $0.9520 \times 10^{-4}$ , so that the calculated  $\theta_{RX}$  agreed with the observed values to one or two digits in the fourth place of decimals. In most cases in physical chemistry this agreement would be considered excellent, but the fact remains that the  $R_i$  found are different from the true values, and we cannot deduce unique values for them. At best we can quote a range of values which will satisfy the equations to a high degree of accuracy. If this is the case we cannot hope to properly refine the  $R_i$  by the least squares methods of Appendix 1, but it is still possible to lay a least squares curve through the original  $\theta_{RX}$ . When the trial  $R_i$  quoted above are varied

in this way, their values undergo small random movements in each cycle, but no convergence is found. For example, after six cycles of full-matrix least squares refinement of the last set of  $R_i$ , we obtain  $R_{RX} = 12.88$ ,  $R_{ROH} = 8.81$  and  $R_{H_2O} = 0.557$ , with the error factor  $0.3564 \times 10^{-4}$  and approximately equal numbers of positive and negative residuals.

When the experimental isotherm data (section 5) were treated similarly, it was found that the parameters were less well defined than in the cases with theoretical data. As before, relatively large values of  $R_{RX}$  were found, signifying a large equilibrium constant for the salt encapsulation process. The ill-definition referred to above, and the possible variation of the  $R_i$  with  $m_{RX}^{\alpha}$  make it impossible to quote values of the  $R_i$  which properly correspond to the several salts considered in the experiments, and which demonstrate differences between them. Neither is it possible to discuss deviations from ideality due to shortcomings of the formulation such as the neglect of sorbate-sorbate interactions. Perhaps the best method of continuing this line of investigation would involve its application to another crystal whose structure is known, and for which salt inclusion data are available, or could be collected. By such means one might resolve some of the problems which have become apparent in this section.

SECTION 8.Conclusions.

A variety of sodalite and cancrinite salt inclusion compounds may be easily synthesized from raw kaolinite at 80°. These have interesting chemical and physical properties and are potentially useful in a number of applications touching upon catalysis, gas storage, and ion-exchange processes. The imbibition of anions from solution during these hydrothermal reactions seems to be a very general phenomenon and therefore may be of use in other systems where it is desired to tailor aluminosilicate crystals to meet specific requirements, for example to alter ion-exchange and thermal characteristics of molecular sieves.

The Langmuir type salt inclusion isotherms on sodalite seem to support an equilibrium encapsulation process which necessitates competition between water, sodium hydroxide and salt for available trapping sites. By suitable adjustment of solution variables, crystal compositions may be fairly accurately prescribed in advance. This may be useful in certain applications.

APPENDIX 1.Problem of Deciding whether a given set of experimental measurements is following a particular law.

In its simplest form this problem is not complex. The experimental variable is merely substituted into the mathematical equation of the law and the agreement noted. However, in many cases of practical interest this simple approach is unsatisfactory, because it is lengthy and inaccurate. In the general case we have a set of experimental measurements of some quantity which is subject to all kinds of errors of observation, and have deduced an equation on theoretical or other grounds, and wish to know whether it will explain the observations. Let us first consider a simple example. The following table represents measurements

| F (obs) | Variable |
|---------|----------|
| 7.5200  | 0.1000   |
| 8.0800  | 0.2000   |
| 8.6800  | 0.3000   |
| 9.3200  | 0.4000   |
| 10.0000 | 0.5000   |
| 10.7200 | 0.6000   |
| 11.4800 | 0.7000   |
| 12.2800 | 0.8000   |
| 13.1200 | 0.9000   |
| 14.0000 | 1.0000   |
| 14.9200 | 1.1000   |
| 15.8800 | 1.2000   |
| 16.8800 | 1.3000   |
| 17.9200 | 1.4000   |
| 19.0000 | 1.5000   |
| 20.1200 | 1.6000   |
| 21.2800 | 1.7000   |

$F_{\text{obs}}$  of a quantity as a function of a variable  $v$ . The fact that this table was constructed at equal intervals of the argument is of no consequence. Let us suppose that all the measurements  $F_{\text{obs}}$  were for some reason equally accurate so that each accords unit weight. Now, any quantitative description of the measurements must connect  $F_{\text{obs}}$  with the variable  $v$  through some function  $f$  thereof. Furthermore,  $f$  should be derived from the axioms of the known theories which are believed to account for these particular data. Suppose that by recourse to these axioms we were able to derive two laws which were supposed to explain the data, namely  $f(v) = a_0 v^2 + a_1$  and  $f(v) = a_0 v^2 + a_1 v + a_2$ . The first law may have been derived from the second by introduction of a simplification. In these laws the  $a_i$  are constants, and we may well have no idea whatsoever about their magnitudes. They may, for example, represent activity coefficients in a complex solution of electrolytes, or internal pressures within porous crystals. The law may not be a simple polynomial as above, but a more complex function eg.  $f(v) = a_0 e^{-a_1 v^2 / (1-v)^{a_2}} + a_3$ . The question we have to answer on this and numerous other occasions during physical chemistry research, is this: do either of these laws describe the observations, and, if a choice exists, as above, which law is the best description?

By application of the mathematical and computational procedures to be described we can, in a very short time, state that the first law is invalid, and that the second law describes the measurements completely, if  $a_0 = 2$ ,  $a_1 = 5$  and  $a_2 = 7$ . The only assumption required is that the  $a_i$  lie inside some vaguely defined range. In the example we assumed that  $0.1 \leq a_i \leq 1000$ . Normally, it is possible to say that the physical quantities represented by the  $a_i$  lie within some wide range, even though we may have no precise idea of their magnitudes.

When theories are adduced to explain the salt inclusion isotherms for sodalite, we must be able to test them in the manner described.

#### A General Approach.

In this work a mathematically accurate procedure suitable for coding (i.e. generalizing in machine language for a digital computer) was required.

Another object was generality; the procedure should be applicable to all problems, not only the present one, and therefore any law which can be expressed in the form  $F_{\text{obs}} = f(a_i)$  must be amenable to analysis. The method developed with success is now described.

#### Formulation of Problem.

The observed quantity  $F_{\text{obs}}$  must be known together with the experimental errors in the independent variables associated with it. For example, if we are measuring under isothermal conditions the pressure ( $F_{\text{obs}}$ ) of a quantity of gas as a function of the volume occupied by that gas, we must know the error in the measurement of volume, so that we can apply a weight to  $F_{\text{obs}}$ ; this is mathematically equivalent to stating that some measurements of  $F_{\text{obs}}$  are more reliable than others, and hence must be given a greater weight.

Next, equations representing the behaviour of the system must be deduced from primitive axioms. In the last example we would deduce Boyle's law from the kinetic theory of gases, and it would remain to evaluate the constant of that law. A little thought at this point shows that some care should be taken in the planning of experiments, lest measurements are made at great pains, which are unsuitable for demonstrating the behaviour required or which produce needless complications. For example, if we were interested in the temperature dependence of solution properties, it would be inexpedient to use volume concentrations  $C_s$ , since  $\frac{\partial C_s}{\partial T} = -\alpha C_s$  where  $\alpha$  is the coefficient of thermal expansion, and if  $C_s$  were chosen as a variable, it would not be independent. It is therefore of great importance to examine the model which is proposed to account for the behaviour after the first few exploratory experiments, and then to design the following experiments so as to give the information required as straightforwardly as possible, holding as many troublesome variables constant as possible.

#### Estimation of the error of approximation.

Assuming that the problem has been correctly formulated we have a list of observed measures,  $F_{\text{obs}}$ , and a function  $f$ . For convenience we designate the function as follows:

$$f = f(v_i, a_i)$$

where the  $v_i$  are variables, experimentally measured with their errors, and the  $a_i$  are fixed unknown constants. Let us take one measurement, the  $j$ th, in the list. Substitute the  $j$ th arguments into  $f$ , and calculate the value of the function using trial values  $a_j$  of the, as yet unknown, parameters and designate this measure  $F_{\text{calc}}$ :

$$F_{\text{calc}} = f(v_j, a_j)$$

The difference ( $F_{\text{obs}} - F_{\text{calc}}$ ) between the observed  $j$ th value of the experimentally determined quantity and the  $j$ th calculated approximation to it is the residual for this set. If these residuals are squared, multiplied by the weight of the observation, and summed over all observations, we have an estimation  $\sigma$  of the error of approximation for the given function  $f$  and the trial parameters  $a_j$ :

$$\sigma = \sum_j [F_{\text{obs}}^j - f(v_j, a_j)]^2 \cdot W_j$$

or

$$\sigma = \sum_j [F_{\text{obs}}^j - F_{\text{calc}}^j]^2 \cdot W_j$$

For  $\sigma = 0$  the measurements will be completely satisfied, but in other cases will have a positive value representing minor (experimental "noise") deviations from satisfaction, or large deviations which disprove the law or remove the possibility of disproving it (experiments too inaccurate).

#### The search for acceptable trial parameters.

For each set  $a_k$  of trial parameters a value of  $\sigma$  can be computed. A large number  $n$  of sets of trial parameters will produce  $n$  values of  $\sigma$ , and the smallest  $\sigma$  will represent that set which causes  $F_{\text{calc}}$  most closely to approach  $F_{\text{obs}}$  over the entire range of measurements. If it is known in advance that the individual parameters lie within a certain numerical range we can search this range and generate all possible combinations of individual parameters in sets  $a_k$ , resulting in a large number of sets of trial parameters. A  $\sigma$  may be

computed for each set, and the best set used to test the law.

### The density of search.

We can now introduce the important concept of searching density. In the event that true parameters lie in a prescribed range, a search of low density may fail to locate them, while a very dense search possibility will. Since the searching is to be done by computer, machine time, an expensive commodity, must be minimized and no unnecessary searching should be done. Monte Carlo methods are commonly used in such problems, but it is one of the beauties of mathematics that there is always a simpler, faster and more elegant way, which is preferable to chance and brute force. Before going on to describe this method, we note the principle which suggested it. In principle, the method of least squares may be used to refine trial parameters, i.e. to adjust them in such a way as to give the most plausible agreement between the observed and calculated values of our measure.

In the event that the original equation of condition, represented by  $f$ , is non-linear, it can be made linear, as follows. Consider only two parameters for the purpose of this example, namely  $x$  and  $y$ . Now suppose that in some way an approximate pair of values of  $x$  and  $y$  have been found, say  $\bar{x}$  and  $\bar{y}$ .

Now, writing  $x = \bar{x} + \xi$  and  $y = \bar{y} + \eta$  we have, for the  $j$ th observation, approximately,

$$f_j(x, y) = f_j(\bar{x} + \xi, \bar{y} + \eta) = f_j(\bar{x}, \bar{y}) + \frac{\partial f_j}{\partial \bar{x}}(\bar{x}, \bar{y}) \xi + \frac{\partial f_j}{\partial \bar{y}}(\bar{x}, \bar{y}) \eta$$

so that the  $j$ th equation of condition becomes

$$\frac{\partial f_j}{\partial \bar{x}}(\bar{x}, \bar{y}) \xi + \frac{\partial f_j}{\partial \bar{y}}(\bar{x}, \bar{y}) \eta = F_{\text{obs}}^j - f_j(\bar{x}, \bar{y}).$$

These equations are now linear in  $(\xi, \eta)$  and may be solved by normal least squares processes. Thus, a searching procedure coupled with the methods of least squares would not need to locate precisely the true values of the parameters, but only approximations thereto. In practice it is found that



the approximations  $\bar{x}$ ,  $\bar{y}$  may be as far as 20% away from the true values in a general non-linear case, with complex derivatives, and provided the numerical procedures are accurate and not susceptible to appreciable rounding errors, a good refinement is possible.

The method of geometric searching for trial parameters naturally presents itself in this context. Consider a parameter whose true value is 2 and which is known to lie in the range 1 to 3. An arithmetic search of this range which began with the minimum value 1 and added increments say of 2, would produce only two trial values, viz. 1 and 3, each of which are 100% from the true value. If we had chosen 0.1 as an increment, we should certainly have found the true value but should have also done twenty times as much work and generated 9 trial parameters within 20%, and 5 within 10%, of the true value. In the event (which would remain unknown) of a less astute choice of increment, we may never hit the true value, and by arithmetic searching may fail even to get within 20% of it, as required for least squares refinement. On the other hand, a geometric search, in which specified fractions of the current parameter are added to itself to give the next trial value, overcomes all these problems, and the amount of work required is reduced by a very considerable factor. The fraction referred to is called the density of searching. Naturally, in problems with many parameters, each parameter is searched independently in its own range, and all possible combinations within the given set are separately considered during substitution into the function.

#### Computer Programmes.

The above problems of (a) searching for trial parameters and (b) refining trial parameters by the method of least squares, were the subjects of two Fortran IV programmes, which may be used separately or together. They will deal with any mathematical function with any number of variables and parameters, but have been tested mainly on problems with one variable and up to three parameters, i.e. problems frequently encountered in a physical chemistry laboratory. Apart from the primary object of examining functional dependence, they may be used to lay a least squares polynomial through any set of data.

The first programme, SRCH, undertakes a geometric search of  $n$  ranges of  $n$  parameters for a function  $f$  programmed by the user. For this purpose the  $n$  maximum and minimum values of the parameters, and the searching density must be specified. SRCH then substitutes all possible combinations of these parameters into  $f$  along with the independent variables, and computes the error of approximation  $\sigma$  for each set. The  $\sigma$  and parameters associated with it are stored in a large multidimensional array which is continually shuffled so that the smallest  $\sigma$  and associated parameters are kept at the top of the list. At the end of this process, the first set of parameters represents the best fit, and is loaded into the data arrays of GLS, the second programme.

GLS (general least squares) refines these trial parameters by full-matrix least squares methods. For this purpose the derivatives of the function with respect to the  $n$  refinable parameters must be programmed by the user. If the function is complex and some doubt exists as to whether the derivatives are correct, GLS can differentiate the functions numerically, but this facility can use appreciable amounts of machine time, so is normally used only to check analytical derivatives.

At the end of a run, the final  $F_{\text{obs}}$  and  $F_{\text{calc}}$  are printed out at the intervals of the arguments originally supplied, together with the refined parameters, and the final error of fit, which is the square root of the sum of the weighted squares of the residuals divided by the number of degrees of freedom. Comparison of this last quantity with the individual weighted residuals allows us to state whether the data are consistent with the function. If they are, the physical significance of the parameters may be discussed in relation to the theory.

#### Some Practical Details.

In some cases the trial parameters generated by SRCH are so good that least squares refinement is unnecessary. In others an initial set gives quite good agreement but least squares refinement does not proceed correctly. This is usual when the function is mathematically ill-defined, and the solutions undergo random motion. The normal equations may also be ill-conditioned giving rise to very small or zero diagonal elements during assembly or inversion of

the matrix.

The value of the method therefore lies not only in its ability to solve well-defined systems completely, but equally in its ability to expose ill-defined functions. The programmes described are self-adjusting, and will note and print out warnings on unfavourable occurrences, and then proceed to generate a new set of parameters. In most cases, however, the whole process is completely straight-forward, and for problems of the size mentioned times of from 30 seconds to 3 minutes are required for complete solution on a machine of medium speed (IBM.7094 or 360/65).

#### Shape of Curves.

In order to better understand the behaviour of unfamiliar functions of several variables, a small programme was written which plots families of plane curves for any specified function of one variable and several parameters. This programme and the others already described were used to examine the rather complicated theories of anion entrainment described in section 7 of the main text.

References.

1. Barrer, R.M., *Trans. Brit. Ceram. Soc.*, 56, 155, (1957).  
"Molecular Sieves", *Soc. Chem. Ind.*, London, 1968, p.39.
2. Eitel, W., "Silicate Science", Vol. 4, "Hydrothermal Silicate Systems"  
Academic Press, New York, 1966.
3. Kerr, G.T., *Inorg. Chem.*, 5, 1539, (1966).
4. Barrer, R.M., *Disc. Faraday Soc.*, No. 5, 326, (1949).
5. Grubner, O., Jírů, P. and Rálek, M. "Molekularsiebe", Deutscher  
Verlag der Wissenschaften, Berlin, 1968.
6. Milton, R.M., "Molecular Sieves", *Soc. Chem. Ind.*, London, 1968, p.199.
7. Barrer, R.M., *Chemistry and Industry*, p.1203, (1968).
8. Demmel, E.J., Perrella, A.V., Stover, W.A. and Shambaugh, J.P.,  
*Oil and Gas Jour.*, May, 1966, 178.
9. Pauling, L., "The Nature of the Chemical Bond", Cornell University  
Press, 1960.
10. Mellor, J.W., "Treatise on Inorganic and Theoretical Chemistry",  
Vol. 6/2, p.567, Longmans, 1947.
11. Barrer, R.M., *Endeavour*, 23, 122, (1964).
12. Amphlett, C.B., "Inorganic Ion Exchangers", Elsevier, 1964.
13. Barrer, R.M., *Nature*, 164, 112, (1949).
14. Venuto, P.B. and Landis, P., *Adv. Catalysis*, 18, 259, (1968).
15. Barrer, R.M., *J. Chem. Soc.*, 127, (1948).
16. Guth, J-L., *Rev. de Chimie Minerale*, 2, 127, (1965).
17. Barrer, R.M., Baynham, J.W., Bultitude, F.W. and Meier, W.M.,  
*J. Chem. Soc.*, 195, (1959).
18. Barrer, R.M., Cole, J.F. and Sticher, H., *J. Chem. Soc. (A)*,  
2475, (1968).
19. White, E.A.D. private communication.
20. Barrer, R.M., Cole, J.F. and Sticher, H., *British Patent Appln.*,  
case no. I-3773.  
Barrer, R.M. and Cole, J.F., *British Patent Appln.*,  
case no. I-3774.

21. Takahashi, H. and Nishimura, Y., *Int. Conf. Clays and Clay Minerals*, 1966, p.185.
22. Barrer, R.M. and Marshall, D.J., *J. Chem. Soc.*, 6621, (1965).
23. Barrer, R.M. and Makki, M.B., *Canad. J. Chem.*, 42, 1481, (1964).
24. Taggart, R.L. and Riband, G.L., United States Patent 3,119,659 (1964)  
(Union Carbide Corporation).  
British Patent 924, 938 (1963), (W.R. Grace and Co.).  
Haden, W.L. and Dzierzanowski, F.J., U.S. Patent 3,123,441, (1964),  
(Minerals and Chemicals Phillipp Co.).
25. Kerr, G.T., *J. Phys. Chem.*, 72, 1385, (1968).
26. Milton, R.M., U.S. Patent 3,008,803, (1961), (Union Carbide Corporation).
27. Breck, D.W. and Flanigen, E.M., "Molecular Sieves", *Soc. Chem. Ind.*  
London, 1968, p.47.
28. "IBM.7094 Data Processing System", IBM Form A22,6703,3.  
IBM Corporation, New York, 1962.
29. Cole, J.F. and Villiger, H. unpublished work.
30. Barrer, R.M., *Brennstoff-Chemie*, 325, (1954).  
Barrer, R.M., *British Chem. Eng.*, May, 1959, p.1.
31. Minachev, Kh. M., Garanin, V.I. and Isakev, Ya. I., *Russian Chemical Revs.*, 35, 903, (1966).
32. Union Carbide Corporation, *Neth. Pat. Appl.* 6,710,729, (1967).
33. Kerr, G.T. and Johnson, G.C., *J. Phys. Chem.*, 64, 381, (1960).
34. Sand, L.B., "Molecular Sieves", *Soc. Chem. Ind.*, London, 1968, p.71.  
Keough, A.H. and Sand, L.B., *J. Am. Chem. Soc.*, 83, 3536, (1961).
35. Sticher, H. private communication.
36. Milton, R.M., U.S. Patent 2,882,243, (1959), Union Carbide Corporation.
37. Milton, R.M., U.S. Patent 2,882,244, (1959), Union Carbide Corporation  
Barrer, R.M., Buser, W. and Grütter, W.F., *Helv. Chim. Acta*,  
39, 518, (1956).
38. Kerr, G.T., U.S. Patent 3,314,752, (1967), Mobil Oil Corporation.

39. (a) Kerr, G.T., J. Amer. Chem. Soc., 83, 4675, (1961),  
(b) Inorg. Chem., 5, 1537, (1966).
40. Barrer, R.M. and Marshall, D.J., J. Chem. Soc., 485, (1964).
41. Barrer, R.M. and Marshall, D.J., Amer. Mineralogist, 50, 484, (1965).
42. Deer, W.A., Howie, R.A. and Zussman, J. "Rock-forming Minerals",  
Vol. 4, Longmans, 1963.
43. Barth, T.F.W., Zeit. für Krist., 83, 405, (1932).
44. Löns, J. and Schulz, H., Acta. Cryst., 23, 434, (1967).
45. Pauling, L., Zeit. für Krist., 74, 213, (1930).
46. Johnson, C.K., "ORTEP, A Fortran Thermal Ellipsoid Plot Programme  
for Crystal Structure Illustrations". Oak Ridge National Laboratory,  
Tennessee 1965. ORNL Document 3794, revised.
47. Barrer, R.M. and Falconer, J.D., Proc. Roy. Soc. (A), 236, 227,  
(1956).
48. Barrer, R.M. and Denny, A.F., J. Chem. Soc., 4684, (1964).
49. Barrer, R.M. and Cole J.F., J. Phys. Chem. Solids, 29, 1755, (1968)
50. Cole, J.F. and Villiger, H., Mineralogical Magazine, (1969), in press.
51. International Tables for X-ray Crystallography, 3 Vols., Kynoch Press,  
Birmingham, (1958).
52. Jarchow, O. Zeit. für Krist., 122, 407, (1965).
53. Barrer, R.M. and Villiger, H., Zeit. für Krist., (1968), in press.
54. Barrer, R.M. and White, E.A.D., J. Chem. Soc., 1561, (1952).
55. Vaughan, D.E.W., Ph.D. Thesis, University of London, 1967.
56. Meier, W.M., Zeit. für Krist., 115, 439, (1961).  
Barrer, R.M. and Peterson, D.L., Proc. Roy. Soc. (A), 280, 466,  
(1964).
57. Fleischer, E.B., J. Am. Chem. Soc., 86, 3889, (1964).
58. Gordon, E.K., Samson, S. and Kamb, B. Science, 154, 1004, (1966).
59. Smith, J.V. and Bailey, S.W., Acta. Cryst., 16, 801, (1963).
60. Meier, W.M. and Villiger, H., Zeit. für Krist. (1968), in press.
61. Azároff, L.V. and Buerger, M.J., "The Powder Method in X-ray  
Crystallography", McGraw Hill, New York, 1958.

62. Burnham, C.W., "An IBM.7090 Computer Programme for Least-Squares Refinement of Crystallographic Lattice Constants", Geophysical Laboratory, Carnegie Institution of Washington, Washington D.C., 1963.
63. Cole, J.F. and Villiger, H., "LCLSQ, A Revised and Expanded FORTRAN IV Version of C.W. Burnham's Lattice Parameter Refinement Programme". Chemistry Department., Imperial College, London, 1968.
64. Cole, J.F. and Villiger, H., FORTRAN IV Computer Programmes for the IBM.7094 to facilitate the rapid indexing of Zeolite X-ray Powder Diffraction Patterns. Chemistry Department, Imperial College, London, 1967.
65. Ito, T.. "X-ray Studies on Polymorphism", Maruzen Co., Tokyo, 1950.
66. McMasters, O.D. and Larsen, W.L., U.S.A.E.C. Research and Development Report TID-4500, 1963.
67. Vand, V. and Johnson, G.G., Acta Cryst., A24, 543, (1968.)
68. Vand, V. and Johnson, G.G., "Generalized Methods of Indexing X-ray Powder Patterns", Materials Research Laboratory, Pennsylvania State University, 1967.
69. Lanczos, C., "Applied Analysis", Pitman, 1957.
70. Donnan, F.G., Zeit. f. Elektrochemie, 17, 572, (1911).  
Donnan, F.G. and Guggenheim, E.A., Zeit. f. phys. Chem., 162,  
Donnan, F.G., Zeit. f. phys. Chem., 168, 369, (1934).
71. Villiger, H., Ph.D. Thesis, University of London, 1968.
72. Meier, W.M., "Molecular Sieves", Soc. Chem. Ind. London, (1968), p.10.
73. Fischer, K.F. and Meier, W.M., Fortsch. Miner., 42, 50, (1965).
74. Busing, W.R., Martin, K.O. and Levy, H.A., "ORFLS, Oak Ridge Fortran Crystallographic Least Squares Programme", Oak Ridge National Laboratory, Oak Ridge, Tennessee, 1962.
75. Villiger, H., A Version of ORFLS suitable for Powder Data, Chemistry Department, Imperial College, London, 1967.

76. X-ray '63 Program System for X-ray Crystallography for the IBM.7094, Department of Chemistry, University of Washington, Seattle, (1965).
77. Zhdanov, S.P., Dokl. Akad. Nauk., 154, 419, (1964).
78. Barrer, R.M. and Mainwaring, D.E., unpublished work.
79. Barrer, R.M. and Marshall, D.J., J. Chem. Soc., 6621, 1965.
80. Barrer, R.M. and Denny, P.J., J. Chem. Soc., 971, (1961).
81. "Inorganic Syntheses", Vol. 4, 164, McGraw Hill, London, 1953.
82. Halstead, P.E. and Moore, A.E., J. Appl. Chem., 12, 413, (1962).
83. Lowenstein, W., Amer. Mineralogist, 39, 92, (1954).
84. Lemberg, J., Zeit. d. deutsche Geol. Gesellschaft, 579, (1883).
85. Thugutt, S.J., "Mineralchemische Studieren", Dorpat, (1891).  
Zeit. f. allg. und anorg. Chemie, 2, 65, (1892).  
Jahrbuch f. Mineral. Beil. Bd., 2, 554, (1894).
86. Knight, B.A.G. and Tomlinson, T.E., J. Soil. Science, 18, 233, (1967).
87. Flint, E.P., Clarke, W.F., Newman, E.S. Shartsis, L., Bishop, D.I. and Wells, L.S., J. Res. Nat. Bur. Stds., 36, 63, (1946).
88. Kirsch, H., N. Jb. Miner. Abh., 106, 287, (1967).
89. Meier, W.M., private communication.
90. Barrer, R.M. and Vaughan, D.E.W., in preparation.
91. Broussard, L. and Shoemaker, D.P., J. Am. Chem. Soc., 82, 1041, (1960).  
Reed, T.B. and Breck, D.W., J. Am. Chem. Soc., 78, 5972, (1956).
92. Nowacki, W. and Bergerhoff, G., Schweiz. miner., petrogr. Mitt., 36, 621, (1958).  
Bergerhoff, G., Bauer, W.H., and Nowacki, W., N. Jb. Miner. Mh., 2, 193, (1958).
93. Barrer, R.M. and Cole, J.F., unpublished observations.
94. Whittaker, E.T. and Robinson, G., "The Calculus of Observations", Blackie, 1960.
95. Breck, D.W., United States Patent 3,130,007, (1964), Union Carbide Corporation.



96. British Patent 1,090,563 (1965), Esso Research and Engineering Co.
97. Kerr, G.T., Science, 140, 1412, (1963).
98. Buerger, M.J., "Crystal Structure Analysis", John Wiley, New York, 1960.
99. Kerr, G.T., J. Phys. Chem., 70, 1047, (1966).
100. Sticher, H., Helv. Chim. Acta, (in press).
101. Domine, D. and Quobex, J., "Molecular Sieves", Soc. Chem. Ind., London, 1968, p.78.
102. Thomas, L.H. and Umeda, K., J. Chem. Phys., 26, 293, (1957).
103. Flanigen, E.M. and Breck, D.W., 137th Meeting of A.C.S., Inorganic Chemistry, Cleveland, Ohio, U.S.A. April, 1960. Abstracts p.33-M.
104. Zhdanov, S.P., "Molecular Sieves", Soc. Chem. Ind., London, 1968, p.62.
105. Dubinin, M.M. and Polstyanov, E.F., Russ. J. Inorg. Chem., 40, 631, (1966).
106. Fahlke, B., Wieker, W. and Thilo, E., Zeit. Anorg. u. allg. Chemie, 347, 82, (1966).
107. Barrer, R.M. and Meier, W.M., J. Chem. Soc., 299, (1958).
108. Barrer, R.M. and Walker, A.J., Trans. Faraday Soc., 60, 171, (1964).
109. Barrer, R.M. and Rees, L.V., Trans. Faraday Soc., 50, 1, (1954).